PhD degree in Molecular Medicine

European School of Molecular Medicine (SEMM),

University of Milan and University of Naples "Federico II"

Faculty of Medicine

Settore disciplinare: BIO/11

VE-cadherin orchestrates epigenetic modifications aimed at endothelial stabilisation

Marco Francesco Morini

IFOM-IEO Campus, Milan

Matricola n. R08901

Supervisor: Prof.ssa Elisabetta Dejana

IFOM-IEO Campus, Milan

Anno accademico 2012-2013

TABLE OF CONTENTS

LIST OF ABBREVIATIONS 4

FIGURE INDEX 8

ABSTRACT 11

INTRODUCTION 13

Development of the vascular system in mammals 13

Endothelial cell-cell junctions: adherens junctions and tight junctions 18

Intracellular signalling emanating from cell-cell junctions 25

The importance of vascular stabilisation 31

Claudin-5, VE-PTP and vWf: three vascular stability genes 38

Polycomb Group proteins and transcription regulation 43

MATERIALS AND METHODS 49

Cell culture 49

Lentiviral and adenoviral preparations 50

Immunofluorescence microscopy 51

Western Blot analysis 52

Co-immunoprecipitation 53

Quantitative RT-PCR analysis 54

Transcription factor binding site analysis 55

Chromatin immunoprecipitation 56

RNA interference 59

Immunohistochemistry 59

Antibodies and chemicals 60

Statistical analysis 61

RESULTS 62

VE-cadherin clustering triggers an endothelial stabilisation transcriptional programme 62

FoxO1 and β-catenin repress *VE-PTP* and *vWf* expression 66

Claudin-5, *VE-PTP* and *vWf* are Polycomb-target genes 72

FoxO1/β-catenin complex recruits PcG proteins at *claudin-5*, *VE-PTP* and *vWf* promoters 80

VE-cadherin associates with Ezh2 and sequesters it at the plasma membrane 88

VE-cadherin regulates Ezh2 expression level 96

Polycomb protein overexpression is accompanied by Claudin-5 repression in human ovarian cancer 98

DISCUSSION 101

REFERENCES 113

ACKNOWLEDGEMENTS 119

LIST OF ABBREVIATIONS

Ang-1: Angiopoietin-1

Ang-2: Angiopoietin-2

APC: Adenomatous Polyposis Coli

AF-6: Afadin-6

AJ: Adherens Junction

βTrCP: beta-transducin repeat containing protein

Bcl9: B-cell CLL/lymphoma 9 protein

BM: basement membrane

Bmi1: B lymphoma Mo-MLV Insertion region 1

bp: base pair

Brg-1: Brahma-related gene-1

BSA: bovine serum albumin

CBP: CREB-Binding Protein

Cbx4: Chromobox protein homolog 4

CD: Cluster of Differentiation

CDS: coding sequence

ChIP-seq: Chromatin-ImmunoPrecipitation-sequencing

CK1: Casein Kinase 1

DAPI: 4', 6-diamidino-2-phenylindole

DEP1: Density Enhanced Protein-1

DLL4: Delta Like 4

DN: dominant negative

DSP: dithiobis(succinimidyl)propionate

DZnep: 3-Deazaneplanocin A

E: embryonic day

EC: Endothelial Cell

Eed: Embryonic Ectoderm Development

eNOS: endothelial Nitric Oxyde Synthase

EPC: endothelial progenitor cell

ERK/MAPK: Extracellular-signal-Regulated Kinases/Mitogen-Activated Protein Kinase

ES: embryonic stem cells

ETS: E-twenty six

Ezh2: Enhancer of zeste homolog 2

FGF: Fibroblast Growth Factor

FKHR-TM: Forkhead in Rhabdomyosarcoma-Triple Mutant

FoxO1: Forkhead-box O1

GAPDH: glyceraldehyde-3-phosphate dehydrogenase

GFP: green fluorescent protein

GSK3β: Glycogen Synthase Kinase 3 β

GUK: guanylate kinase

H2AK119Ub1: mono-ubiquitylation of lysine 119 on histone H2A

H3K4me3: trimethylation of lysine 4 on histone H3

H3K27me3: trimethylation of lysine 27 on histone H3

H3K36me2/me3: di- or tri-methylation of lysine 36 of histone H3

HOX: homeobox

HRP: horseradish peroxidase

Ig: immunoglobulin

IkBa: Nuclear factor of kappa light polypeptide gene enhancer in B cells inhibitor, alpha

IL: interleukin

JAM: Junctional Adhesion Molecule

Jarid2: Jumonji- and AT-rich interaction domain (ARID)-domain-containing protein 2

lncRNAs: long non coding RNAs

LRP5: Low-density lipoprotein receptor-related protein 5

MDCK: Madin-Darby Canine Kidney cells

MLL1: Mixed Lineage Leukemia 1

MMP: Matrix Metalloprotease

Myc: myelocytomatosis oncogene

PcG: Polycomb Group

Pcl: Polycomb-like

PDGF-B: platelet-derived growth factor B

PDGFR-β: platelet-derived growth factor receptor β

PDZ: Post synaptic density protein, Drosophila disc large tumor suppressor and Zonula occludens-1 protein

PECAM: Platelet Endothelial Cell Adhesion Molecule

PFA: paraformaldehyde

Phc1: Polyhomeotic protein 1

PI3K: PhosphatidylInositol 3-Kinase

PlGF: Placental-derived Growth Factor

pRb: Retinoblastoma protein

Ptprb: Protein Tyrosine Phosphatase Receptor Type B

PRC: Polycomb Repressive Complex

qChIP: quantitative chromatin immunoprecipitation

REST: RE1-silencing transcription factor

Ring1B: Really interesting new gene 1B

RNA Pol II: RNA Polymerase II

SET: Su(var)3-9, Enhancer of Zeste, Trithorax

SH: Src Homology

sh: short hairpin

SOX: sex-determining region (SRY)-box

Suz12: Suppressor of Zeste 12

TAL1: T-cell Acute lymphocitic Lymphocytic Leukaemia protein 1

TBST: Tris buffered saline tween

TCF: T-Cell Factor

TNF-α: Tumour Necrosis Factor-α

TrxG: Trithorax Group

TSS: transcription start site

VASH1: vasohibin1

VE-cadherin or **VEC**: Vascular Endothelial-cadherin

VE-PTP: Vascular Endothelial-Protein Tyrosine Phosphatase

VEGF: Vascular Endothelial Growth Factor

VEGFR: Vascular Endothelial Growth Factor Receptor (a.k.a Flk1, Foetal Liver Kinase 1)

VWD: von Willebrand disease

vWf: von Willebrand factor

Wnt: Wingless-related MMTV integration site

WT: wild type

Yy1: Yin and Yang 1

ZO: Zonula Occludens

ZONAB: ZO-1-associated nucleic acid binding protein

FIGURE INDEX

INTRODUCTION

Figure 1 The development of the vascular network

Figure 2 Angiogenic sprouting: tip cells, stalk cells and lumen formation

Figure 3 Schematic representation of endothelial AJs

Figure 4 Schematic representation of endothelial TJs

Figure 5 Schematic representation of the Wnt/β-catenin pathway

Figure 6 AKT-dependent regulation of FoxO1

Figure 7 Tumour vessels are structurally and functionally abnormal

Figure 8 The coordinated activities of PRC1 and PRC2

MATERIALS AND METHODS

Figure 9 An aliquot of fragmented chromatin from ECs run on a 1% agarose gel

RESULTS

Figure 10 Claudin-5 expression in confluent VEC-null and VEC-positive ECs

Figure 11 VE-cadherin clustering upregulates the endothelial-stabilisation gene *VE-PTP*

Figure 12 VE-cadherin clustering upregulates the endothelial-stabilisation gene *vWf*

Figure 13 VE-cadherin clustering is required for *VE-PTP* and *vWf* expression

Figure 14 Analysis of *VE-PTP* and *vWf* expression upon FKHR-TM overexpression

Figure 15 Analysis of *VE-PTP* and *vWf* expression upon pharmacological inhibition of PI3K/AKT pathway

Figure 16 Analysis of *VE-PTP* and *vWf* expression upon ΔN-β-catenin overexpression

Figure 17 Schematic representation of the putative promoter regions of *VE-PTP* and *vWf*

Figure 18 FoxO1 binds to *VE-PTP* and *vWf* promoter regions

Figure 19 β-catenin binds to *VE-PTP* and *vWf* promoter regions

Figure 20 PcG proteins bind the TSS of *claudin-5*, *VE-PTP* and *vWf* genes in VEC-null ECs

Figure 21 Histone density on the TSS of *claudin-5*, *VE-PTP* and *vWf* genes is not affected by the absence of VE-cadherin

Figure 22 Activation marks decorate the TSS of *claudin-5*, *VE-PTP* and *vWf* genes in VEC-positive ECs

Figure 23 Suz12 overexpression in VEC-positive ECs

Figure 24 Suz12 overexpression represses *claudin-5*, *VE-PTP* and *vWf* expression

Figure 25 Suz12 knockdown in VEC-null ECs

Figure 26 Analysis of *FoxO1* expression upon stable Suz12 knockdown

Figure 27 PcG protein binding to the TSS of *claudin-5*, *VE-PTP* and *vWf* genes upon Suz12 stable knockdown

Figure 28 Analysis of *claudin-5*, *VE-PTP* and *vWf* expression upon stable Suz12 knockdown

Figure 29 FKHR-TM interacts with PcG proteins

Figure 30 Endogenous FoxO1 interacts with PcG proteins

Figure 31 FKHR-TM overexpression increases H3K27me3 levels on the TSS of *claudin-5*, *VE-PTP* and *vWf* genes

Figure 32 FoxO1 knockdown impairs Ezh2 binding to the TSS of *claudin-5*, *VE-PTP* and *vWf* genes

Figure 33 FKHR-TM and Suz12 cooperate in repressing *claudin-5* gene

Figure 34 β-catenin interacts with PcG proteins

Figure 35 β-catenin stabilises Ezh2 to the the TSS of *claudin-5*, *VE-PTP* and *vWf* genes

Figure 36 Ezh2 associates with VE-cadherin but not with N-cadherin *in vitro*

Figure 37 Ezh2 association with VE-cadherin probed with a different antibody (Millipore)

Figure 38 Ezh2 associates with VE-cadherin *in vivo*

Figure 39 Suz12 does not interact with VE-cadherin

Figure 40 Ezh2 interacts with VE-cadherin at the plasma membrane

Figure 41 β-catenin mediates Ezh2 binding to VE-cadherin

Figure 42 Ezh2/VE-cadherin association is reduced in both Δβcat and Δp120 ECs

Figure 43 Ezh2 interacts with p120 catenin

Figure 44 Δp120 ECs fail to upregulate *claudin-5*, *VE-PTP* and *vWf*

Figure 45 *Ezh2* transcript levels are reduced in VEC-positive ECs

Figure 46 *Hif1α* transcript and protein levels are reduced in VEC-positive ECs

Figure 47 pRb is hypophosphorylated in VEC-positive ECs

Figure 48 IHC analyses of EZH2 and Claudin-5 in normal and malignant ovarian tissue

DISCUSSION

Figure 49 Schematic representation of PcG-protein-dependent regulation of vascular stability genes in VEC-null ECs

Figure 50 Schematic representation of vascular stability gene activation in VEC-positive ECs

Figure 51 Proposed model for PcG-protein recruitment by FoxO1 (FKHR-TM) in VEC-positive ECs

ABSTRACT

In healthy tissues blood vessels undergo a process known as vascular stabilisation in order to tightly control vascular permeability and ensure an optimal perfusion of the tissue. Vascular stabilisation is accomplished through endothelial cell-cell contact formation, basement membrane deposition and mural cell recruitment. Conversely, tumor vessels lack vascular stability features leading to increased interstitial fluid pressure, reduced drug delivery and easier metastatic dissemination. Vascular Endothelial (VE)-cadherin plays a crucial role in adherens junction (AJ) formation between endothelial cells (ECs) and in the regulation of vascular permeability. Given this, we sought to determine in more details how VE-cadherin promotes the expression of vascular stability genes in ECs.

We found that the expression and clustering of VE-cadherin at AJs upregulates a subset of endothelial-specific genes encoding the tight junction protein claudin-5, Vascular Endothelial-Protein Tyrosine Phosphatase (VE-PTP) and von Willebrand factor (vWf). Most importantly, these genes are well-known for their key role in promoting vascular stabilisation. In the absence of VE-cadherin *claudin-5*, *VE-PTP* and *vWf* are repressed by the combined activity of the transcription factor Forkhead-box O1 (FoxO1), β-catenin and Polycomb Group (PcG) proteins, a family of epigenetic repressors of transcription. Here we show that FoxO1 and β-catenin interact with PcG proteins in ECs and that they work as PcG protein recruiters on *claudin-5*, *VE-PTP* and *vWf* promoters. Strikingly, we found also that VE-cadherin is able to sequester part of Enhancer of Zeste homolog 2 (Ezh2), a key PcG protein, out of the nucleus in a β-catenin- and p120-catenin-dependent manner. Preventing p120-dependent Ezh2 sequestration at the plasma membrane leads to the repression of *claudin-5*, *VE-PTP* and *vWf*, thus suggesting that the sequestered pool of Ezh2 is functionally relevant for gene expression. Since in human ovarian cancer EZH2 is often upregulated in tumor vessels, we took advantage of this condition to demonstrate that CLAUDIN-5 expression is strongly downregulated when EZH2 expression is increased.

This suggests that CLAUDIN-5 undergoes an epigenetic regulation exerted by PcG proteins *in vivo* as well. To conclude, our findings prove for the first time that AJ organisation can influence gene expression at the epigenetic level and provide new insights into the understanding of vascular stabilisation paving the way for developing new therapies for diseases characterized by vessel instability such as cancer.

INTRODUCTION

Development of the vascular system in mammals

Single cells and organisms as small as *Caenorhabditis elegans* and *Drosophila melanogaster* do not have a cardiocirculatory system because they rely on the simple process of diffusion of oxygen and nutrients through their different cellular compartments [1]. On the contrary, large multicellular organisms would not survive without a cardiocirculatory system able to convey oxygen and nutrients to all tissues. The cardiocirculatory system is composed of an organ, the heart, which drives the blood circulation, and a vascular tree of arteries, veins and capillaries that convey blood and fluids to all the districts of the body. In addition, the vascular system has other fundamental functions such as to discard waste products and provide a fast track for patrolling immune cells [1-3].

In mammals the formation of the vascular system takes place through two different sequential processes: vasculogenesis and angiogenesis [2, 4]. Vasculogenesis is defined as the *de novo* formation of blood vessels starting from mesodermal precursor cells or angioblasts that form clumps known as blood islands in the embryo (Figure 1). In mice this process takes place between embryonic day E6.5 and E9.5. Vasculogenesis starts at E6.5 in extrambryonic tissues and between E7 and E7.5 in intraembryonic tissues with the appearence of dispersed T-cell Acute lymphocitic Lymphocitic Leukaemia protein 1^+/Vascular Endothelial Growth Factor Receptor 2^+ (VEGFR-2 also known as Foetal liver kinase 1, Flk1) ($TAL1^+/Flk1^+$) angioblasts. Later on, $TAL1^+/Flk1^-$ progenitors residing inside the blood island differentiate into haematopoietic cells while more external $TAL1^+/Flk1^+$ cells become endothelial cells (ECs) [5]. Of note, the expression of these markers precedes the expression of well-established EC markers such as Platelet

Endothelial Cell Adhesion Molecule (PECAM), CD34, and VE-cadherin, which are detected only from E8 onwards. Subsequently, blood islands fuse together to create a network of blood vessels called primitive vascular plexus, needed to convey blood to the developing tissues once the heart starts to beat around E8.5. At this point, the primitive network of blood vessels must undergo a massive expansion and remodelling phase, a process referred to as angiogenesis. Angiogenesis, by definition, is the process of new vessel formation starting from pre-existing ones [2, 4, 6]. During the angiogenic phase, the primitive network of vessels must reshape into a highly organized and hierarchical structure composed of larger vessels ramifying into small ones. Vessels must also acquire a further specialized identity in term of arteries, veins, capillaries and lymphatics (Figure 1). Arteries cope with strong haemodynamic forces and consist of a layer of ECs surrounded by multiple layers of smooth muscle cells that provide contractility and structural support. Veins, conversely, support a lower blood pressure and therefore are enclosed in a thinner layer of smooth muscle cells. Capillaries are the structures where the exchange of gases and nutrients takes place. They present a very thin vessel wall associated with pericytes: perivascular cells able to provide a degree of contractility and which help regulate permeability. Lymphatic vessels, instead, are needed to drain interstitial fluids from the tissues in order to take them back into the venous circulation [1-3, 7].

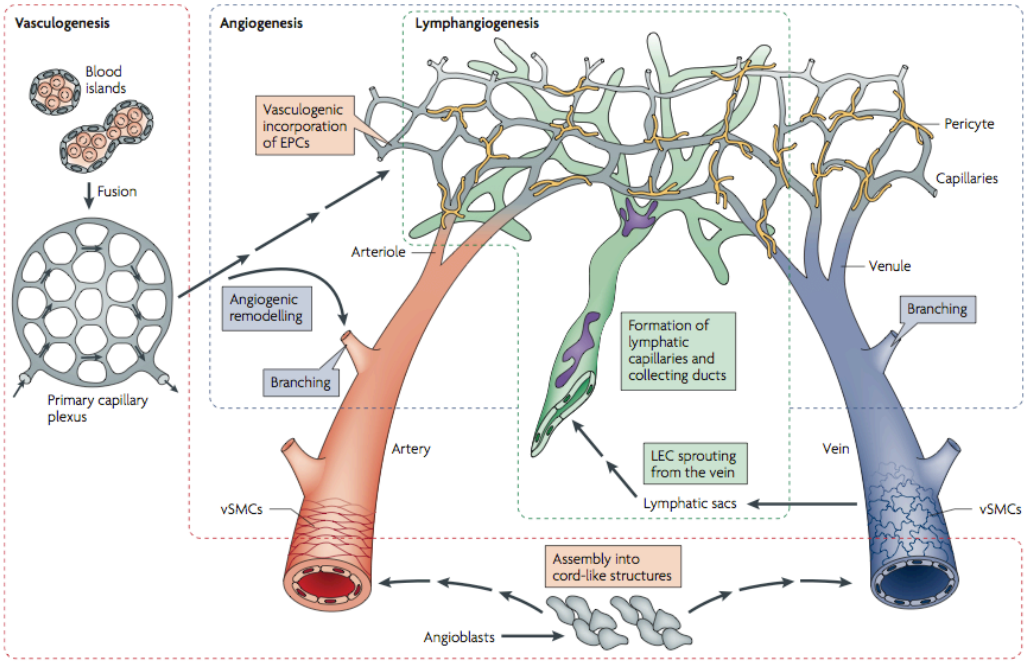

Figure 1 The development of the vascular network

During embryonic development endothelial precursor cells (angioblasts) form aggregates called blood islands that later on will fuse together to create cord-like structures and the primary capillary plexus. These events occur during the vasculogenesis phase. Once the heart starts beating the primitive plexus must undergo a remodelling phase that will provide the embryo with a hierarchical network of arteries, capillaries, veins and lymphatics [8].

Angiogenesis does not occur exclusively during embryo development but also during adult life in both physiological and pathological conditions. Regardless of the situation in which angiogenesis takes place, similar events are involved in the formation of new vessels. At the onset of sprouting, a stimulus (such as hypoxia) triggers the local production of proangiogenic molecules, such as Vascular Endothelial Growth Factors (VEGFs), which stimulate new vessel formation (Figure 2). First, ECs degrade the surrounding extracellular matrix by upregulating matrix metalloproteases (MMPs). These events are important both for allowing EC migration and for freeing pro/antiangiogenic molecules trapped inside the extracellular matrix, which finely regulate vessel sprouting.

Within the growing vessel, ECs undergo specification into tip and stalk cell depending on their position in the sprout. A tip cell is defined as the EC that drives sprout growth by probing the environment following, for instance, VEGF gradients, while stalk cells follow the tip cell, convey strength and support to the sprout and participate in lumen formation [3, 9, 10]. Among the numerous signalling pathways involved in tip and stalk cell specification, VEGFR and Notch pathways play a pivotal role. Tip cells respond to VEGF gradients via VEGFR2-mediated filopodia formation and upregulation of Delta Like 4 (DLL4), which in turn engages Notch1 receptors expressed by stalk cells (Figure 2). As a result, Notch1 receptor activation represses tip cell phenotype in stalk cells [3, 8]. Stalk cells produce fewer filopodia compared to tip cells and are more proliferative. Furthermore, they establish junctions with neighbouring cells and produce basement membrane components to ensure the stability of the sprout. It is worth to notice that tip and stalk cell identities are transient and that during sprout growth cell position might shuffle and tip/stalk roles can be redefined [9].

In order to expand the vessel network, ECs undergo iterative cycles of sprouting, branching and tubulogenesis. Stalk cells organize to form a hollow lumen that permits blood flow. At least two different mechanisms have been proposed for lumen formation: cell hollowing and cord hollowing (Figure 2). The former mechanism has been observed in intersomitic vessels and requires the coalescence of intracellular vacuoles, further connecting with vacuoles of neighbouring ECs, leading to lumen formation. Cord hollowing, instead, consists in endothelial cell-cell junction reorganization, definition of apical-basal polarity and secretion from the apical (luminal) membrane of negatively charged glycoproteins that facilitate the opening of the lumen via electrostatic repulsion. Eventually, the growth of the sprout ends when another sprout is reached, and once the contact between tip cells is established, VE-cadherin-containing junctions form and stabilise the connection [3, 11]. Recent studies in zebrafish embryo confirm the central role of VE-cadherin in regulating the early steps of vascular anastomosis [12]. To conclude, newly

formed vessels deliver oxygen and nutrients to the hypoxic tissue, thus counterbalacing the proangiogenic stimuli involved in starting the entire angiogenic process and shifting EC behaviour towards a quiescent phenotype [3].

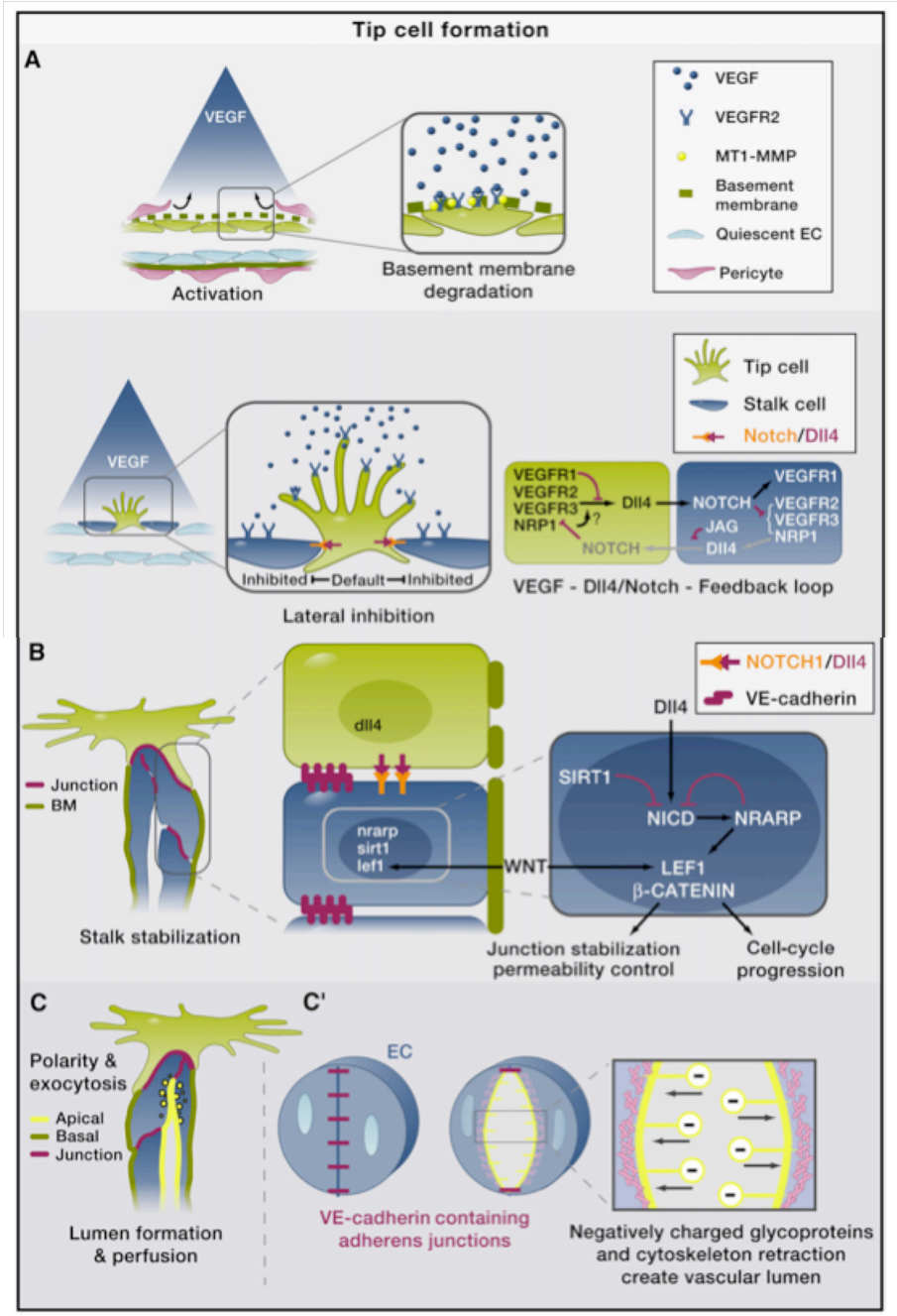

Figure 2 Angiogenic sprouting: tip cells, stalk cells and lumen formation

(**a**) In hypoxic conditions, VEGF gradients promote sprouting. Tip cells extend filopodia to follow VEGF gradients, upregulate Dll4 expression and lead the sprout. (**b**) Notch1 expressed on stalk cells binds Dll4 expressed on tip cells with the ensuing inhibition of VEGFR signalling and promotion of stalk cell

phenotype. (**c** and **c'**) Stalk cells form junctions with neighbouring cells and subsequently a new lumen is formed. Adapted from Potente *et al.* 2011.

Endothelial cell-cell junctions: adherens junctions and tight junctions

ECs are equipped with highly organized cell-cell junctions that are responsible for many of the characteristics of ECs. ECs possess two types of cell-cell junctions: adherens junctions (AJs) and tight junctions (TJs). Unlike epithelial cells, ECs lack desmosomes, and display AJs and TJs frequently intermingled along the cell border. Endothelial AJs are formed by cell adhesion molecules of the cadherin family (Figure 3). Two types of cadherins are expressed by ECs: VE-cadherin and Neuronal (N)-cadherin. VE-cadherin expression is strictly limited to ECs, while N-cadherin is not EC-specific and mediates EC interaction with pericytes [13, 14]. Both VE-cadherin and N-cadherin belong to the family of "classical" type I cadherins, made up of 5 extracellular domains located at the N-terminus, a transmembrane region and a cytoplasmic tail at the C-terminus serving as a binding platform for cadherin intracellular partners. Of note, cadherins engage Ca^{2+}-dependent homophylic *trans*-interactions by binding to identical cadherins expressed on neighbouring cells. In addition, cadherins are also able to cluster laterally in *cis* (homophylic *cis*-interactions) at cell-cell junctions forming a zipper-like structure along the cell border. The binding strength between two single classical cadherins is quite weak and transient [15, 16]. Therefore, many cadherin molecules need to cooperate to allow for an effective intercellular adhesion. It has been calculated that the number of cadherin molecules at AJs ranges between 700 and 1200 per μm^2 [14, 16]. In particular, the first two extracellular cadherin domains are reported to mediate homophylic interactions. More in detail, two contacting extracellular cadherin domains extend β-sheet arms which associate with hydrophobic grooves in their counterpart on the adjacent cell forming a "strand exchange

dimer" [16]. These properties enable cadherins to promote homophylic cell-cell adhesion, which exerts a key role in generating and maintaining tissue integrity during development. The adhesive properties of cadherins are also important for creating a physical separation of plasma membrane proteins in epithelial and endothelial cells, thus establishing apico-basal polarity [14, 17, 18].

Of note, VE-cadherin and N-cadherin expression is mutually regulated in ECs. In the absence of VE-cadherin, N-cadherin is expressed and localized at cell-cell contacts. However, upon VE-cadherin expression, N-cadherin is downregulated and excluded from cell-cell contacts. VE-cadherin/β-catenin association prevents β-catenin nuclear translocation and transcriptional activity, thus reducing the expression of N-cadherin which is a β-catenin transcriptional target [19].

Cadherin levels in ECs are not just important for adhesion *per se* but strongly influence EC behaviour. Indeed, both N-cadherin and VE-cadherin expression enhance EC proliferation and limit apoptosis. Together with preventing β-catenin nuclear translocation and transcriptional activity, the levels of N-cadherin and VE-cadherin correlate with the degree of activation of the phosphatidylinositol 3-kinase (PI3K)/AKT pathway that results in the phosphorylation and subsequent inactivation of the transcription factor FoxO1 (also known as Forkhead in rhabdomyosarcoma, FKHR), involved in cell growth inhibition and induction of apoptotic death [19].

The importance of VE-cadherin and N-cadherin in ECs is highlighted by the vascular phenotype displayed by mice lacking either of these two cadherins. Briefly, N-cadherin deletion in ECs results in developmental delay and in defective embryonic and yolk sac vasculature. At the ultrastructural level, ECs show signs of apoptosis [20]. Similarly, VE-cadherin-null mice die at E9.5 because of severe vascular defects. Interestingly, VE-cadherin deficiency does not affect angioblast differentiation to ECs and vasculogenesis in mutant embryos occurs normally. However, by E8.5 vascular defects start to be visible in VE-cadherin-null embryos with impairment of vascular lumen formation and

disconnection between ECs in the yolk sac. Vascular defects become even more severe beyond E8.75 when the primitive vascular network needs to undergo sprouting, angiogenesis and remodelling. At this point ECs throughout the vasculature become progressively disconnected from each other, showing gaps, losing contacts with the underlying basement membrane and displaying features of apoptotic cell death [21]. Beyond E9.25, vessels in VE-cadherin-null embryos regress and collapse causing circulatory insufficiency and extensive necrosis. This demonstrates that VE-cadherin expression is dispensable during vasculogenesis but it has a central role in the remodelling, expansion and maturation of the primitive vascular network. Of note, the majority of vascular defects in VE-cadherin-null mice occurs before the onset of blood flow, thus suggesting that the lack of VE-cadherin in ECs has profound consequences on EC intracellular signalling as well. The apoptotic cell death of ECs observed in VE-cadherin-null embryos is attributed to the disruption of a multiprotein complex composed of VE-cadherin, VEGFR2, β-catenin and PI3K which is required to respond to VEGF-A survival signal. VE-cadherin/VEGFR2 partnership is important not only during embryonic development but also in the adult organisms, in the regulation of EC quiescence (see below) [22, 23].

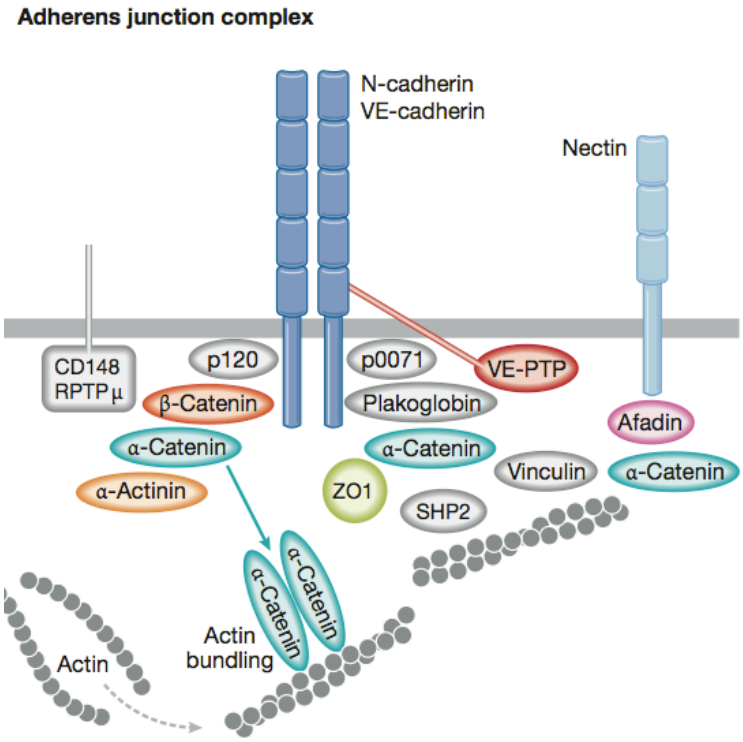

Figure 3 Schematic representation of endothelial AJs

Endothelial AJs are composed of proteins of the cadherin family such as VE-cadherin and N-cadherin. VE-cadherin mediates interaction between neighbouring ECs while N-cadherin mediates interaction between ECs and pericytes. Among the numerous cadherin intracellular partners p120, α-catenin, β-catenin and plakoglobin regulate cadherin stability at junctions, binding with actin cytoskeleton and intracellular signalling. Adapted from Nyqvist *et al.*, 2008.

Besides AJs, the other major component of endothelial cell-cell contacts are TJs (also called zonula occludens) (Figure 4). These are intercellular junctional complexes present in epithelial and endothelial cells which are able to physically seal the plasma membrane of two adjacent cells, regulating the passage of cells and solutes through the paracellular space [24]. While in epithelial cells TJs are the most apical components of the junctional complex, in ECs TJs are often intermingled with AJs along the cell cleft. TJs are multiprotein structures composed of transmembrane proteins such as claudins, occludin, Junctional Adhesion Molecules (JAMs) and membrane-associated proteins such as Zonula Occludens (ZO)-1, -2 and -3 and cingulin [25]. Claudins exert their main biological function

by sealing the membranes of neighbouring cells and are crucial determinants for the fine regulation of the paracellular permeability to ions and plasma proteins. They form a large family composed of 24 different members in human and mouse, some of which (i.e. claudin-1, claudin-3, claudin-5 and claudin-12) are expressed in ECs. Among these only claudin-5 shows an EC-restricted expression pattern [26-28]. Claudins are 21-28 kDa proteins and consist of four transmembrane domains, two extracellular loops, amino- and carboxy-terminal cytoplasmic domains and a short cytoplasmic turn. Most claudins contain the conserved aminoacid motif GLWxxC(8-10 aa)C in the first extracellular loop and a PDZ (Post synaptic density protein, Drosophila disc large tumor suppressor and Zonula occludens-1 protein) domain-binding motif at the carboxy terminus, which is needed for the association with PDZ-containing TJ proteins such as ZO-1, ZO-2 and ZO-3 [24]. Claudins expressed on the same plasma membrane laterally associate with each other to form the so-called TJ strands. TJ strands present on adjacent cells are further involved in homotypic interactions in order to form “paired” strands and seal the two membranes [29]. The distinct tightness properties of a given tissue seem to be largely dependent on the combination of the claudins composing such stands and on the manner in which they co-polimerize. A certain claudin family member may associate with identical molecules (homophilic interaction) or with other family members (heterophilic interaction) [30]. Overall, this suggests that TJ strands are usually composed of a "mosaic" of different claudins involved in homotypic and heterotypic interactions depending on the claudin expression pattern of the tissue [24, 30].

Besides claudins, other proteins are key components of TJs (Figure 4). Occludin, like claudins, is a four-pass transmembrane protein with both N-terminal and C-terminal cytoplasmic domains. The carboxy-terminal cytoplasmic region of occludin binds to other TJ-associated proteins such as ZO-1, ZO-2 and ZO-3. Occludin-deficient epithelial cells do not show any overt abnormality in the morphology and physiology of TJs and mice knockout for this protein are viable [24]. Tricellulin, instead, is the only known TJ protein

that concentrates at the conjunction between three cells. Tricellulin contains four transmembrane domains and a carboxy-terminal cytoplasmic domain that shares sequence similarity with occludin. Tricellulin knockdown in epithelial cells leads to alteration of tricellular TJs and epithelial barrier function [31, 32]. Other important TJ proteins such as ZOs do not contain any transmembrane region but present PDZ domains that enable them to interact with TJ-associated integral membrane proteins. ZO-1, ZO-2 and ZO-3 consist of three PDZ domains, a Src Homology (SH)3 domain and a guanylate kinase (GUK) domain. The first PDZ domain directly binds to the C-terminus of claudins [33]. Interestingly, it has been demonstrated that ZO-1 and ZO-2 are indispensable for TJ formation in epithelial cells. Umeda and coworkers generated epithelial cells simultaneously lacking the expression of ZO-1, ZO-2 and ZO-3 and noticed that these cells, despite showing a normal epithelial morphology and AJ protein expression and distribution, completely lack TJs. By re-expressing ZO-1 and/or ZO-2 in these cells the authors rescued claudin polymerization at TJs and identified the SH3/GUK domain of ZO-1 as an essential domain for this function [34, 35].

Epithelial and endothelial TJs also contain proteins of the JAM family. JAM proteins belong to the immunoglobulin (Ig) superfamily and have two extracellular N-terminal Ig-like domains, a transmembrane region and a short cytoplasmic tail harbouring a PDZ-binding domain. This latter is responsible for the interaction of JAMs with other TJ components such as ZO-1 and Afadin-6 (AF-6) [36-38]. The JAM family consists of 5 members, JAM-A, -B and -C being the most studied and JAM-4 and JAM-L the most obscure. Every JAM displays its own peculiar pattern of expression. JAM-A is reported to be the most widely expressed in endothelial and epithelial tissues of many organs and in platelets, erythrocytes and leukocytes. JAM-B, instead, is expressed exclusively by ECs while JAM-C is present both in ECs and leukocytes. Much less is known about the expression pattern of JAM-4 and JAM-L. Of note, also JAM proteins are engaged in both homophilic (i.e. with identical JAM molecules) and heterophilic (i.e. with different JAMs

or other unrelated proteins) interactions. JAM-A, JAM-B, JAM-C and JAM-L contain a putative dimerization loop in their N-terminal region and are able to localize at cell-cell contacts in close proximity with TJ strands. In addition to their role in promoting TJ formation in epithelial and endothelial cells, JAMs modulate other important processes such as leukocyte adhesion and transmigration through EC monolayers and platelet activation [36-38].

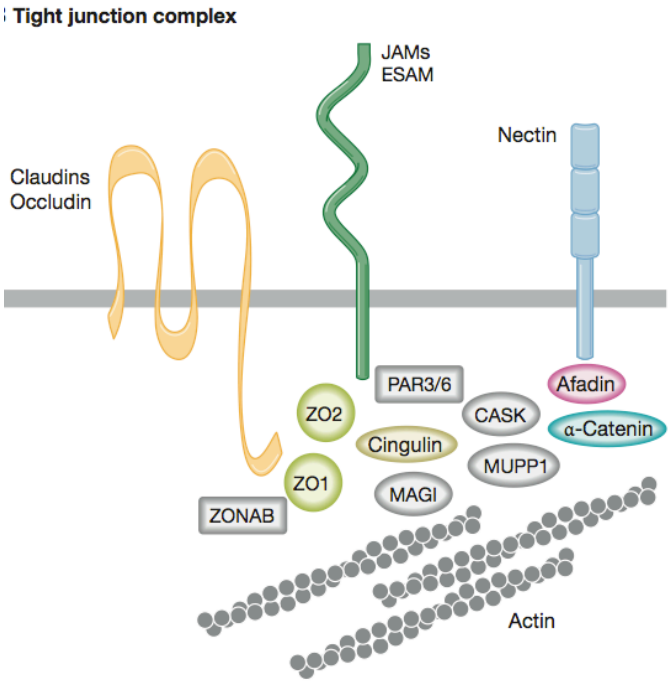

Figure 4 Schematic representation of endothelial TJs

Claudins play a central role in the formation of TJ strands between ECs. Other proteins such as JAMs, ZO-1, ZO-2 and cingulin take part in the formation of TJs. ZO-1 and ZO-2 bind to claudins cytoplasmic domain and are necessary for claudin polymerization at TJs. Adapted from Nyqvist *et al.*, 2008.

Intracellular signalling emanating from cell-cell junctions

Junctions between both epithelial and ECs have long been considered simply as adhesive structures. However, during the last decades it has been clearly demonstrated that a plethora of intracellular signalling pathways is modulated by cell-cell contacts. EC junctions exert two major roles: they maintain the integrity of the endothelium and they are able to convey intracellular signals which modulate key aspects of EC physiology such as cell growth, apoptosis, cell polarity and migration [13, 14, 39]. Indeed, intercellular contacts are now seen as signalling units that enable ECs to probe the surrounding environment and feel their neighbouring cells, thus regulating themselves according to such clues [13]. The final outcome of junction-triggered signalling pathways is often the regulation of the expression of specific target genes with profound consequences on cell behaviour or cell-cell junctions themselves: contact inhibition versus proliferation, remodelling of cell-cell contacts causing epithelial or endothelial to mesenchymal transition for instance. The functional link between cell-cell adhesion and the modulation of nuclear activity resides in the ability of several junctional proteins to translocate to the nucleus under certain conditions and to alter the transcriptional output of the cell.

Many different proteins are reported to interact with the cytoplasmic tail of cadherins in ECs. Among these intracellular partners, α-, β-, γ- and p120-catenin have been reported to exert fundamental roles in regulating cadherin behaviour. A key regulator of both cell-cell junction stability and gene transcription in ECs is β-catenin. Actually it has been reported that the binding of β-catenin to the cytoplasmic tail of classical cadherins starts in the endoplasmic reticulum and is required for the correct transport of cadherins through the biosynthetic pathway [16]. Furthermore β-catenin is a well-known transcriptional co-activator composed of 12 armadillo repeats that enable it to bind to multiple partners both at junctions and in the nucleus. In resting non-stimulated cells the steady state levels of β-

catenin are kept under control by the activity of the so-called β-catenin destruction complex composed of Adenomatous Polyposis Coli (APC), Casein Kinase 1 (CK1), Axin and Glycogen Synthase Kinase 3 β (GSK3β). This complex promotes N-terminal β-catenin phosphorylation, flagging it for beta-transducin repeat containing protein (βTrCP)-dependent ubiquitylation and proteasomal degradation. Upon the binding of the Wingless-related MMTV integration site (Wnt) ligand to Low-density lipoprotein receptor-related protein 5 (LRP5)/Frizzled 4 receptors, the β-catenin destruction complex falls apart, β-catenin accumulates inside the cell and can translocate into the nucleus via mechanisms that are still not well understood [40] (Figure 5). Once inside the nucleus, β-catenin binds to DNA-bound T-Cell Factor (TCF) transcription factors that recognize the nucleotide sequence AGATCAAAGG. In the absence of Wnt stimulation, TCFs bind the transcriptional repressor Groucho that keeps Wnt/β-catenin target genes in an "off" state. When Wnt ligands are present, nuclear β-catenin accumulates and displaces Groucho factors from TCFs, thus promoting Wnt/β-catenin target gene activation [40]. Other proteins associate to the TCF/β-catenin complex in order to drive gene expression. B-cell CLL/lymphoma 9 protein (Bcl9)/Legless and Pygopus, for instance, are key partner of the TCF/β-catenin complex in *Drosophila melanogaster* but knockout studies in mice suggest that they seem to be dispensable for Wnt/β-catenin target gene activation in mammals [40]. Other β-catenin nuclear partners that participate in gene activation are the histone acetyl transferase CREB-Binding Protein (CBP) and Brahma-related gene-1 (Brg-1) [40, 41] (Figure 5). Different cellular pools of β-catenin, characterized by different features, exist. While the half life of the signalling pool of β-catenin is in the order of minutes, the pool residing at AJs is considered to be highly stable and less dynamic [18, 40, 42, 43]. Moreover, binding of β-catenin to cadherins limits cell growth by preventing β-catenin-dependent transcription of two genes involved in cell cycle progression like *cyclin D1* and *Myc* [14]. Another way through which cadherins restrain cell proliferation is mediated by the induction of cell

cycle arrest in G1 phase by the dephosphorylation of Retinoblastoma protein (pRb) and the increase in cyclin-D1-dependent kinase inhibitor p27KIP1 levels [44].

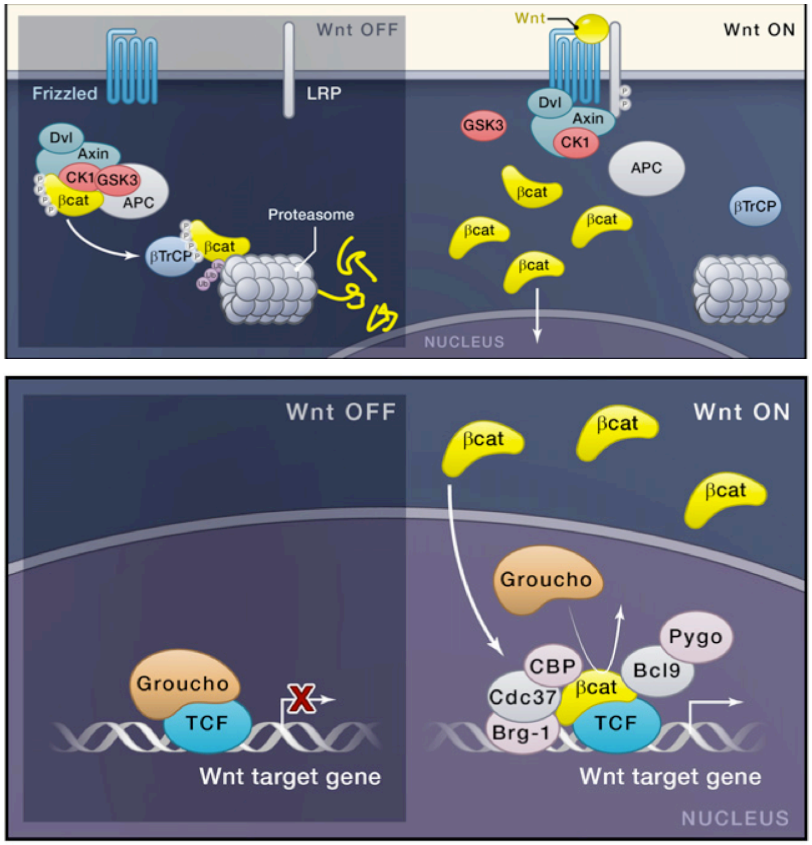

Figure 5 Schematic representation of the Wnt/β-catenin pathway

Top panel: in the absence of Wnt ligands β-catenin is degraded by the β-catenin destruction complex (left). Wnt stimulation promotes the disassembly of the β-catenin destruction complex, thus leading to β-catenin accumulation inside the cell (right). Lower panel: in the presence of Wnt, β-catenin accumulates in the nuclus and displaces the transcriptional repressor Groucho to promote the activation of Wnt-target genes. Adapted from Clevers and Nusse, 2010.

Like β-catenin, other proteins belonging to the catenin family, such as p120 and γ-catenin, have functions both at cell-cell contacts and in the nucleus. p120-catenin, for instance, binds the cytoplasmic tail of classical cadherins stabilizing them at cell-cell contacts by preventing their internalisation and recycling. In addition, p120-catenin has been reported to translocate to the nucleus where it displaces the transcriptional repressor

Kaiso from target gene promoters [18, 43]. γ-catenin (also known as plakoglobin) has been reported to localise both at cell-cell contacts and nuclei and to exert a role in the regulation of Wnt/β-catenin pathway. In addition, it has also been found that plakoglobin is insufficient *per se* for TCF-dependent transcriptional activation under Wnt-3a stimulation [43, 45].

ZO-1-associated nucleic acid binding protein (ZONAB) is a Y-box transcription factor that is reported to localize both at TJs and in the nucleus and to promote cell proliferation. ZONAB binds to the SH3 domain of ZO-1 and this interaction is required for sequestering ZONAB at the plasma membrane and restraining its nuclear localization, thus reducing cell proliferation. Interestingly, in Madin-Darby Canine Kidney MDCK cells ZO-1 and ZONAB expression are inversely regulated by cell density: ZO-1 expression rises with increasing culture density while ZONAB shows the opposite trend of regulation. Taken together, these data point to a role for these TJ proteins in contact-dependent inhibition of cell growth [43, 46].

Cell-cell junctions are able to influence cell cycle progression and intracellular signalling also because junctional components such as cadherins bind to growth factor receptors like VEGFR2. When ECs are confluent, they are considered to be in a quiescent state, however they are able to readily re-enter the cell cycle or begin to migrate in response to stimuli or when endothelial junctions are dismantled. In accordance with this, it has been demonstrated that when ECs are confluent, VE-cadherin clusters at AJs and forms a complex with VEGFR2, promoting its dephosphorylation by Density Enhanced Protein-1 (DEP1). These events lead to the inhibition of cell growth while promoting cell survival via AKT pathway activation. In sparse ECs, on the other hand, VE-cadherin/VEGFR2 association is reduced and VEGFR2 signals mainly to promote proliferation through the activation of the Extracellular-signal-Regulated Kinases/Mitogen-Activated Protein Kinase (ERK/MAPK) pathway.

The expression and clustering of VE-cadherin at endothelial cell-cell junctions is of central importance for mediating pro-survival signals in ECs. This is accomplished through the formation of a multiprotein complex composed of VE-cadherin/VEGFR-2/β-catenin/PI3K that, upon VEGF-A stimulation, promotes AKT activation and phosphorylation. Aside from VEGF-dependent activation in ECs, AKT can be activated also by VE-cadherin clustering at AJs, thus leading to the phosphorylation and inactivation of FoxO transcription factors [19, 21, 26, 47, 47] (Figure 6).

FoxO transcription factors are involved in the development, remodelling and maintenance of the vasculature. Three different FoxO proteins are expressed in ECs: FoxO1, FoxO3a and FoxO4. All these transcription factors are similarly regulated by the AKT pathway. FoxO1 is expressed at highest levels in ECs and it undergoes AKT-dependent phosphorylation on three residues: Thr 24, Ser 256 and Ser 319 [47, 48]. These phosphorylation events negatively regulate FoxO1 function by altering its capacity to bind the DNA and promoting its nuclear exclusion [47] (Figure 6).

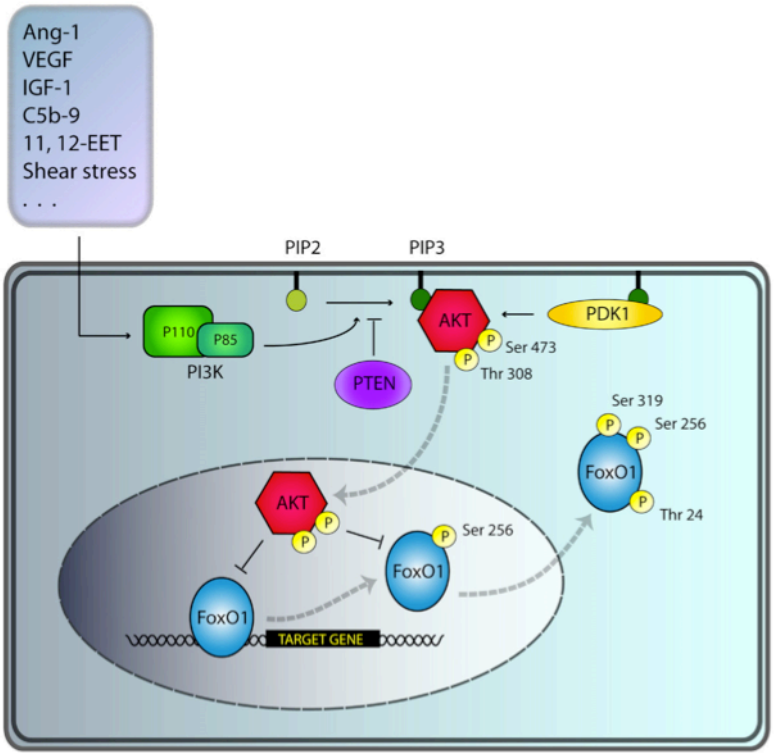

Figure 6 AKT-dependent regulation of FoxO1

Once activated by several stimuli, PI3K phosphorylates AKT on Ser 473 and Thr 308. Active (phosphorylated) AKT traslocates to the nucleus where it phosphorylates and inactivates FoxO1 transcription factor [47].

In line with its high expression in ECs, FoxO1 knockout mice show a vascular phenotype, while animals devoid of FoxO3a and FoxO4 display only a modest phenotype, if any [49]. More in detail, FoxO1$^{-/-}$ mice at E9.5 show severe vascular defects in both extraembryonic and embryonic tissues. Yolk sacs lack well-developed blood vessels, heart looping is retarded and there are major defects in the development of dorsal aorta, intersomitic vessels and of the vasculature of the head. All these defects are in line with the growth retardation shown by FoxO1$^{-/-}$ mice. Eventually these mice do not survive beyond E10.5. These findings are in agreement with the reported strong and widespread FoxO1 expression in the developing vasculature in the embryo and suggest that FoxO1 activity is dispensable for vasculogenesis while seems to be crucial for the subsequent steps of

angiogenesis and remodelling of the primitive vascular network. Furthermore, deregulated connexin 37, connexin 40 and Ephrin B2 expression, together with mild defects in VEGF response have been reported to occurr in FoxO1$^{-/-}$ ECs [50]. Interestingly, Potente et al. demonstrated an antiangiogenic role of FoxO1 in ECs *in vitro*. The authors showed that FoxO1 and FoxO3a overexpression in ECs strongly impairs EC tube formation and VEGF-mediated EC migration. Conversely, FoxO1 or FoxO3a knockdown results in an increase in EC sprouting assessed by spheroid assay. In addition, it has been shown that FoxO1 and FoxO3a regulate the expression of several important genes involved in angiogenesis and vascular remodelling. Briefly, upon FoxO1 knockdown endothelial Nitric Oxyde Synthase (eNOS), E-twenty six (ETS) domain protein Elk3 and the apoptosis inhibitor survivin are upregulated, while Angiopoietin-2 (Ang-2) is downregulated [51]. In agreement with these data, Daly and coworkers found that ECs treated with Angiopoietin-1 (Ang-1) undergo strong AKT activation with subsequent FoxO1 phosphorylation and inactivation. Conversely, FoxO1 overexpression led to a strong induction of genes linked to vascular remodelling, extracellular matrix reorganization and cell migration such as Ang-2, decorin, lumican, collagen type-3 and fibulin-5 [52]. Given the role of FoxO1 as an inhibitor of eNOS and as an activator of Ang-2, we can envision that FoxO1 is a transcription factor promoting vascular remodelling and vessel destabilisation [47, 51, 52].

The importance of vascular stabilisation

In order to fulfill the metabolic requirements of a given tissue, sprouting angiogenesis is only the first step of a much more complex process. Indeed, once new vessels are formed, they need to undergo a maturation or stabilisation phase in order to become fully competent and functional. Vascular maturation occurs both at the EC level through the

deposition of new basement membrane, the recruitment of mural cells, the reduction of EC proliferation and the sustained endothelial cell-cell junction formation but also, in a broader sense, at the network level. This means that new vessels must be organised into a hierarchically ordered network that is able to cope with the metabolic requirements of the perfused tissue [53, 54].

A fundamental feature of vessel maturation is the recruitment of mural cells (pericytes and smooth muscle cells). Pericytes are stellate-shaped cells that wrap the endothelium providing mechanical stability to capillaries. In addition, thanks to their position around endothelial cell-cell junctions, pericytes cover gaps between ECs and regulate barrier function [54]. Pericytes establish direct cell-cell contacts with ECs in capillaries and immature vessels via N-cadherin expressed on both ECs and pericytes themselves. Arteries and veins, instead, are covered by a layer of extracellular matrix and by vascular smooth muscle cells. Recruitment of mural cells is controlled by platelet-derived growth factor receptor β (PDGFR-β) signalling. Endothelial PDGF-B signals to PDGFR-β expressed by mural cells, stimulating their migration and proliferation. Inactivation of either *Pdgfb* or *Pdgfrb* induces pericyte deficiency, vascular dysfunction, micro aneurysm formation and bleeding [55, 56].

As already mentioned, the deposition and remodelling of the extracellular matrix and basal membrane surrounding blood vessels has an important role in regulating neoangiogenesis as well as vessel stabilisation [3, 6, 57]. It has been recently demonstrated that the proteolytic processing of extracellular matrix components can promote or inihibit angiogenesis in a context-dependent manner. For instance, MMP or plasmin activity can promote angiogenesis and EC migration by multiple mechanisms such as decreasing the stiffness and density of extracellular matrix and by releasing matrix-bound proangiogenic molecules such as VEGF and Fibroblast Growth Factor-2 (FGF-2). On the contrary, by cleaving extracellular matrix proteins, proteases can create proteolytic fragments that have anti-angiogenic properties. For example, endostatin, an anti-angiogenic factor, is generated

by proteolytic processing of collagen XVIII by elastase or other proteases [57, 58]. Many publications highlight also an important role for extracellular matrix proteins in vessel stabilisation. Of note, mice lacking fibronectin die during embryogenesis due to cardiovascular defects and alterations in vessel lumen formation and maintenance [57, 59, 60]. Furthermore, the genetic inactivation of collagen I, collagen III and fibrillin in mice leads to vascular stability defects and blood vessel rupture [61, 62].

Endothelial cell-cell junction formation and strengthening is another key aspect of vascular stabilisation. Intercellular contacts stabilise new vessel through different mechanisms. First, when ECs come into contact, new junctions are formed through homophilic interaction of cell adhesion molecules such as cadherins. Subsequently, AJ formation promotes the correct organization of TJs and ECs become fully competent for a precise control of vessel permeability [14, 26]. Moreover, as already discussed, cell-cell contact formation has a crucial role in limiting EC growth and apoptosis thus leading to the quiescent state of ECs observed in resting and stabilised vessels [14, 23].

In the adult organism, the turnover of ECs and extracellular matrix surrounding blood vessels is considered to be very low. In healthy conditions, ECs are in a quiescent state and the vasculature is stabilised. Angiogenesis in the adult is generally confined to pregnancy, menstrual cycle and wound healing processes [6, 55, 63]. In contrast, new blood vessel formation acquires a central importance in many pathological conditions such as chronic inflammation, stroke and cancer. As discussed in detail below, many aspects and features of blood vessels are altered during tumour angiogenesis. These anomalies are present in a wide range of solid tumour types both in mice and humans and can vary among different neoplastic tissues [6]. Tumour vessels are tortuous, follow a serpentine course, branch irregularly in a chaotic network of tangles (Figure 7). Inside the same tumour mass, vessels exhibit also a striking heterogeneity ranging from capillary-like to big, leaky, thin-walled, pericyte-depleted fenestrated sinusoids, or glomeruloid vessels and other vascular malformations [6, 63, 64]. Tumours have developed several different strategies to attract and

co-opt blood vessels in order to sustain their growth. New blood vessel sprouting from pre-existing ones is the most obvious way that tumour cell exploit to gain new vessels but increasing evidence in the literature suggests that other mechanisms could occur, at least in some kinds of tumours: 1) the recruitment of bone marrow-derived endothelial progenitor cells (EPCs) to newly forming vessels, 2) intussusception, defined as the splitting of a pre-existing vessel into two (also known as splitting angiogenesis), 3) vessel co-option, defined as the growth of cancer cells in close proximity to pre-existing vessels, 4) vascular mimicry, meaning that cancer cells get incorporated into the vessel wall, thus creating "mosaic vessels", 5) tumour stem cell to EC differentiation [6, 53, 63, 64]. In tumours, vessel diameters are often uneven given the different compression of tumour cells and stroma on the vessels in the different areas of the neoplastic mass. Most importantly, in contrast with normal vessels, which are lined by a monolayer of quiescent ECs and displaying a clear apical-basal polarity, tumour endothelial cells are often hyperactivated and display loose intercellular contacts. In this context ECs have an altered cell polarity, detach from the basement membrane and might eventually die, therefore creating an easy route for cancer cells to enter the circulation and cause peripheral metastases (Figure 7). ECs lining tumour vessels often undergo endothelial-to-mesenchymal transition and move away from their resident site, thus leaving behind empty sleeves of EC-devoid matrix channels (also known as string vessels). Pericyte abnormalities add up to EC defects in tumour vessels. In most cancers, vessels are poorly covered by pericytes, which are activated and loosely associated to ECs [54] (Figure 7). Because of the continuous remodelling occurring in tumour vessels, also the basement membrane is often altered and loosely associated to ECs. It is not uncommon to find vessels no longer surrounded by a basement membrane, very fragile and prone to rupture. Conversely, in some specific tumour contexts, vascular basement membrane could undergo opposite alterations. In hepatocellular carcinoma, for instance, tumour vessels deposit an ectopic basement membrane, not present in the healthy tissue [54, 64]. All these abnormalities profoundly alter vascular functionality. Indeed, tumour

blood flow is chaotic and even stagnant in several areas of the tumour mass. As tumour vessels are leaky, they cannot maintain pressure gradients across their walls. Normally, fluid pressure inside healthy vessels is higher than in the surrounding tissue. However, owing to the leakiness of tumour vessels, fluids and plasma proteins escape from the vessel lumen and accumulate in the interstitial space. These events result in an uncontrolled increase of the extravascular oncotic pressure dragging further liquid into the interstitium, thus raising even more the interstitial fluid pressure (IFP) and producing tissue swelling (oedema) [64]. These uneven flow patterns, together with the unnatural pressure gradient, not only create an obstacle to the transport of oxygen and nutrients, but also dramatically reduce the delivery of drugs to cancer cells and, consequently, their effectiveness [54]. The raised intratumoural IFP reduces the hydrostatic pressure gradient between the intravascular and extravascular compartments such that the two essentially equilibrate. In addition, the mechanical stress from the solid mass of proliferative cancer cells is able to collapse tumour vessels, closing their lumen through compressive forces.

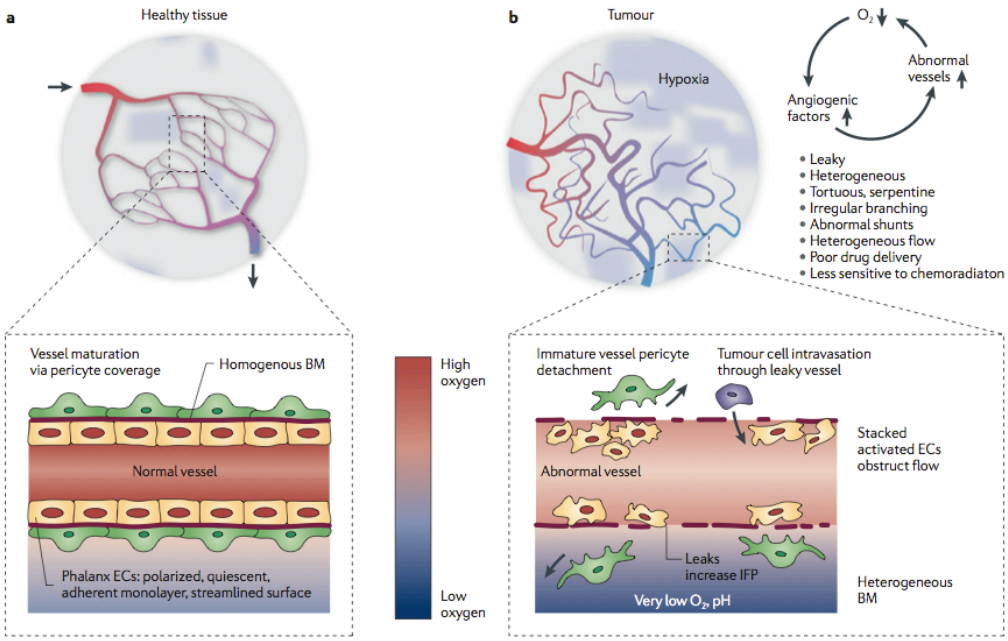

Figure 7 Tumour vessels are structurally and functionally abnormal

(**a**) In healthy tissues vessels display a hierarchical organization, are lined with a continuous monolayer of quiescent ECs and are covered by pericytes and by a homogeneous basement membrane (BM). In this way the vasculature ensures an optimal delivery of oxygen and nutrients.

(**b**) In tumors, vessels are leaky and tortuous. In this context, there are often gaps between ECs, basement membrane is discontinuous and pericytes are detached. These features lead to poor perfusion of the tumor mass with ensuing hypoxia, reduced drug delivery and oedema [54].

Rapidly growing tumour cells are in continuous demand for oxygen and nutrients. However, the non-productive form of angiogenesis which arises fails to meet the needs of the tumour mass. While in physiological conditions proangiogenic factors promote new vessel growth in a controlled manner and anti-angiogenic molecules tightly limit this process, in the tumour microenvironment proangiogenic molecules are produced in large excess by tumour and stromal cells. This profoundly unbalanced microenvironment is thought to be the cause of the discussed vascular abnormalities. Given the uneven blood flow and the suboptimal delivery of oxygen and nutrients inside the tumour mass, cancer cells often experience severe hypoxic conditions and acidosis that can alter their gene expression profile, making them more aggressive and more prone to metastasise [64].

In the last decade, research has been focusing on the identification of possible approaches to restore the imbalance between pro and antiangiogenic factors in tumours, aimed at inducing a reversion of tumour vessels from an altered towards a more normal phenotype, a process known as "vascular normalisation" [64]. Unlike antiangiogenic therapies, consisting in the destruction of tumour vasculature, vessel normalisation aims at the use of pharmacological and/or genetic approaches to revert the gross morphological and functional abnormalities of such vessels. Vascular normalisation might occur through different mechanisms such as increasing the homogeneity of vascular density, restoring vessel hierarchy within the tumour vascular bed and improving endothelial cell-cell junction organization and perivascular cell coverage in order to recover the control of vessel permeability [54, 63, 64]. Although tumour vessels may never become completely "normal", these changes would yield a more even distribution of blood flow with a subsequent reduction of tissue hypoxia and acidosis. This would also impede cancer cell metastatic behaviour and improve drug delivery.

Traditionally, given the widely recognized importance of VEGF in promoting tumour angiogenesis, many groups aimed at blocking VEGF signalling in order to dramatically reduce vessel growth with the ultimate goal of starving tumour cells. Among the numerous tools generated to block VEGF signalling it is worth to mention Bevacizumab, an anti-human VEGF antibody; Aflibercept (also known as VEGF-Trap) that binds VEGF-A, VEGF-B and Placental-derived Growth Factor (PlGF); DC101, an antibody recognizing VEGFR2; and several small molecules that inhibit VEGFR2 tyrosine kinase activity. Despite the promising results obtained in pre-clinical models, Bevacizumab as monotherapy failed to induce significant benefits to patients in several phase III clinical trials while it improves the progression-free survival and overall survival when given in combination with traditional chemotherapy [54, 64, 65]

Several studies have pointed out the existence of a "time window" in which the pharmacological induction of vascular normalisation is effective. Therefore, vascular

normalisation seems to be a transient phenomenon typically starting 1 or 2 days after the beginning of the therapy and followed by an eventual "closure" of the normalisation window, when features of normalisation are lost. This is due either to an excessive dose of the antiangiogenic drug or to the development of resistence via the activation of other proangiogenic pathways. Importantly, it has been shown that cancer cells are more vulnerable to cytotoxic therapies specifically during the normalisation window [6, 63, 64]. Taken together, these findings point out that we still need an in depth understanding of the mechanisms that govern vascular stabilisation. By exploiting these findings we will be able to design new therapies aimed at extending the so called "vascular normalisation window" to improve cancer treatment.

Claudin-5, VE-PTP and vWf: three vascular stability genes

Many different genes have been reported to have a role in vascular stabilisation but only some of them are expressed in an endothelial-restricted manner. Among these, we focused on *claudin-5*, Vascular Endothelial Protein Tyrosine Phosphatase, *VE-PTP* (also known as Protein Tyrosine Phosphatase Receptor Type B, *Ptprb*) and von Willebrand Factor (*vWf*), because, as extensively explored in the following chapter, they seemed, from previous observations, to be regulated in the same fashion. Remarkably these proteins, although exerting very different functions and showing different subcellular localizations, play an important role in the establishment of a stabilised vessel phenotype.

Claudin-5 is the only member of the claudin family of genes that shows an endothelial-restricted expression pattern. Evidence in the literature points to a crucial role for *claudin-5* in vascular stabilisation. VE-cadherin clustering at the plasma membrane has been shown

to upregulate *claudin-5* expression through the activation of the PI3K/AKT pathway leading to the phosphorylation and subsequent cytoplasmic relocalization of FoxO1 and to the inhibition of its transcriptional activity. When VE-cadherin is absent or not clustered at junctions, FoxO1 and β-catenin bind to *claudin-5* gene promoter inhibiting its expression. VE-cadherin clustering, through PI3K/AKT activation and the sequestration of β-catenin at the plasma membrane, relieves FoxO1/β-catenin-mediated inhibition of *claudin-5* transcription and promotes the correct organization of TJs and permeability control [26]. In addition, these data confirm that an interplay and a hierarchy exist between AJs and TJs. Indeed, other reports demonstrated that AJ formation precedes and promotes TJ formation and that interfering with AJ establishment leads to TJ impairment [14, 66]. Junctional maturation in ECs is of key importance for vessel stabilisation and is strictly required to create morphologically and functionally competent blood vessels [13, 53, 54]. The importance of *claudin-5* expression in ECs has been further demonstrated by the generation of *claudin-5* knockout mice. These mice show normal embryo development and are born alive but die within 10 hours after birth. Microscopic evaluation of brain vasculature at E9.5 and E18.5 shows no overt abnormalities, no signs of oedema or bleeding. Surprisingly, by electron microscopy it is still possible to appreciate TJs of normal appearance between brain ECs. However, brain vessels display a size-selective loosening in the absence of claudin-5. The authors report that the blood-brain barrier of *claudin-5*$^{-/-}$ mice is permeable to molecules weighing less than 800 Da, while bigger tracers are retained inside the vessels [67, 68].

VE-PTP is an endothelial-specific gene encoding a protein tyrosine phosphatase involved in the regulation of crucial players in vascular development and function such as VE-cadherin, angiopoietin receptor Tie2, VEGFR-2 and plakoglobin. Mouse VE-PTP protein is composed of 17 extracellular fibronectin type III-like repeats (FN3), one transmembrane domain and one intracellular phosphatase domain (PTP). The importance of *VE-PTP* in the establishment of a correct vascular network has been highlighted by the generation of *VE-PTP* knockout mice and zebrafish morphants. *VE-PTP*$^{-/-}$ mice die around

E10 most probably because of a plethora of severe vascular and cardiac defects. For instance, these mutants show yolk sacs without hierarchically organized vessels, often lack intersomitic vessels and display dilated pericardial cavity and incomplete turning of the heart. These vascular alterations suggest that *VE-PTP*$^{-/-}$ mice can not undergo a productive remodelling phase of the primitive vascular network, while the vasculogenesis phase seems to be unaffected [69, 70]. As expected, *VE-PTP* expression is restricted to blood vessels and in particular the highest expression levels are reported to be in arteries. Knockdown experiments in zebrafish using morpholino injection confirmed the findings obtained with *VE-PTP*$^{-/-}$ mice. Also in zebrafish *zve-ptp* shows a widespread expression in the developing vascular system of embryos and early larvae. Morpholinos blocking mRNA translation and splice-blocking morpholinos altering the extracellular domain of the protein, without affecting the intracellular catalytic domain, cause vascular fragility and other defects. These comprise intersomitic vessels with anomalous branching or truncations, blood stasis in the caudal region of the axial vein and in some cases leakage of blood out the vessel wall. Of note, all *zve-ptp* morphants show strong ultrastructural alterations of endothelial cell-cell junctions and an increase in the number of ECs extending filopodia [71]. VE-PTP is reported to interact and dephosphorylate angiopoietin receptor Tie2, thus modulating its activity [72, 73]. More in details, Winderlich et al. demonstrated that treatment of allantois explants or ECs with anti-VE-PTP antibodies leads to the specific dissociation of VE-PTP from Tie2, resulting in an increase of Tie2 phosphorylation that mimics Ang-1 stimulation. Interestingly, the authors found that upon Ang-1 stimulation Tie2 phosphorylation increases but at the same time Tie2 associates more with VE-PTP, establishing a negative feedback loop that controls Tie2 signalling. ECs either stimulated with Ang-1 or treated with anti-VE-PTP antibodies undergo an increase in their proliferation rate that is mediated by ERK1/2 and AKT pathway activation [73]. Saharinen and coworkers demonstrated that in confluent ECs Ang-1 stimulation leads to Tie2 translocation to cell-cell contacts where it binds VE-PTP and Tie1. In this context Tie2 preferentially signals through AKT which

phosphorylates and activates eNOS, thus leading to vascular stabilisation and reducing monolayer permeability [74]. VE-PTP has been also reported to interact with VE-cadherin and to reduce VEGFR2-dependent VE-cadherin phosphorylation, thus increasing VE-cadherin-mediated barrier integrity [75]. In agreement with these findings, Nottebaum et al. reported that VE-PTP interacts with VE-cadherin at cell-cell contacts and that VE-PTP expression levels increase with increasing EC confluence, along with its interaction with VE-cadherin. Treatment of ECs with siRNAs targeting VE-PTP causes a significant increase in EC permeability and neutrophil transendothelial transmigration [76]. Very recently it has been demonstrated that VE-PTP is also able to modulate VEGFR-2 activity in a Tie2-dependent manner. Consistently with its role in vascular stabilisation, the authors demonstrated that sprouts arising from *VE-PTP*$^{-/-}$ embryoid bodies show much less pericyte coverage compared to WT sprouts. Moreover, mutant sprouts display also altered apical/luminal polarity as assessed by the distribution of podocalyxin and moesin markers and strikingly *VE-PTP*$^{-/-}$ sprouts often do not contain any lumen. The authors propose a model through which Tie2 mediates the suppression of VEGFR-2 activity by promoting the formation of a multiprotein complex with VE-PTP in order to create functional blood vessels. This is of particular interest in pathological contexts where an excess of VEGF or a deregulated expression of VE-PTP could profoundly alter EC polarization and lead to the formation of poorly functional vessels [10]. All these results point to a stabilizing function for VE-PTP on blood vasculature.

VWf is a large multimeric glycoprotein with crucial roles in haemostasis, platelet aggregation and transportation of the pro-coagulant Factor VIII (FVIII). Recently this molecule has been involved in regulating angiogenesis and vessel stabilisation [77-79]. VWf is produced by ECs and megakaryocytes as a precursor (pro-vWf) consisting of 2813 aminoacids that include a 22 aminoacid signal peptide, a 741 aminoacid propeptide and a 2050 aminoacid mature vWf subunit. Pro-vWf needs to undergo a series of subsequent modifications along with its transport through the secretory pathway in order to give rise to

the mature vWf protein. In the endoplasmic reticulum pro-vWf undergoes dimerization via disulphide bond generation and N-linked glycosylation, then in the Golgi apparatus it is further processed with O-linked glycosylation and processing of the N-linked carbohydrate side-chains [77-79]. Eventually, in the trans-Golgi network pro-vWf is subjected to endoproteolytic cleavage and dimers are disulphide-linked in multimers. At this point, mature vWf protein can undergo either a constitutive secretion, meaning that the protein is released as soon as it is synthesized by the cell as dimers or small multimers, otherwise it can be stored in rod-shaped intracellular organelles called Weibel-Palade bodies in ECs and α-granules in megakaryocytes and platelets. Once vWf is stored in these intracellular organelles, it is secreted as high-molecular-weight multimers together with its propeptide in a tightly regulated manner following stimuli such as thrombin, histamine and mediators of inflammation such as Tumour Necrosis Factor-α (TNF-α), Interleukin-8 (IL-8) and IL-6. In circulating platelets only the regulated secretion occurs, so the vast majority of circulating vWf protein comes from ECs that release it both in the vessel lumen and in the subendothelial matrix. VWf protein harbours several functional domains that are important for its functions: A1 domain is required for vWf interaction with the platelet receptor glycoprotein GPIbα, A3 domain binds to collagen, C1 domain contains the RGD sequence recognized by the β3 integrins ($\alpha_{IIb}\beta3$ and $\alpha_v\beta3$) and the D'-D3 domains bind FVIII. Von Willebrand disease (VWD) is a bleeding disorder characterized by either a quantitative deficit in vWf production (type 1 and type 3 VWD) or by the production of dysfunctional vWf protein (type 2 VWD) [80]. Very interestingly, Starke et al. recently demonstrated an unprecedented role for vWf in restraining angiogenesis by inhibiting the function of several important molecules in ECs such as VEGFR2, Ang-2 and integrin $\alpha_v\beta3$, the most characterized endothelial receptor for vWf. The authors found that ECs taken from patients affected from von Willebrand disease or wild type (WT) ECs knockdown for vWf show an increase in tube formation and in VEGF-dependent EC migration. Moreover knockdown

of vWf results in the concomitant downregulation of $\alpha_v\beta3$ integrin both at the transcriptional level and via protein internalisation. Weibel-Palade bodies do not store only vWf but also other important regulators of angiogenesis and vessel stability such as Ang-2. Most importantly, vWf–knockdown ECs show increased levels of Ang-2 release compared to control cells. These data are of particular interest given that Ang-2 is a major player in vessel destabilisation and remodelling and it unravels an unprecedented role for vWf in promoting vessel stabilisation. In agreement with these findings, it has also been demonstrated that vWf-deficient mice show an increase in the vascular infiltration in subcutaneous Matrigel plugs compared to WT mice [81]. Altogether these observations clearly show vWf involvement in regulating the quiescent phenotype of stabilised vasculature.

Polycomb Group proteins and transcription regulation

Cells continuously adapt their transcriptional output depending on their needs and on the stimuli coming from the surrounding environment, both *in vitro* and *in vivo* in living organisms. Recently, it has been shown that genes encoding important developmental transcription factors are marked with specific histone modifications named "bivalent domains" that consist of broad regions harbouring both trimethylation of lysine 27 on histone H3 (H3K27me3), a well-established histone mark leading to gene repression, and trimethylation of lysine 4 on histone H3 (H3K4me3), a marker of active gene transcription [82]. In embryonic stem (ES) cells, the developmental genes marked by bivalent domains are usually expressed at low levels and these histone modifications are thought to be required for keeping these genes poised for activation and ready to be turned on when cells undergo differentiation. When this occurs, bivalent domains are resolved in either H3K27me3-rich

regions or H3K4me3-rich regions and this determines the activation status of the gene [82, 83].

Polycomb Group (PcG) and Trithorax Group (TrxG) proteins are the two families of epigenetic regulators of transcription that catalyse the H3K27me3 and the H3K4me3 histone marks, respectively. Both PcG and TrxG proteins were first described in *Drosophila melanogaster* as regulators of Homeobox (HOX) gene expression and body segmentation and are very well conserved from plants to vertebrates and mammals, thus suggesting their crucial role in the regulation of gene expression [86, 87, 102]. PcG proteins operate through two different Polycomb Repressive Complexes (PRC) made up of different subunits and harbouring different functions (Figure 8). Both PRC1 and PRC2 complexes have core subunits, *i.e.* molecules that are invariably present in the complex and accessory ones which bind the complex only in certain contexts. Not surprisingly, these accessory subunits seem to be involved in finely regulating the activities of PRC complexes and the way they are targeted to genomic loci [84-86]. Core subunits of the PRC1 complex are B lymphoma Mo-MLV Insertion region 1 (Bmi1), Really interesting new gene 1B (Ring1B), Polyhomeotic protein 1 (Phc1) and Chromobox protein homolog 4 (Cbx4). The PRC2 complex contains Enhancer of Zeste Homologue 2 (Ezh2), Suppressor of Zeste 12 (Suz12) and Embryonic Ectoderm Development (Eed) as core subunits. The principal function of the PRC2 complex is to catalyze H3K27 trimethylation, while PRC1 complex has the ability to ubiquitylate lysine 119 on histone H2A (H2AK119Ub1), another repressive histone mark [84, 86] (Figure 8). PRC complexes are classically thought to act sequentially on the chromatin. First, PRC2 complex is recruited to the target gene and deposits H3K27me3. Subsequently, PRC1 complex recognizes the H3K27me3 mark and deposits H2AK119Ub1 [86, 87]. Through this mechanism PcG proteins are believed to restrain RNA Polymerase II (RNA Pol II) initiation and elongation of transcription and to compact chromatin structure. However, a clear picture of how PcG proteins repress their target genes is still missing [87].

More in details, the PRC2 complex is able to perform the di-/tri methylation H3K27 thanks to its catalytically active subunit, Ezh2, which bears a Su(var)3-9, Enhancer of Zeste, Trithorax (SET) domain. Of note, Ezh2 protein *per se* is not functional and requires the association with at least Suz12 and Eed in order to work efficiently [88]. Suz12 is another crucial member of the PRC2 complex. In cells lacking Suz12, the PRC2 can not assemble and H3K27me3 levels are strongly impaired [89]. Eed subunit of PRC2 complex has the ability to recognize the H3K27me3 histone mark thanks to its donut-like β-propeller structure. This interaction boosts the activity of the PRC2 complex itself by targeting it where H3K27me3 is already present. This positive feedback loop helps to localize PRC2 activity only to certain regions of the chromatin and to maintain H3K27me3 levels during cell cycle progression [90, 91].

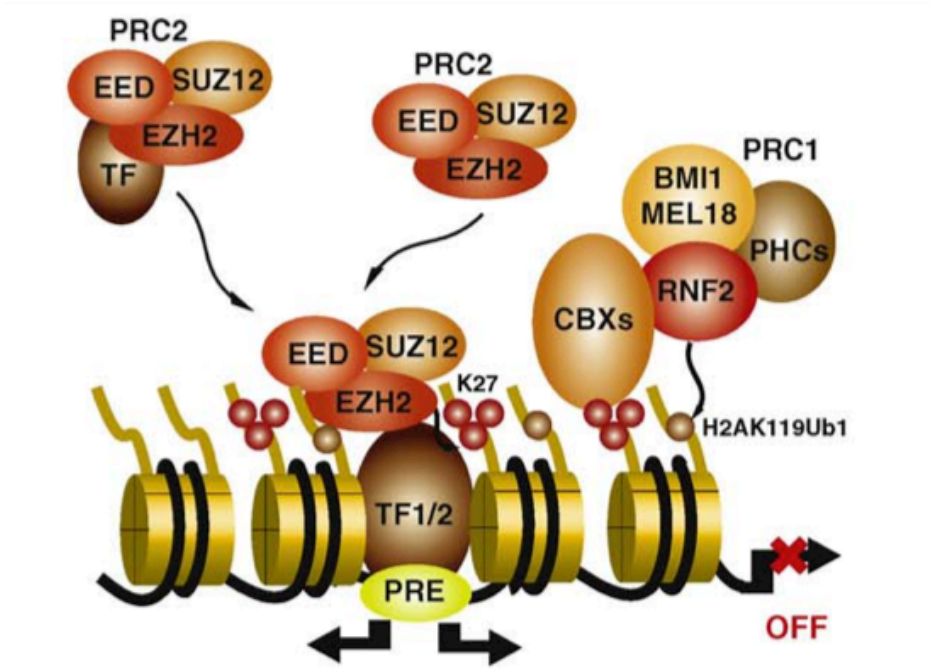

Figure 8 The coordinated activities of PRC1 and PRC2

PcG protein recruitment is still obscure. PRC binding to TFs may mediate cell type-specific PcG protein targeting to chromatin. Once bound to the DNA, PRC2 mediates the deposition of H3K27me3 repressive histone mark that can be recognized by Cbx-containing PRC1. Then, PRC1 deposits H2AK119Ub1 and the nearby gene is switched off. Adapted from Morey and Helin, 2010.

The activity of the PRC2 complex can be modulated by changing the core subunits composition, by the binding of accessory proteins and also by post-translational modifications. For instance, Ezh2 subunit in some instances can be interchanged with Ezh1 [92] and multiple Eed isoforms can take part to the formation of the complex [88]. In addition, recent publications demonstrated that several accessory subunits take part in the formation of the PRC2 complex and in modulating its activity and targeting to genomic loci. The Polycomb-like (Pcl) proteins are a family of cofactors that modulate PRC2 activity. Pcl proteins have been reported to stimulate the capacity of PRC2 complex to convert the K27me2 to K27me3 and to increase PRC2 levels at target chromatin sites [93, 94]. Another recently discovered PRC2 accessory protein is Jumonji- and AT-rich interaction domain (ARID)-domain-containing protein (Jarid)2, an enzymatically inactive member of the Jumonji (Jmj) family of histone demethylase that contains also a DNA-binding domain. Jarid2 binding to chromatin shows a significant overlap with Suz12 and H3K27me3 and Jarid2 knockdown strongly reduces PcG protein binding to target genes [95]. Moreover, local chromatin histone modifications related to active transcription, such as H3K4me3 and di- or tri-methylation of lysine 36 of histone H3 (H3K36me2/me3) can influence the activity of the PRC2 complex [96]. H3K4me3 is usually found near the promoter of the transcribed gene, while H3K36me2/me3 accumulate in gene bodies and towards the 3' end of the coding sequence [97]. Interestingly, it has been recently demonstrated that the presence of either H3K4me3 or H3K36me2/me3 inhibits PRC2 function *in cis* via allosteric modulation of the PRC2 complex that involves Suz12 subunit. These findings suggest that PRC2 complex modulates its own activity depending on the histone modifications which are already present in the genomic context [87, 96].

Recent publications suggest that PRC1 complex exists in forms containing or not Cbx proteins. The presence or absence of Cbx proteins influences PRC1 genome occupancy and function. Indeed, Cbx-containing PRC1 complex tends to colocalise with H3K27me3 while Cbx-lacking PRC1 complex does not require the interaction with H3K27me3 to bind

to chromatin [98, 99]. Taken together, these recent findings challenge the proposed dependence of PRC1 on PRC2 function for being targeted to chromatin.

One of the most active areas of research about PcG proteins deals with understanding how these are recruited to the target genes. In *Drosophila melanogaster* the existence of DNA sequences able to recruit PcG proteins to chromatin has been clearly demonstrated. These are called Polycomb Response Elements (PREs): clusters of DNA binding sites for known PcG protein-recruting factors. In mammals, instead, very little is known about PcG protein recruitment. Many proteins have been proposed as putative PcG-recruiters. Yin and Yang 1 (Yy1) was shown to modulate Ezh2 binding to the chromatin but chromatin immunoprecipitation-sequencing (ChIP-seq) data show only a limited overlap between PRC2 and Yy1 genome occupancy. Oct4 has also been proposed as a PcG recruiter given that its knockdown in ES cells reduces both PRC1 and PRC2 chromatin occupancy. Interestingly, 97% of PRC2 ChIP-seq peaks in ES cells overlap with CG-rich regions, thus pointing to a possible role for CpG islands in PcG proteins recruitment. The transcription factor Snail1 has been shown to bind PcG proteins and to target them to E-cadherin promoter in order to repress it. PRC2 component knockdown impairs Snail1 ability to repress E-cadherin expression [100]. Furthermore, long non coding RNAs (lncRNAs) have been shown to play a role in targeting PRCs to genomic loci [86].

PcG protein-mediated repression of transcription can be antagonized by TrxG proteins, which mediate the deposition of the H3K4me3 histone mark. TrxG proteins are a large family of transcriptional regulators that can be classified in three different categories: 1) SET-domain-containing proteins that trimethylate histone tails, 2) ATP-dependent chromatin-remodelling factors and 3) specific DNA-binding proteins and other TrxG proteins that are not included in the first two categories [101]. Mammalian cells contain six non-redundant COMPASS-like complexes that are able to trimethylate lysine 4 on histone H3. COMPASS-like complexes are further classified depending on their subunit composition: Set1A- and Set1B-containing complexes mediate the bulk of H3K4me3

methylation in mammalian cells; Mixed Lineage Leukemia 1 (Mll1)-containing complexes deposit H3K4me3 on a smaller subset of genes, including *Hox* genes; Mll3- and Mll4-containing complexes are involved in the activation of retinoic acid target genes. To conclude, even if we still miss the big picture, there is an increasing amount of data suggesting that the balance between PcG and TrxG proteins at a particular genomic locus is what determines the activation state of the target genes and is influenced by many different factor such as nucleosome positioning, the presence of activating or repressing histone marks, transcription of lncRNAs, the binding with basal transcription machinery and transcription factors [101, 102].

MATERIALS AND METHODS

Cell culture

The cell lines used in this study were:

- ECs derived from murine embryonic stem cells with homozygous null mutation of the VE-cadherin gene (VEC-null) [103]. The wild-type form of VE-cadherin was introduced in these cells (VEC-positive) using retrovirus-mediated transfer as described in detail by Lampugnani et al. [22];
- Δβcat cells, ECs expressing a truncated mutant of VE-cadherin (lacking residues 703-784 of human VE-cadherin) [104], which correspond to the β-catenin-binding region [22];
- IL2-VEC cells, ECs expressing a mutated version of VE-cadherin made up of the VE-cadherin cytoplasmic domain (aminoacids 621-784) fused to the extracellular and transmembrane domains of IL-2 receptor α-chain (from Andrew Kowalczyk, Emory University, Atlanta, GA) [105, 106];
- Δp120 cells, ECs expressing a truncated mutant of VE-cadherin (lacking residues 621–702 of human VE-cadherin), which corresponds to the p120-binding region [105, 107]
- β-catenin WT and β-catenin KO ECs were derived from lungs of adult β-catenin$^{flox/flox}$ mice and immortalized with as previously described [103] and infected with an adenovirus encoding GFP (control) or CRE recombinase to obtain β-catenin gene recombination (Monica Corada, unpublished data).

For all ECs of murine origin, culture medium was DMEM (GIBCO) with 20% North American (NA) fetal bovine serum (FBS) (HyClone), glutamine (2 mM; Sigma), penicillin/streptomycin (100 units/l; Sigma), sodium pyruvate (1 mM; Sigma), heparin

(100 μg/ml, from porcine intestinal mucosa; Sigma), and EC growth supplement (ECGS) (5 μg/ml, made in our lab from calf brain) (complete culture medium).

Starving medium was MCDB 131 (GIBCO) with 1% bovine serum albumin (BSA) (EuroClone), glutamine (2 mM), penicillin/streptomycin (100 units/l) and sodium pyruvate (1mM).

293T-Phoenix-Ecotropic packaging cells were provided by IFOM Cell Culture facility and cultured in DMEM medium supplemented with 10 % South American (SA) FBS (Hyclone), glutamine (2 mM) and sodium pyruvate (1 mM).

Low passage AD-HEK293 cell line (human embryonic kidney, American Type Culture Collection, Manassas, VA), used for adenoviral production, were provided by IFOM Cell Culture facility and grown in DMEM medium supplemented with 10% FBS NA, glutamine (4 mM), penicillin/streptomycin (100 units/l), and sodium pyruvate (1 mM).

All cells were cultured at 37°C in a humidified atmosphere with 5% CO_2.

Lentiviral and adenoviral preparations

The following lentiviral constructs were used:

- ΔN-βcatenin: encoding a stabilized mutant of β-catenin was obtained from C. Brancolini, University of Udine, Udine, Italy.
- lentiviruses used to express a stable short hairpin RNA against Suz12 (shSuz12), for the overexpression of Suz12 and the respective control vectors were a kind gift of Diego Pasini, IEO, Milan.

Packaging plasmids were kindly donated by L. Naldini (HSR-TIGET, San Raffaele Telethon Institute for Gene Therapy, Milan, Italy). Lentiviral vectors were produced as described by Dull et al. [108]. Briefly, on day 1 293T-Phoenix-Ecotropic packaging cells were transfected with the viral genome using calcium phosphate and incubated overnight

with the transfection mix. On day 2 the medium containing the transfection mix was removed and 293T-Phoenix-Ecotropic cells were grown in as little medium as possible to concentrate the virus. On day 3 the medium containing the virus was removed, passed through a 0,45 μm diameter filter, supplemented with Polybrene (8 ug/ml, from IFOM Cell Culture facility) and placed on cells to be infected. The same procedure was repeated on day 4. shSuz12- and shEmpty-infected cells were selected with hygromycin 300 ug/ml. Cells were kept under selection until control non-infected cells died. Suz12-overexpressing cells and their Empty control were selected with Puromycin 3 ug/ml. Cells were kept under selection until control non-infected cells died.

The FKHR-TM adenovirus has been previously described [52]. The TCF4-DN adenovirus was kindly donated by S. J. George (Bristol Heart Institute, Bristol, UK) [109]. Infectious viruses were purified and titered using standard techniques. Briefly, for adenovirus production AD-293T cells were infected with 2 pfu/cell in DMEM without serum for 1 h at 37°C. Then, the infection medium was removed and cells were grown in an appropriate volume of DMEM + 5% horse serum until complete cell lysis is obtained (usually 72h later). The medium containing the viruses was then subjected to 3 freeze-and-thaw cycles in order to destroy all the cells and to set as many virions as possible free. The resulting supernatant was then centrifuged at 3000 rpm for 30 min at +4°C to eliminate the cellular debris, aliquoted and stored at -80°C. For the infection of ECs two consecutive cycles of infection [5 h and overnight (O/N)] were performed with MOI of 300 in 1 ml of complete culture medium.

Immunofluorescence microscopy

Immunofluorescence microscopy staining was performed using standard technique, as previously described [107]. Briefly, cells were seeded on 0,5% cross-linked gelatin. Cells

were fixed and permeabilized in methanol at -20°C for 5 min. Fixed cells were incubated for 30 min in a blocking solution (PBS, phosphate buffer saline, containing Ca^{2+} and Mg^{2+}, +/+, 2.5% skim-milk, 0.3% TritonX-100). Cells were then incubated for 1 h at RT with primary antibodies diluted in blocking buffer. Appropriate secondary antibodies were applied on cells for 45 min at RT and mounted with VECTASHIELD with DAPI (Vector Biolabs).

Samples were observed under an epifluorescence microscope (DMR; Leica) using a 63X objective. Images were captured using a charge-coupled camera and processed with Adobe Photoshop. Only adjustments of brightness and contrast were used in the preparation of the figures. For comparison purposes, different sample images of the same antigen were acquired under constant acquisition settings.

Western blot analysis

Total proteins were extracted by solubilising cells in boiling Laemmli buffer [2.5% SDS and 0.125 M Tris-HCl (pH 6.8)]. Lysates were incubated for 5 min at 100°C to allow protein denaturation and then spinned for 5 min at 13200 rpm to discard cell debris. The supernatants were collected and the concentration of protein was determined using a BCA™ Protein Assay Kit (Pierce) according to manufacturer's instructions. Equal amounts of proteins were loaded on gel and separated by SDS-PAGE, transferred to a Protran Nitrocellulose Hybridization Transfer Membrane 0.2 µm pore size (Whatman) and blocked for 1 h at RT in 1X Tris Buffered Saline Tween (TBST) [150 mM NaCl, 10 mM Tris-HCl (pH 7.4), and 0.05% Tween] containing 5% (w/v) powdered milk. The membranes were incubated overnight at 4°C or 1 h at RT with primary antibodies diluted in 1X TBST-5% BSA. Next, membranes were rinsed 3 times with 1X TBST for 5 min each and incubated for 1 h at RT with HRP-linked secondary antibodies (diluted in 1X

TBST-5% BSA). Membranes were rinsed 3 times with TBST for 5 min each and specific binding was detected by the enhanced chemiluminescence (ECL) system (Amersham Biosciences) using HyperfilmTM (Amersham Biosciences) or the ChemiDoc gel imaging system (BIORAD). The molecular masses of proteins were estimated relatively to the electrophoretic mobility of co-transferred prestained protein marker, Broad Range (Cell Signalling Technology).

Co-immunoprecipitation

Cells were grown until confluent and starved overnight. Cells were then washed once with DMEM without serum and incubated with 0,4 mg/ml of dithiobis(succinimidyl)propionate (DSP) (Pierce) for 30 min at 37°C. After several washes with ice-cold PBS, cells were lysed in ice-cold modified RadioImmunoPrecipitation Assay (RIPA) buffer (Tris HCl pH 7.5 100 mM, NaCl 150 mM, Deoxycholic acid 1%, SDS 0,1%, $CaCl_2$ 2 mM). The protein lysate was precleared with an appropriate volume of Protein G Sepharose 4B (Zymed) for 3 h at +4°C. Then, protein concentration was determined with BCA™ Protein Assay Kit and an equal amount of protein was incubated with either immune antibodies or species-matched control antibodies overnight at +4°C. On the following day immunocomplexes were collected using Protein G Sepharose 4B for 3 h at +4°C. Beads were then washed several times with modified RIPA buffer and boiled in an appropriate volume of Laemmli buffer. Samples were analysed by standard Western blot analysis as described above [107].
CoIP following biotinylation of membrane proteins was performed using the same protocol as above. Before cell lysis with modified RIPA buffer cells were incubated with Sulfo-NHS-LC-Biotin (Pierce ThermoScientific) 0,55 mg/ml in PBS +/+ pH 8.0 for 30 min at +4°C. After biotinylation cells were washed with PBS +/+ pH 8.0 + Glycine 100 mM to quench the reaction.

CoIP from lung tissue: lungs from adult age-matched mice were lysed in ice-cold modified JS buffer (Hepes pH 7.5 72 mM, NaCl 210 mM, glycerol 0,5 %, Triton X-100 1%, $MgCl_2$ 2 mM, EGTA 7.2 mM, SDS 0,1 %, Sodium Orthovanadate 300 μM, Pefabloc SC 1 mM [Sigma] and Sodium Fluoride 1 mM) using Tissue Lyser II (Quiagen) (two 30-sec pulses at maximum frequency). Samples were precleared for 4 h at +4°C with an appropriate volume of Protein G Sepharose 4B. Then, protein concentration was determined with BCA™ Protein Assay Kit and an equal amount of protein was incubated with Protein G Sepharose 4B pre-coupled with either immune antibodies or species-matched control antibodies overnight at +4°C. The day after, beads were then washed with modified JS buffer and boiled in an appropriate volume of Laemmli buffer. Samples were analysed by standard Western blot analysis [107]. All the buffers contained freshly added protease inhibitor cocktail (IFOM Kitchen Facility).

Quantitative Real Time-Polymerase Chain Reaction (qRT-PCR) analysis

Total RNA was isolated by RNeasy kit (QIAGEN) and 1 μg was reverse transcribed with random hexamers (High Capacity cDNA Archive Kit, Applied Biosystems) according to the manufacturer's instructions. cDNA (5 ng) was amplified in triplicate in a reaction volume of 15 μl using TaqMan Gene Expression Assay (Applied Biosystems) and an ABI/Prism 7900 HT thermocycler, using a pre-PCR step of 10 min at 95°C, followed by 40 cycles of 15 sec at 95°C and 60 sec at 60°C. Preparations of RNA template without reverse transcriptase were used as negative controls. For any sample the expression level, normalized to the housekeeping gene 18S, glyceraldehyde-3-phosphate dehydrogenase (GAPDH) or β2-microglobulin, was determined using the comparative threshold cycle (CT) method as previously described [110].

Transcription factor binding site analysis

In order to identify FoxO1 and Tcf/β-catenin consensus sequences on the putative *claudin-5*, *VE-PTP* and *vWf* promoter region we used the program MatInspector [111], which identifies transcription factor binding sites (TFBS) in nucleotide sequences using a large library of weight matrices. We analyzed the sequence spanning from 6000 bp upstream and 500 bp downstream the coding sequence (CDS) of the genes and obtained a prediction of a potential combination of TFBS. The TFBS sequences considered in the analysis were [AG][GA][TG][AC]AACAA[AC] for FoxO1 binding and [TAG][GT][AG][CT][AT]x(2)CAAAG[GCT][GAC][AC][GCA] for Tcf/β-catenin binding. Apart from *VE-PTP* promoter which has not been characterized yet, *claudin-5* and *vWf* promoters have been at least in part investigated in previous works [112-114] . Burek et al. studied the 1000 bp residing 5' to murine *claudin-5* transcription start site (TSS) and found six glucocorticoid-response elements (GREs), two NFkB sites, three Sp1, one Sp2, one Ap2 and three E-boxes [114]. Taddei et al. investigated a larger portion of the regulatory regions flanking murine *claudin-5* gene spanning from 6000 bp upstream to 500 bp downstream and found three clusters of predicted binding sites for FoxO1 and β-catenin. Among these regions, the one located most at 5' was found to be bound by both FoxO1 and β-catenin, while the 3' most region was bound only by β-catenin [26]. In another report, human *CLDN5* gene was found to contain a SOX-18 between -183 and -167 bp and four ETS consensus sites between -165 and -74 bp relative to the TSS of the gene. The authors show the importance of Sox18 for the proper expression of claudin-5 in confluent ECs [112]. Since its cloning in 1987 [115], *vWf* promoter has been extensively studied and, like in the case of *claudin-5*, many different TFs seem to participate to drive proper vWf expression in the vasculature. Murine *vWf* promoter contains a conserved GATA-binding site at -80 bp and an ETS-binding site at -60 bp relative to its TSS [116]. Interestingly, while the 110 bp downstream the TSS of murine *vWf* promoter have enhancing activity when cloned

upstream of Luciferase reporter gene, the regions that are located 5' to *vWf* TSS have repressive activity [116].

Chromatin immunoprecipitation

Chromatin immunoprecipitation (ChIP) assays were carried out as previously described [117]. Briefly, cells were starved overnight and cross-linked with 1% PFA for 10 min at RT. PFA was then inactivated by the addition of 125 mM glycine for 5 min at RT. Cells were then washed twice with ice-cold PBS and resuspended in ice-cold SDS buffer (NaCl 100 mM, Tris HCl pH 8,1 50 mM, EDTA 5mM, NaN3 0,2%, SDS 0,5%). The lysate was then centrifuged at 1300 rpm for 5 min at +4°C and the pellet was resuspended in IP buffer (1 vol of SDS Buffer + 0,5 vol of Triton Dilution Buffer [NaCl 100 mM, Tris HCl pH 8,6 100 mM, EDTA 5 mM, NaN3 0,2%, Triton X-100 5%]). Samples were sonicated with a BIORUPTOR^{TM} 200 using the following conditions: H power, 30 sec ON-60 sec OFF for 20 min. To check the size of the sonicated chromatin, an aliquot is taken and digested with Proteinase K 1 ug/ul for 30 min at 55°C and incubated at 65°C for 3h to revert the cross-linking. The samples are then purified using the QIAquick Gel extraction Kit (QIAGEN) and loaded on 1% agarose gel (Figure 9).

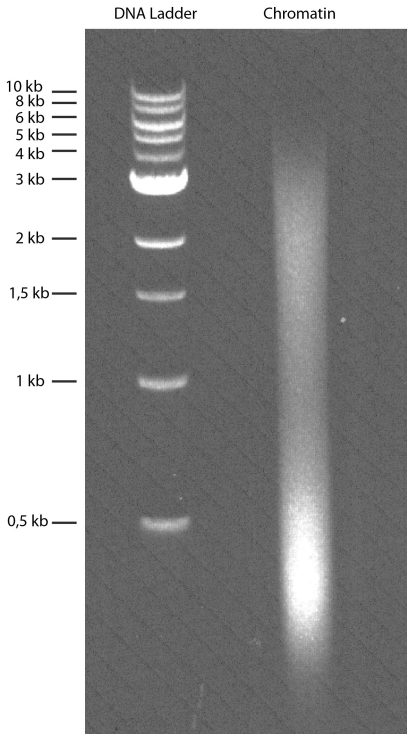

Figure 9 An aliquot of fragmented chromatin from ECs run on a 1% agarose gel

Chromatin extracts containing from 200 µg to 1000 µg of DNA with an average size of 500 bp were incubated overnight at +4°C with 5 µg of either immune antibody or matched non-immune antibodies and Dynabeads protein G (Invitrogen) or Ultralink resin protein A/G (Pierce ThermoScientific). On the following day, beads were recovered and washed twice with Mixed Micelle Wash Buffer (NaCl 150 mM, TrisHCl pH 8.1 20 mM, EDTA 5 mM, Sucrose 5,2 % w/v, NaN_3 0,02%, Triton X-100 1%, 0,2 % SDS), 500 Buffer (Deoxycholic acid 0,1% w/v, NaCl 500 mM, HEPES pH 7.5 25 mM, EDTA 1 mM, NaN_3 0,02%, Triton X-100 1%), LiCl Detergent wash Buffer (Deoxycholic acid 0,5% w/v, LiCl 250 mM, EDTA 1 mM, NP-40 0,5% v/v, NaN_3 0,02%, Tris HCl pH 8.0 10 mM). Proteins/DNA complexes were detached from beads by heating the samples at 65°C for 10 min. De-crosslinking was performed at 65°C overnight. DNA was purified using phenol/chloroform and precipitated in 70% ethanol according to standard protocol. DNA was amplified by qRT-PCR techniques using oligonucleotides flanking the assayed

promoter regions. Every couple of primers was tested in advance to avoid "auto-amplification" due to self-complementarity.

For qRT-PCR analyses DNA was diluted in the presence of specific primers (0.4 μM each) to a final volume of 25 μl in SYBR Green Reaction Mix (Perkin Elmer).

qRT-PCR curves were converted in Ct values using S.D.S 2.2.1 and further analyzed as follows. For each region the mean of the Cts of the inputs was calculated and subtracted to the Ct values of the immune samples (ΔCt). Then, the % of enrichment of input for the immune samples was obtained as 2^-ΔCt and multiplied by the % of input taken during the experiment. The same was performed for the non-immune (IgG control) samples and the non-immune values were subtracted from the immune samples to eliminate unspecific signal. In order to pool together ChIP experiments to perform statistical analysis, each technical replicate of at least 2 biological replicates was normalized to the average of the replicates of the respective reference condition (usually VEC-null cells). In this way the reference condition was set to 1 and the other experimental conditions were represented as fold change of the signal of the reference condition. Means were compared by Student's t-test and significance was set at 0.05.

List of primers used for ChIP experiments

GTCGGGTGAGCATTCAGTCT	Claudin-5 TSS Fw
ATCAAGCCCACCCATCCTAC	Claudin-5 TSS Rv
TGCAGAAGGAGAAAACAATGC	VE-PTP Reg 1 Fw
GCAGCAACGTGTGTCAGTGT	VE-PTP Reg 1 Rv
TGGATCCTGTAGCCATATTTGA	VE-PTP Reg 2 Fw
CATCATATAACTGCAACAAAGCAC	VE-PTP Reg 2 Rv
GACATAAGTAGCCAAGAACAGGTTT	VE-PTP Reg 3 Fw
TCAAATCACTAGGAGGAATAAGACA	VE-PTP Reg 3 Rv
GCTCAACAAGTGGTACCCAGA	VE-PTP TSS Fw
TGCACGACGCTCAGTGTTAT	VE-PTP TSS Rv
GTTTGTTTGAGCCAGGGTCT	vWf Reg 1 Fw
CAGGAGGTCGAAGCAAGATG	vWf Reg 1 Rv
GCAGGTCTTGGGTTCTATGC	vWf Reg 2 Fw
GGGGTGGAAATGATGGTTC	vWf Reg 2 Rv
TGGTGGCAACTTGGAGCTAT	vWf Reg 3/TSS Fw
AGGGGCTTCAAAGTCCTCAG	vWf Reg 3/TSS Rv

RNA interference

Stealth RNAi Duplexes (Life Technologies) and the correspondent Low GC Stealth RNAi Control Duplexes (Life Technologies) were used to knockdown FoxO1. The sequences of the two siRNAs used were the following: 5'-CCAAGUGACUUGGAUGGCAUGUUUA-3' and 5'-CAGACACUUCAGGACAGCAAAUCAA-3'. Transfection was performed using LipofectAMINE 2000 (Invitrogen) according to the manufacturer's instructions.

Immunohistochemistry (IHC)

Paraffin-embedded human ovarian tissue samples were kindly provided by Ugo Cavallaro (European Instiute of Oncology, IEO, Milan) and scored as pathologic or non-pathologic by a trained pathologist. Samples were de-paraffinized and hydrated as follows: Histolemon (Carlo Erba) 3 min, Ethanol (EtOH) 100% 3 min, EtOH 95% 3 min, EtOH 80% 3 min, H2O 5 min. Samples underwent antigen unmasking in Sodium Citrate Buffer pH 6 for 45 min at 95°C and allowed to recover for 30 min at room temperature. Endogenous peroxydase activity was inhibited with H_2O_2 3% for 10 min and then washed with PBS. Slices were blocked in Preincubation Buffer (PBS containing FBS 1% and BSA 0,6%) for 90 min at room temperature. Samples were incubated with primary antibodies diluted in Preincubation Buffer overnight at +4°C. Then, samples were washed several times with PBS and incubated for 20 min with MATCH 2 Double Stain 2 Kit (Biocare) containing anti-mouse HRP-conjugated and anti-rabbit alkaline phosphatase-conjugated secondary antibodies. Incubation with Vulcan Red and DAB were done subsequently for 15 and 5 min, respectively. After several washes with H_2O, haematoxylin/eosin staining was performed according to standard protocol and samples were mounted in Eukitt (Bio-

Optica). Samples were then imaged under a transmission light microscope at the indicated magnification.

Antibodies and chemicals

Antibodies used in this study were: anti-claudin-5 mouse monoclonal clone 4C3C2, anti-V5 tag mouse monoclonal R960-25 (Life Technologies); anti-claudin-5 rabbit polyclonal ab-53765, anti-total histone H3 ab1791 and anti-H3K4me3 RNA pol II phospho ser 5 ab8580 (ABCAM); anti-β-catenin mouse monoclonal 610154, anti-Ezh2 mouse monoclonal 612666, anti-N-cadherin mouse monoclonal 610921, anti-pRB mouse monoclonal 554136, anti-p120 mouse monoclonal 610133 (BD Biosciences); anti-β-catenin rabbit polyclonal 06-734, anti-Ezh2 rabbit polyclonal 07-689, anti-H3K27me3 07-449, anti-TCF4 mouse monoclonal clone 6H5-3 05-511 (Millipore); anti-FKHR (H-130X) rabbit polyclonal sc-67140, anti-VE-cadherin goat polyclonal sc-6458, anti-vWf clone H-300 rabbit polyclonal sc-14014, anti-Suz12 goat polyclonal sc-46264 (Santa Cruz Biotechnology); anti-vWf rabbit polyclonal AB7356 (Chemicon); anti-Hif1α rabbit polyclonal A300-286A (Bethyl Laboratories); anti-FoxO1 rabbit monoclonal clone C29H4 2880, anti-phospho-FoxO1 (Ser 256) rabbit polyclonal 9461, anti-phospho-FoxO1 (Thr 24) rabbit polyclonal 9464, anti-Akt rabbit polyclonal 9272, anti-phospho-Akt (Thr 308) rabbit polyclonal 9275; anti-Myc-tag rabbit polyclonal 2272, anti-Suz12 rabbit monoclonal D39F6, anti-H3K27me3 clone C36B11 rabbit monoclonal BK9733BFS (Cell Signalling), peroxidase-conjugated streptavidin (Jackson ImmunoResearch Laboratories), anti-HA-tag mouse monoclonal clone 12CA5, anti-Bmi1 mouse monoclonal clone AF27 (from Kristian Helin), anti-Ezh2 clone AC22 and AE25-13, anti-α-tubulin mouse monoclonal, anti-

vinculin mouse monoclonal (from internal service); anti-human VE-cadherin mouse monoclonal (BV9) [118], anti-VE-PTP Rabbit polyclonal (produced in our laboratory).

The following reagents were used in this study: pan-caspase inhibitor Z-VAD-FMK (Promega); PI(3)K inhibitor LY 294002 (Cell Signalling Technology). To inhibit AKT activity, cells were starved for 24h in starving medium + 1% BSA and then treated overnight with LY 294002 20 μM or Dimethyl sufoxide (DMSO) 20 μM as a control. To avoid apoptotic cell death during FKHR-TM overexpression experiments, 24h after the beginning of the infection, cells were treated with Z-VAD-FMK 50 μM for 24h and with Z-VAD-FMK 100 μM for the next 24h hours.

Statistical analysis

Student's two-tailed unpaired t-test was used to determine statistical significance. The significance level was set at $P < 0.05$.

RESULTS

VE-cadherin clustering triggers an endothelial stabilisation transcriptional programme

Previous work demonstrated that VE-cadherin expression and clustering at AJs is necessary for claudin-5 upregulation [26] (see also Figure 10). In order to investigate whether VE-cadherin was able to regulate in the same fashion other genes related to vascular stabilisation, we exploited previously generated Affymetrix data [26], comparing a mouse *VE-cadherin*-null cell line (VEC-null) with the same line reconstituted with *VE-cadherin* wild type cDNA (VEC-positive), described previously [22]. We identified two other genes that are preferentially expressed in the endothelium and that are fundamental for vessel stabilisation: *VE-PTP* and *vWf* [26]. As confirmed by quantitative real-time PCR (qRT-PCR), both genes were strongly upregulated by VE-cadherin expression (compare confluent VEC-null with VEC-positive) and cell confluence (compare VEC-positive in sparse and confluent conditions) (Figure 11a and 12a). Data were confirmed by western blot (WB) and immunofluorescence (IF) (Figure 11b and c and 12b and c).

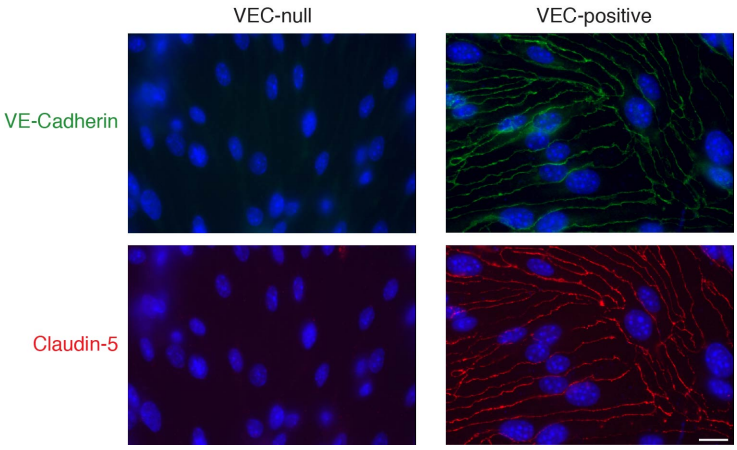

Figure 10 Claudin-5 expression in confluent VEC-null and VEC-positive ECs

IF microscopy analysis of claudin-5 expression and confluent VEC-null and VEC-positive ECs. Cells were double stained with anti-claudin-5 (red) and anti-VE-cadherin (green) antibodies. Scale bar = 10 μm.

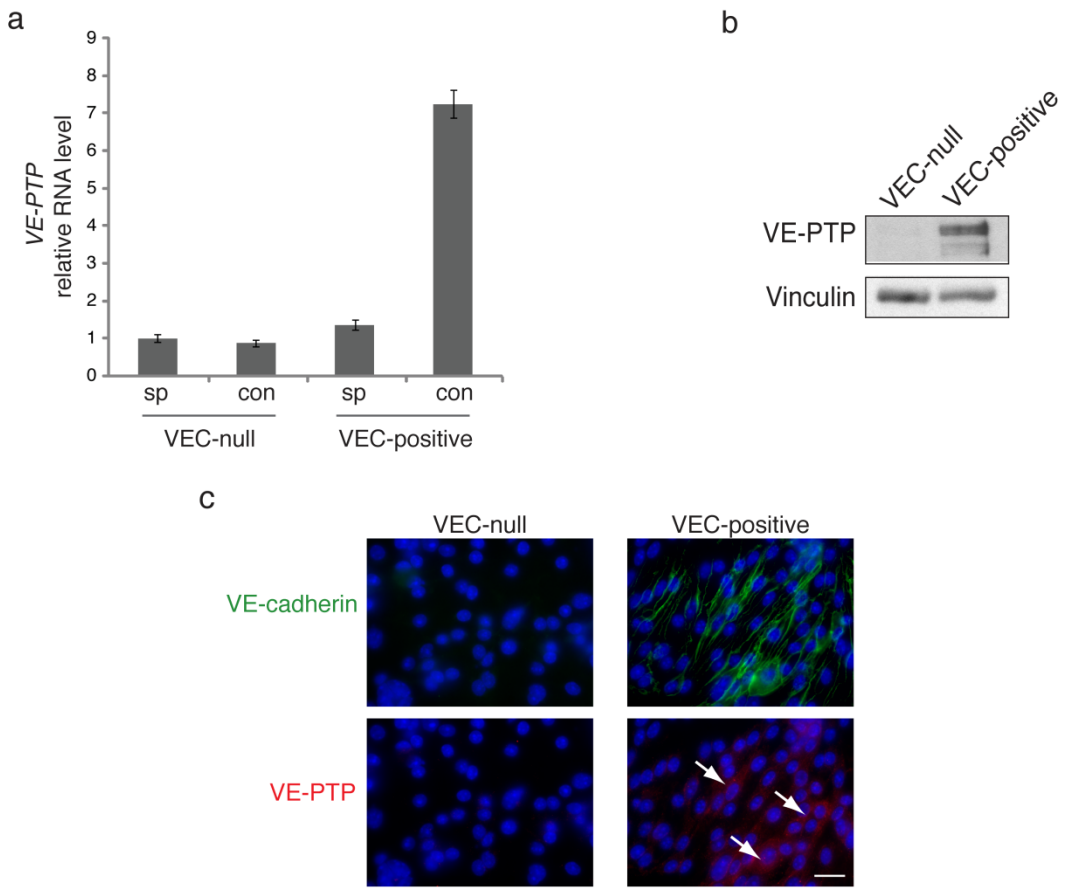

Figure 11 VE-cadherin clustering upregulates the endothelial-stabilisation gene *VE-PTP*

(**a**) qRT-PCR analysis of *VE-PTP* expression in sparse (sp) and confluent (con) VEC-null and VEC-positive ECs. The levels of mRNA are normalized to 18S; columns are means ± s.e.m. of triplicates from a representative experiment (n=3). (**b**) WB analysis of VE-PTP in extracts of confluent VEC-null and VEC-positive ECs. Vinculin was used as a loading control. (**c**) IF microscopy analysis of VE-PTP expression and confluent VEC-null and VEC-positive ECs. Cells were double stained with anti-VE-PTP (red) and anti-VE-cadherin (green) antibodies. Scale bar = 10 μm.

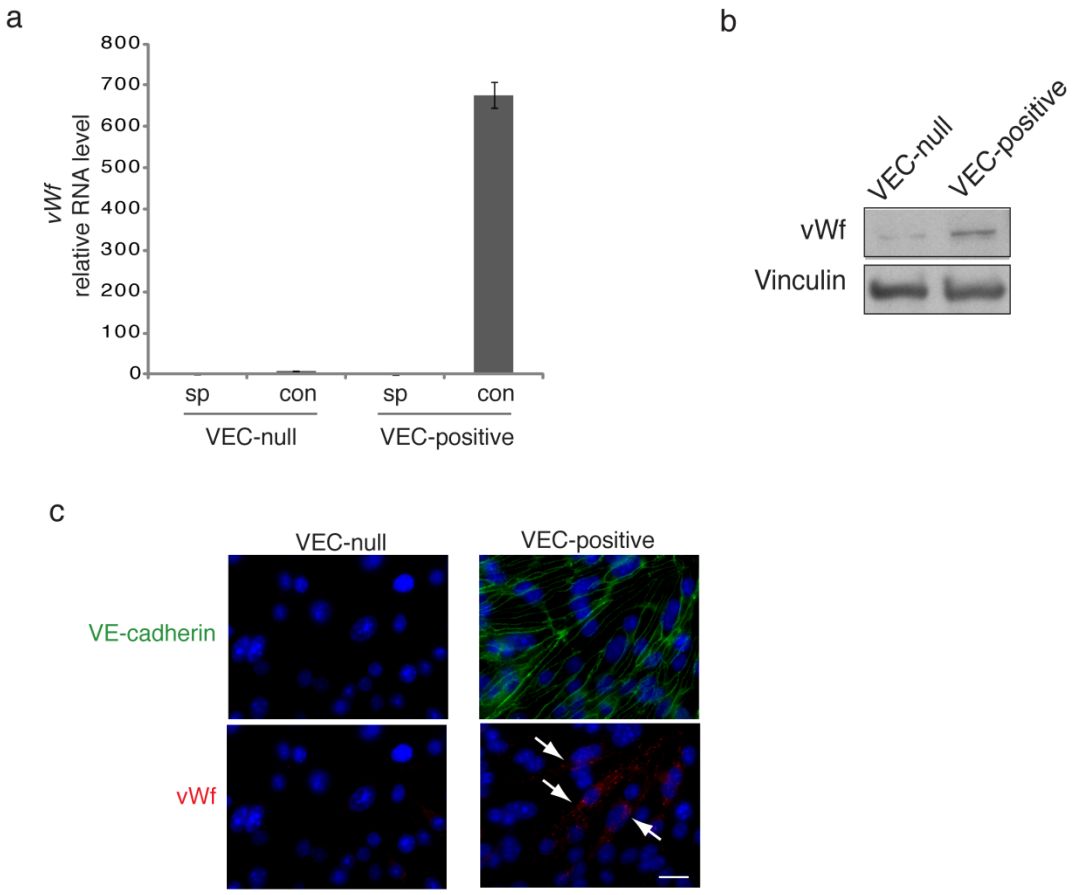

Figure 12 VE-cadherin clustering upregulates the endothelial-stabilisation gene *vWf*

(**a**) qRT-PCR analysis of *vWf* expression in sparse (sp) and confluent (con) VEC-null and VEC-positive ECs. The levels of mRNA are normalized to 18S; columns are means ± s.e.m. of triplicates from a representative experiment (n=3). (**b**) WB analysis of vWf in extracts of confluent VEC-null and VEC-positive ECs. Vinculin was used as a loading control. (**c**) IF microscopy analysis of vWf expression and confluent VEC-null and VEC-positive ECs. Cells were double stained with anti-vWf (red) and anti-VE-cadherin (green) antibodies. Scale bar = 10 μm.

Other evidence in the literature point to a confluence-dependent expression of VE-PTP and vWf in primary and immortalized ECs. Nottebaum et al., for instance have shown that VE-PTP expression is increased in long-confluent mouse bEnd.3 endothelioma cell line compared to the subconfluent counterpart [76]. Similarly, Howell et al. showed that vWf accumulates inside Weibel-Palade bodies in HUVECs primary ECs as cells reach confluency [127].

To demonstrate how VE-cadherin clustering was essential for *VE-PTP* and *vWf* upregulation we expressed in VEC-null cells a mutant version of VE-cadherin composed of the cadherin cytoplasmic tail fused to the transmembrane and extracellular domains of interleukin-2 receptor α-chain (IL2-VEC). This mutant is unable to cluster at cell-cell contacts, although it retains the capacity to associate with VE-cadherin intracellular partners [105, 106]. Neither of the two analysed genes was upregulated upon IL2-VEC expression in confluent endothelial cells, confirming the need for VE-cadherin clustering for their full expression (Figure 13a and b). These data extend what previously demonstrated for *claudin-5* [26], indicating that VE-cadherin clustering at AJs is required for the expression of a set of vascular stability genes.

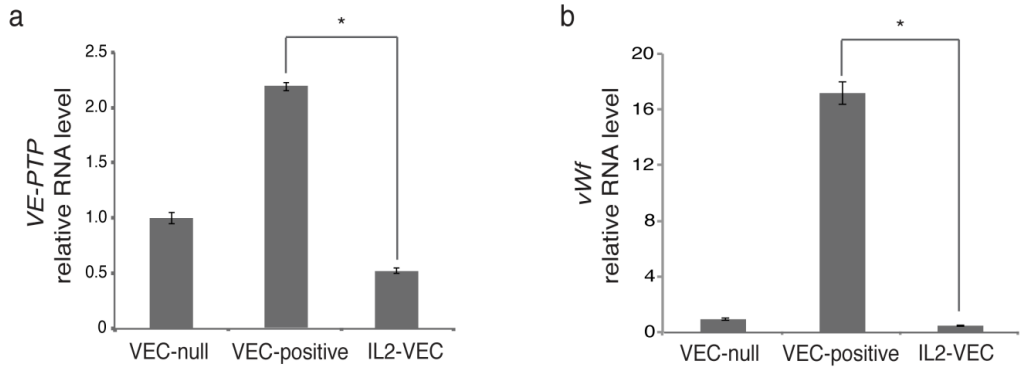

Figure 13 VE-cadherin clustering is required for *VE-PTP* and *vWf* expression

qRT-PCR analysis of *VE-PTP* (**a**) and *vWf* (**b**) expression in confluent VEC-null, VEC-positive and IL2-VEC ECs. The levels of mRNA are normalized to 18S; columns are means ± s.e.m. of replicates of a representative experiment (n=3). *t*-test: **P* < 0.01

FoxO1 and β-catenin repress *VE-PTP* and *vWf* expression

FoxO1 and β-catenin have previously been shown to associate with each other and bind *claudin-5* promoter to induce gene repression. This is counteracted by VE-cadherin clustering, which reduces FoxO1 and β-catenin nuclear levels [26]. We aimed at verifying if this same mechanism was involved in VE-cadherin-mediated induction of *VE-PTP* and *vWf* expression. We infected confluent VEC-positive cells with adenoviruses encoding control green fluorescent protein (GFP) or a constitutively active form of FoxO1 (FKHR-TM, triple mutant) which contains mutations of all three AKT-target phosphorylation sites (Thr 24, Ser 256 and Ser 319) and therefore can not be inhibited [52]. FKHR-TM expression led to a strong downregulation of both *VE-PTP* and *vWf* expression (Figure 14a and b).

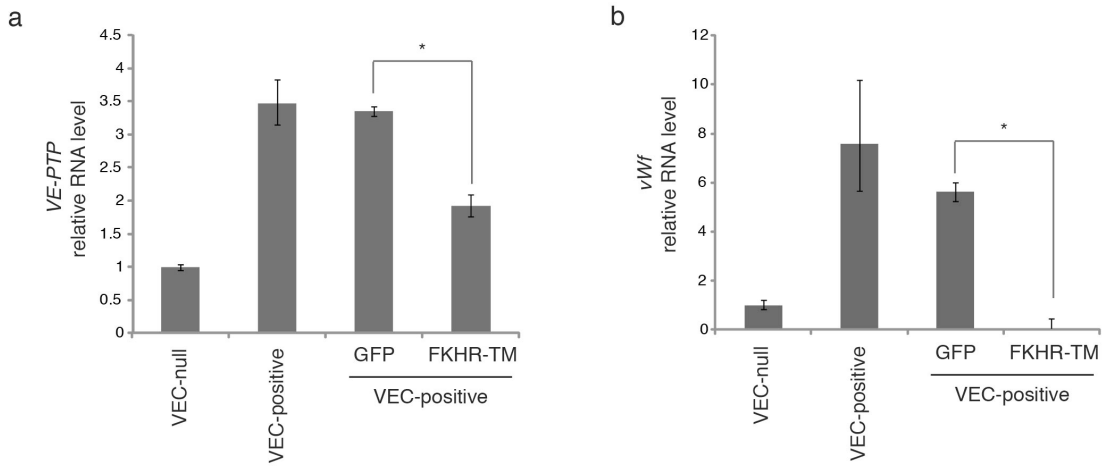

Figure 14 Analysis of *VE-PTP* and *vWf* expression upon FKHR-TM overexpression

qRT-PCR analysis of *VE-PTP* (**a**) and *vWf* (**b**) expression in VEC-null and VEC-positive ECs either uninfected or infected with adenoviral vectors encoding FKHR-TM or GFP as a negative control. 24h after the infection cells were cultured in the presence of the pan-caspase inhibitor Z-VAD-FMK to limit the proapoptotic effect of FKHR-TM (see more details in Materials and Methods). The levels of mRNA are normalized to GAPDH, columns are means ± s.e.m. of triplicates from a representative experiment (n=3). *t*-test: $*P < 0.01$.

Results were confirmed by increasing endogenous FoxO1 activity via LY 294002-mediated inhibition of PI3K. Treatment reduced FoxO1 Ser 256 phosphorylation level (Figure 15c) and yielded the downregulation of both analysed genes (Figure 15a and b).

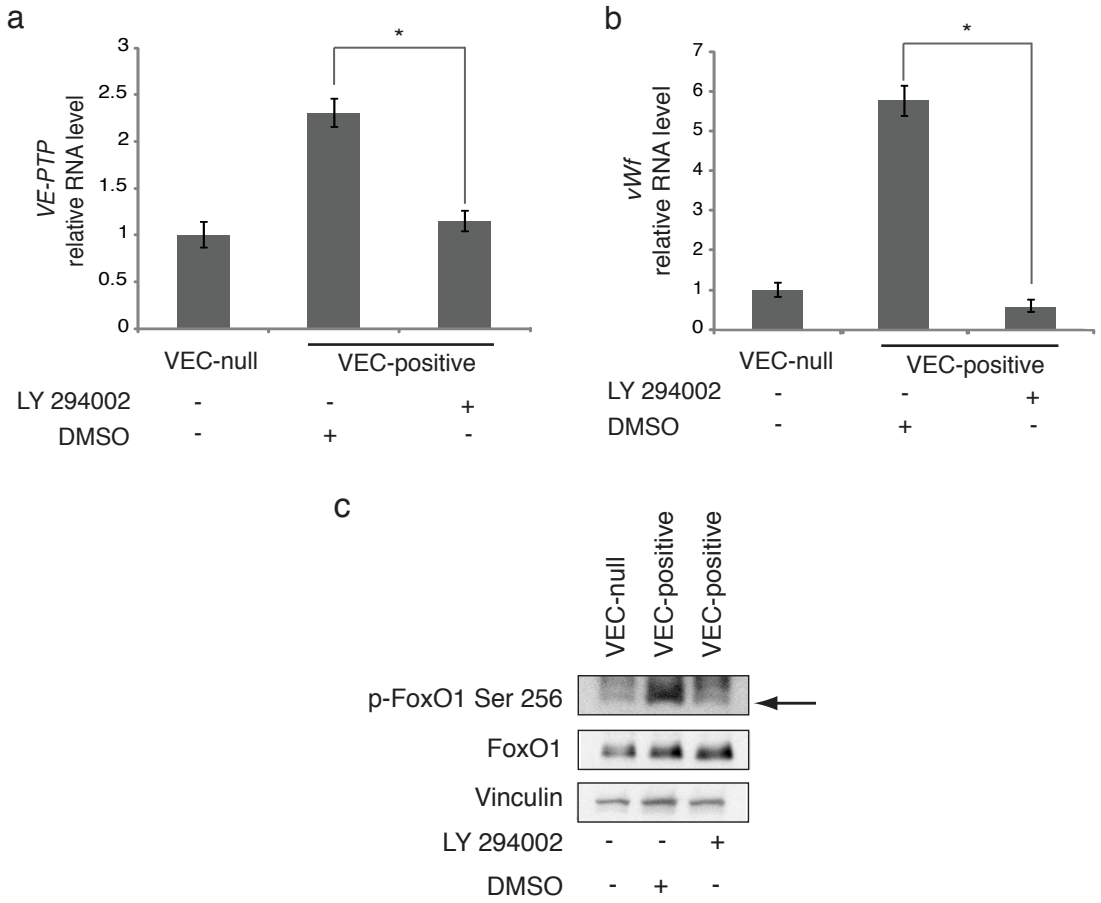

Figure 15 Analysis of *VE-PTP* and *vWf* expression upon pharmacological inhibition of PI3K/AKT pathway

qRT-PCR analysis of *VE-PTP* (**a**) *vWf* (**b**) expression in confluent VEC-null and VEC-positive ECs treated with the PI(3)K inhibitor LY294002 or DMSO as control. (**c**) WB analysis of of p-FoxO1 Ser 256 and total FoxO1 protein. Vinculin was used as loading control. The levels of mRNA are normalized to GAPDH, columns are means ± s.e.m. of triplicates from a representative experiment (n=3). *t*-test: $*P < 0.01$.

β-Catenin is known to associate with FoxO1 increasing its repressor activity on *claudin-5* by stabilizing its binding to gene promoters [26]. Interestingly, the expression of a stabilised version of β-catenin lacking the GSK3β phosphorylation site (ΔN-β-catenin), led to a marked downregulation of both *VE-PTP* and *vWf* genes, suggesting a similar mechanism to *claudin-5* regulation (Figure 16a and b).

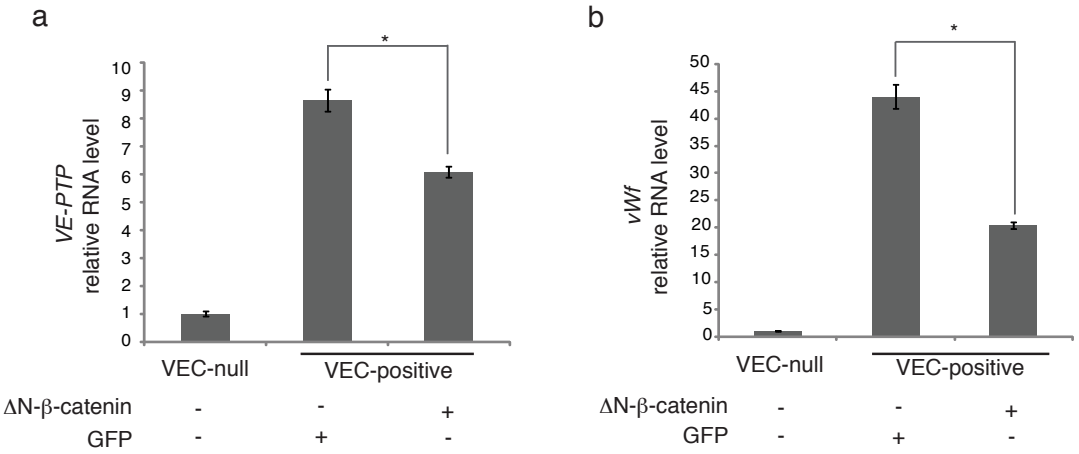

Figure 16 Analysis of *VE-PTP* and *vWf* expression upon ΔN-β-catenin overexpression

qRT-PCR analysis of *VE-PTP* (**a**) and *vWf* (**b**) expression in confluent VEC-null and VEC-positive cells expressing ΔN-β-catenin or GFP as negative control. The levels of mRNA are normalized to GAPDH, columns are means ± s.e.m. of triplicates from a representative experiment (n=3). *t*-test: **P* < 0.01.

We performed a promoter analysis spanning from 6000 base pairs (bp) upstream to 500 bp downstream of the transcription start site (TSS) of *VE-PTP* and *vWf* genes and identified a series of paired Tcf/β-catenin-FoxO1 binding sites localized in three different regions on both promoters: Region 1 (position -5,257/-5,158 for *VE-PTP*; -3,836/-3,354 for *vWf*); Region 2 (position -3,206/-2,656 for *VE-PTP*; -733/-556 for *vWf*); Region 3 (position -1,697/-1,263 for *VE-PTP*; -49/+83 for *vWf*) (Figure 17a and b).

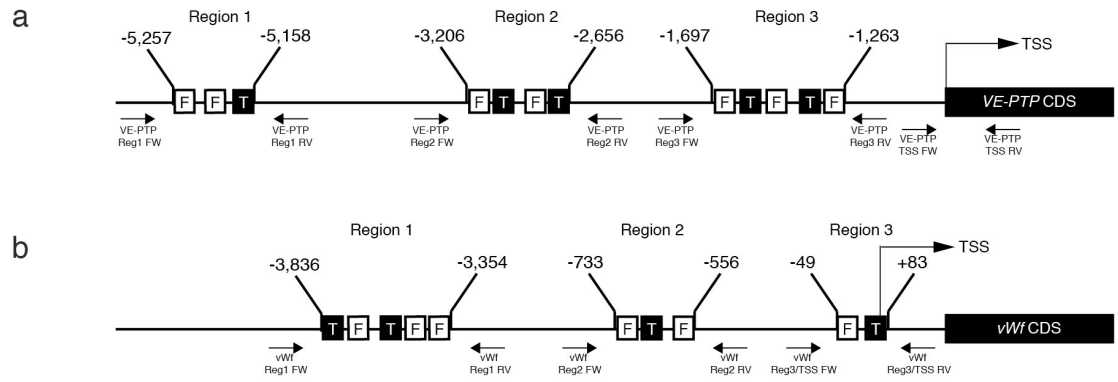

Figure 17 Schematic representation of the putative promoter regions of *VE-PTP* and *vWf*

Tcf/β-catenin and FoxO binding sites identified on the putative promoter region of *VE-PTP* (**a**) and *vWf* (**b**) gene. FoxO1 (F) binding sites are depicted as white boxes and Tcf/β catenin (T) binding sites as black boxes. CDS, coding sequence. Primers are depicted as black arrows. TSS, transcription start site. Promoter analysis was performed using MatInspector software (see Materials and Methods).

Quantitative chromatin immunoprecipitation (qChIP) showed that FoxO1 binds all three regions in both promoters (Figure 18a and b). Binding occurred only in confluent VEC-null and not in confluent VEC-positive cells, correlating with gene repression. Furthermore, β-catenin also bound all identified regions with different affinity (Figure 19a and b). Overall, these data show that VE-cadherin clustering at AJs triggers a vascular stabilisation transcriptional programme, consisting at least in the expression of *claudin-5*, *VE-PTP* and *vWf* through the inhibition of the repressive activity exerted by FoxO1/β-catenin-binding to their promoters.

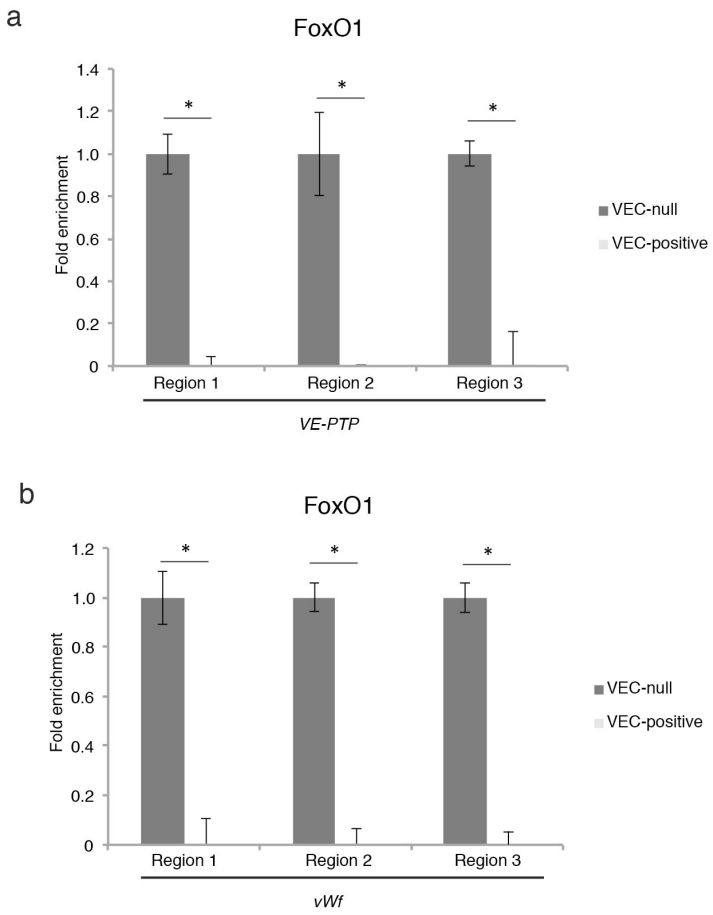

Figure 18 FoxO1 binds to *VE-PTP* and *vWf* promoter regions

qRT-PCR for Region 1, 2 and 3 of *VE-PTP* (**a**) and vWf (**b**) putative promoter regions performed on endogenous FoxO1-bound chromatin immunoprecipitated from confluent VEC-null and VEC-positive ECs. Columns are means ± s.d. of the fold enrichment normalized on the signal of VEC-null cells (n=3). *t*-test: **P* < 0.01.

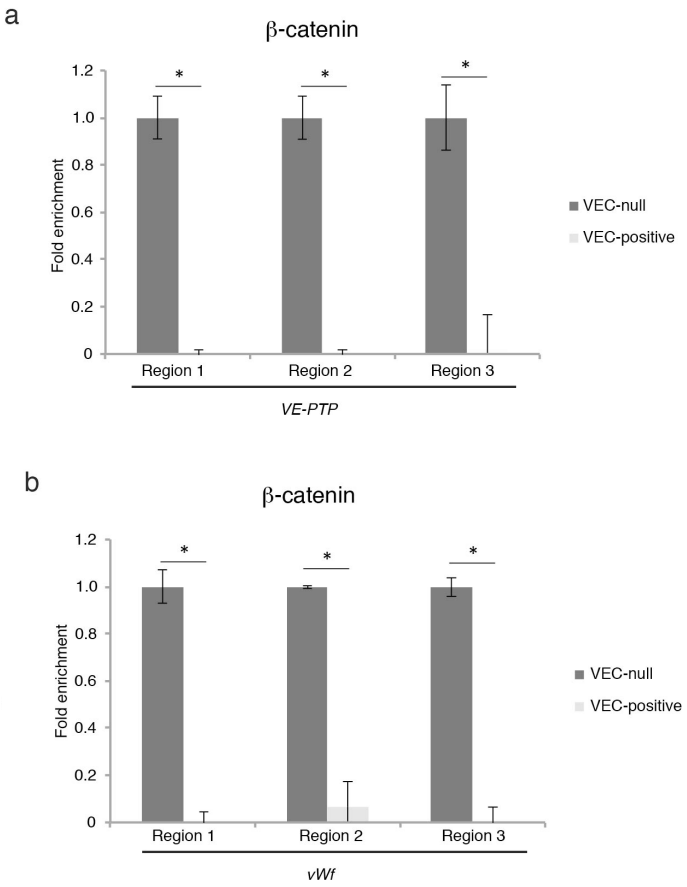

Figure 19 β-catenin binds to *VE-PTP* and *vWf* promoter regions

qRT-PCR for Region 1, 2 and 3 of *VE-PTP* (**a**) and *vWf* (**b**) putative promoter regions performed on endogenous β-catenin-bound chromatin immunoprecipitated from confluent VEC-null and VEC-positive ECs. Columns are means ± s.d. of the fold enrichment normalized on the signal of VEC-null cells (n=3). *t*-test: $*P < 0.01$.

Claudin-5, *VE-PTP* and *vWf* are Polycomb-target genes

The mechanism through which FoxO factors can downregulate several target genes is still a matter of investigation. We aimed at clarifying how the FoxO1/β-catenin complex might act on *claudin-5*, *VE-PTP* and *vWf* genes to induce their repression. The observed regulation consists of a reversible inhibition of gene expression, depending on the state of cell confluence and AJ organization. Given the endothelial-specificity of the identified genes we hypothesized the possible involvement of PcG proteins, a group of transcriptional regulators involved in cell specification, which mediate reversible inhibition of transcription [87]. In order to investigate this possibility we performed qChIP for PcG proteins on the TSS of *claudin-5*, *VE-PTP* and *vWf* genes. Gene TSSs displayed higher enrichments in the components of both PRC2 (Ezh2 and Suz12) and PRC1 (Bmi1) in confluent VEC-null than in VEC-positive cells (Figure 20 b, c and d).

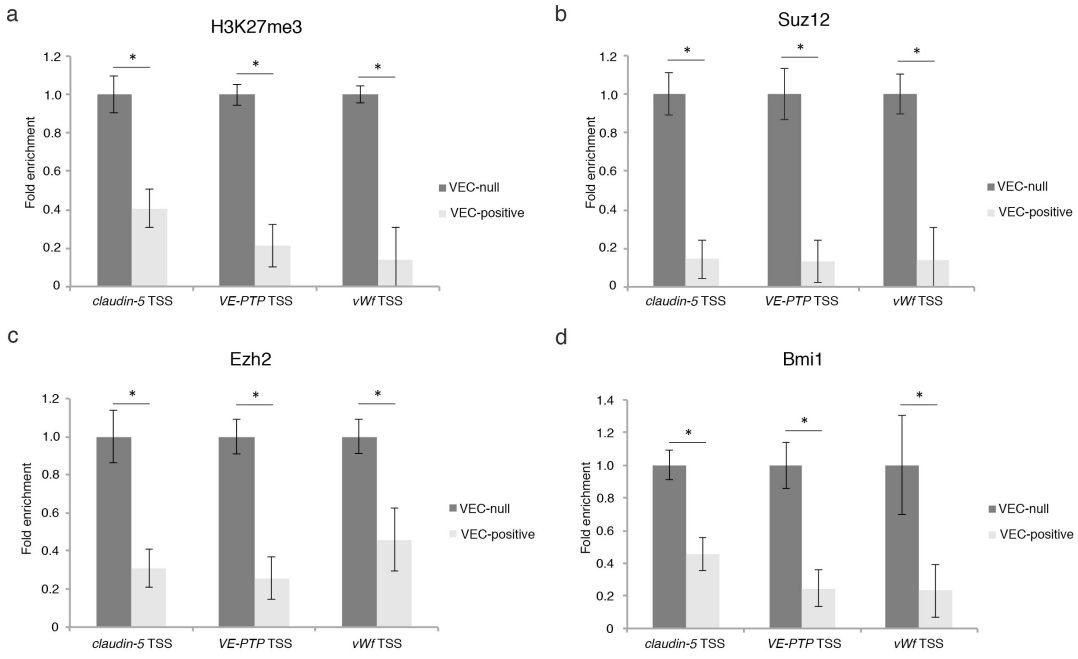

Figure 20 PcG proteins bind the TSS of *claudin-5*, *VE-PTP* and *vWf* genes in VEC-null ECs

qRT-PCR for the TSS of *claudin-5*, *VE-PTP* and *vWf* performed on endogenous H3K27me3- (**a**), Suz12- (**b**), Ezh2- (**c**) and Bmi1- (**d**) bound chromatin immunoprecipitated from confluent VEC-null and VEC-positive

ECs. Columns are means ± s.d. of the fold enrichment normalized on the signal of VEC-null cells (n=3). *t*-test: **P* < 0.01.

The mark of Ezh2 enzymatic activity, H3K27me3, also showed a similar enrichment pattern (Figure 20a), and qChIP for total histone H3 showed comparable enrichments at the analysed regions in VEC-null and VEC-positive cells (Figure 21), ruling out the possibility that the higher H3K27me3 signal in VEC-null cells could be due to higher histone density.

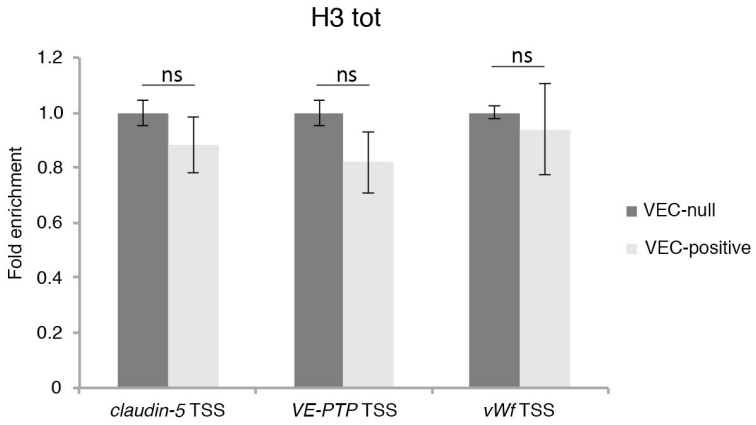

Figure 21 Histone density on the TSS of *claudin-5*, *VE-PTP* and *vWf* genes is not affected by the absence of VE-cadherin

qRT-PCR for the TSS of *claudin-5*, *VE-PTP* and *vWf* performed on total H3-bound chromatin immunoprecipitated from confluent VEC-null and VEC-positive ECs. Columns are means ± s.d. of the fold enrichment normalized on the signal of VEC-null cells (n=3). *t*-test: ns, not significant.

PcG protein-mediated repression is counteracted by the activity of Trithorax group (TrxG) proteins, which catalyse the deposition of H3K4me3 histone mark, leading to gene activation [101]. As expected, *claudin-5*, *VE-PTP* and *vWf* TSSs showed a higher enrichment for H3K4me3 in confluent VEC-positive cells than in VEC-null (Figure 22a), consistently with gene activation in the presence of VE-cadherin clustering. In line with this

observation, RNA Pol II phosphorylated on Ser 5, a modification needed for the enzyme to escape the promoter and transcribe the gene [119], was present to a higher extent at the TSSs of genes in confluent VEC-positive cells (Figure 22b), where genes are actively transcribed.

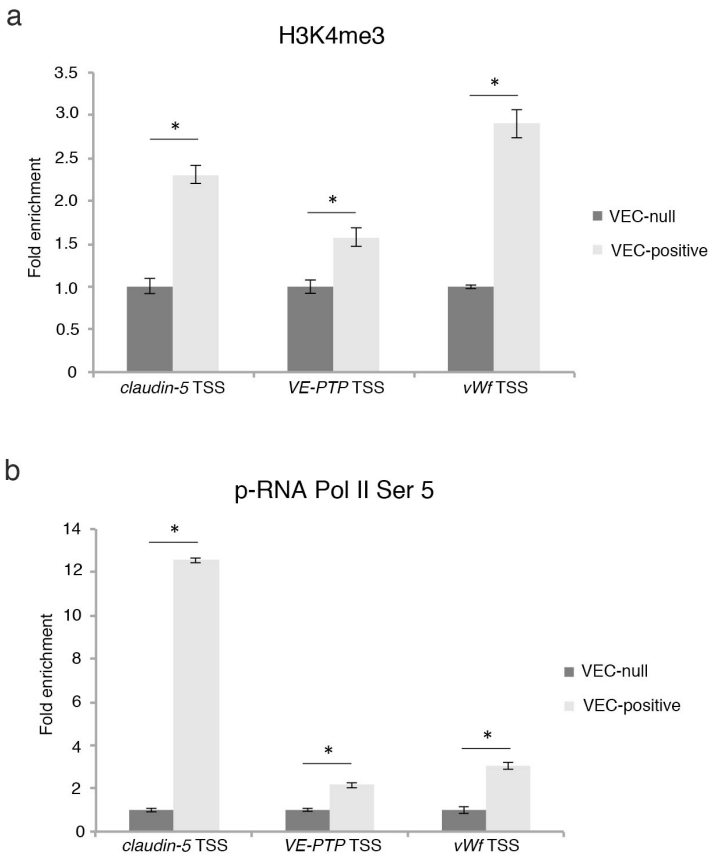

Figure 22 Activation marks decorate the TSS of *claudin-5*, *VE-PTP* and *vWf* genes in VEC-positive ECs

qRT-PCR for the TSS of *claudin-5*, *VE-PTP* and *vWf* performed on endogenous H3K4me3- (**a**) and pRNAPolII Ser 5- (**b**) bound chromatin immunoprecipitated from confluent VEC-null and VEC-positive ECs. Columns are means ± s.d. of the fold enrichment normalized on the signal of VEC-null cells (n=3). *t*-test: $*P < 0.01$.

To further prove the role of PcG proteins in the transcriptional regulation of *claudin-5*, *VE-PTP* and *vWf* genes we overexpressed the PRC2 member Suz12 in confluent VEC-positive cells using lentiviral-mediated gene delivery (Figure 23a). Even if PRC2 proteins are known to promote each other stability by physical interaction [120, 121], Suz12 overexpression

led only to a minor increase of Ezh2 protein levels that did not reach statistical significance (Figure 23b). Upon Suz12 overexpression in VEC-positive ECs *claudin-5*, *VE-PTP* and *vWf* expression was reduced (Figure 24a, b and c). As control, *claudin-12* mRNA levels were unaffected by Suz12 overexpression in VEC-positive ECs (Figure 24 d).

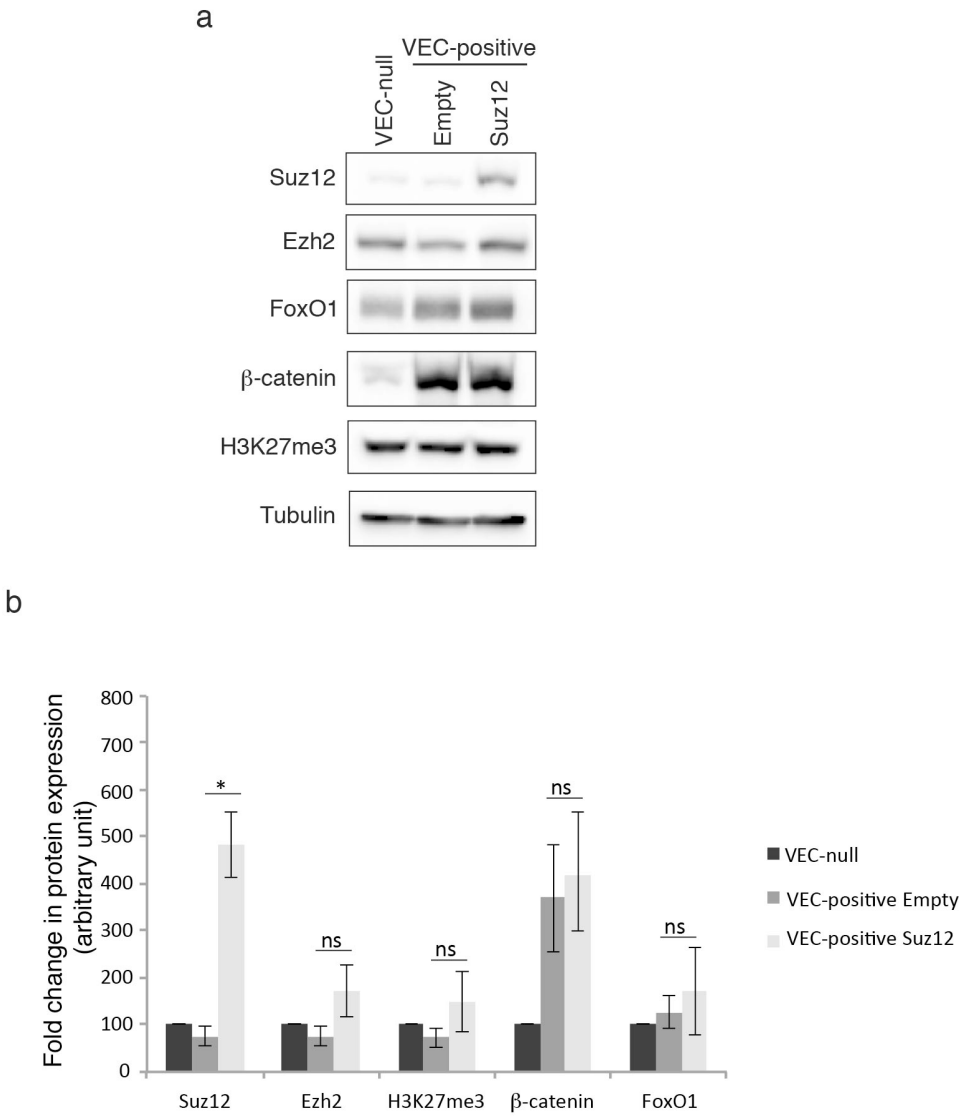

Figure 23 Suz12 overexpression in VEC-positive ECs

(**a**) WB analysis of Suz12, Ezh2, FoxO1, β-catenin and H3K27me3 in extracts of confluent VEC-null and VEC-positive ECs infected with lentiviral vectors inducing Suz12 overexpression or Empty control. Tubulin was used as loading control. (**b**) WB quantification. For each protein, bands are normalized on tubulin and represented as percentage of the signal in VEC-null cells (n=3). *t*-test: **P*<0.01; ns, not significant.

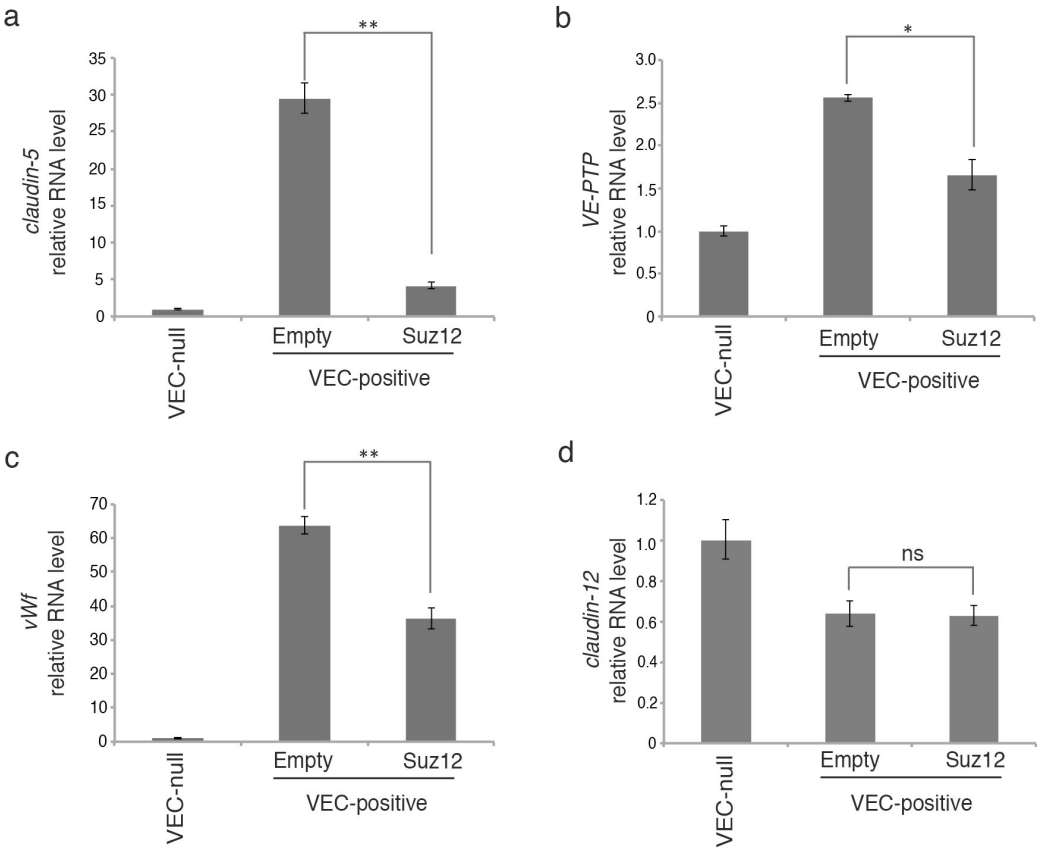

Figure 24 Suz12 overexpression represses *claudin-5*, *VE-PTP* and *vWf* expression

qRT-PCR analysis of *claudin-5* (**a**), *VE-PTP* (**b**) and *vWf* (**c**) in confluent VEC-null and VEC-positive ECs infected with lentiviral vectors inducing Suz12 overexpression or with an Empty control. *Claudin-12* (**d**) levels are unchanged upon Suz12 overexpression. The levels of mRNA are normalized to 18S, columns are means ± s.e.m. of triplicates from a representative experiment (n=3). *t*-test: **P* < 0.05; ** *P*<0.01; ns, not significant.

Conversely, lentiviral delivery of short hairpin (sh)RNA was used to stably knockdown Suz12 in confluent VEC-null cells. As expected, Suz12 knockdown led to a marked decrease in Ezh2 and H3K27me3 levels, while β-catenin was unaltered (Figure 25a). Of note, FoxO1 protein level was about 30% lower upon Suz12 knockdown (Figure 25b), although FoxO1 mRNA expression was not influenced (Figure 26). This is suggestive of a possible effect of Suz12 on the regulation of FoxO1 protein stability.

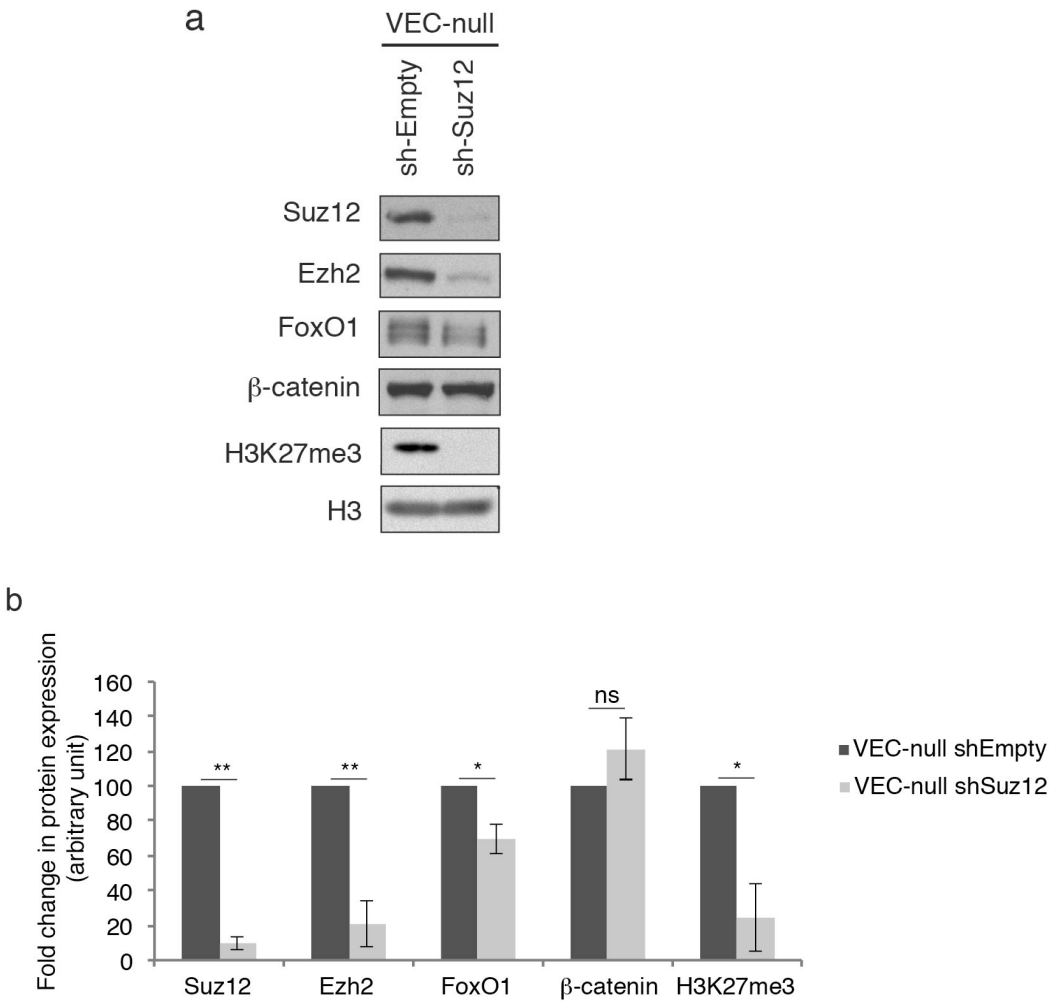

Figure 25 Suz12 knockdown in VEC-null ECs

(**a**) WB analysis of Suz12, Ezh2, FoxO1, β-catenin, H3K27me3 in extracts of confluent VEC-null ECs infected with lentiviral vectors inducing Suz12 knockdown (sh-Suz12) or Empty control (sh-Empty). (**b**) WB quantification. For each protein, bands are normalized on total histone H3 and represented as percentage of the signal in VEC-null sh-Empty cells (n=3). *t*-test: **P* < 0.05; ** *P*<0.01; ns, not significant.

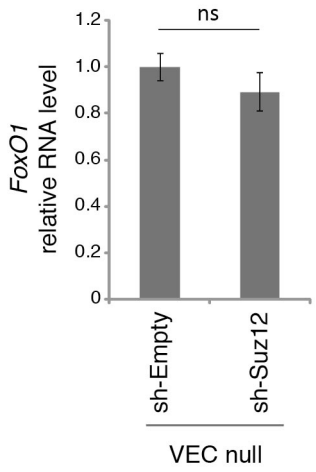

Figure 26 Analysis of *FoxO1* expression upon stable Suz12 knockdown

qRT-PCR analysis of *FoxO1* expression in confluent VEC-null sh-Empty and VEC-null sh-Suz12 ECs. The levels of mRNA are normalized to 18S; columns are means ± s.e.m. of replicates of a representative experiment (n=3). *t*-test: ns, not significant.

Suz12 knockdown abolished Suz12 signal at the TSS of *claudin-5*, *VE-PTP* and *vWf* genes (Figure 27) causing a partial reactivation of their expression (Figure 28). Together these data prove that the expression of the identified stabilisation genes is finely tuned at the epigenetic level by the balanced activity of PcG and TrxG proteins, which depends on the state of cell confluence and AJ organization.

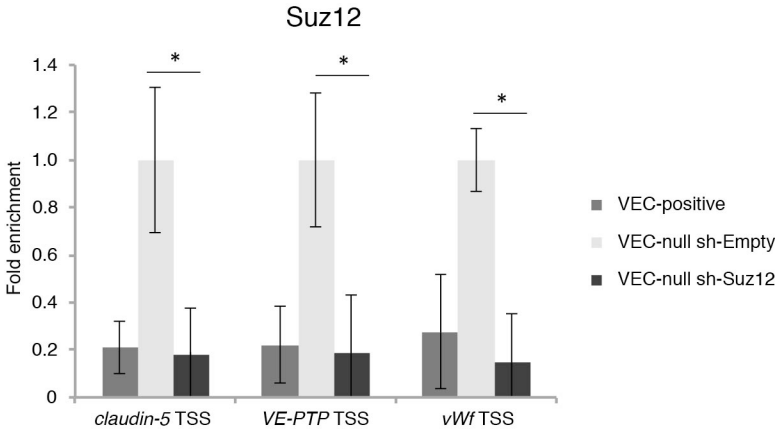

Figure 27 Suz12 binding to the TSS of *claudin-5*, *VE-PTP* and *vWf* genes upon Suz12 stable knockdown

qRT-PCR for the TSS of *claudin-5*, *VE-PTP* and *vWf* performed on endogenous Suz12-bound chromatin immunoprecipitated from confluent VEC-null, VEC-null-sh-Empty and VEC-null-sh-Suz12 ECs. Columns are means ± s.d. of the fold enrichment normalized on the signal of VEC-null sh-Empty cells (n=3). *t*-test: **P* < 0.01.

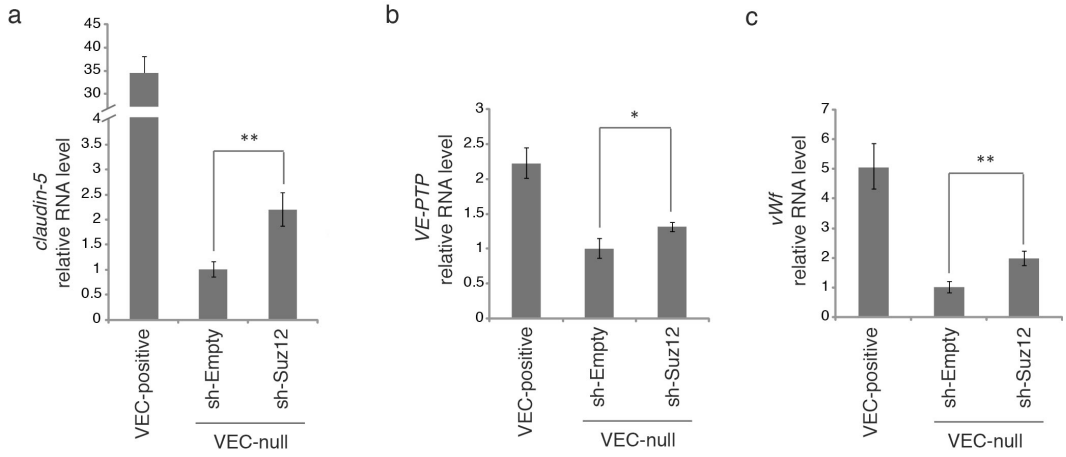

Figure 28 Analysis of *claudin-5*, *VE-PTP* and *vWf* expression upon stable Suz12 knockdown

qRT-PCR analysis of *claudin-5* (**a**), *VE-PTP* (**b**) and *vWf* (**c**) in confluent VEC-null-sh-Empty and VEC-null-sh-Suz12 ECs. The levels of mRNA are normalized to 18S; columns are means ± s.e.m. of replicates of a representative experiment (n=3). *t*-test: **P* < 0.05; ** *P*<0.01.

FoxO1/β-catenin complex recruits PcG proteins at *claudin-5*, *VE-PTP* and *vWf* promoters

A key aspect of PcG protein biology which still remains largely unravelled deals with PcG protein recruitment to their target sites [87]. Given the absence of defined mammalian PREs, PcG protein recruitment to chromatin has been suggested to occur through PRC-interaction with specific DNA-binding partners. For instance, Snail1 transcription factor has been proved to associate to PRC2 components and target them to E-cadherin promoter to induce gene repression [100]. We hypothesized that the FoxO1/β-catenin complex could act as PcG protein-recruiter to the promoters of the identified genes. We checked by co-immunoprecipitation the association of Ezh2 and Suz12 with overexpressed constitutively active FKHR-TM and found this transcription factor interacting with both PcG proteins (Figure 29). This association was confirmed also in basal conditions, between Ezh2, Suz12 and endogenous FoxO1 (Figure 30).

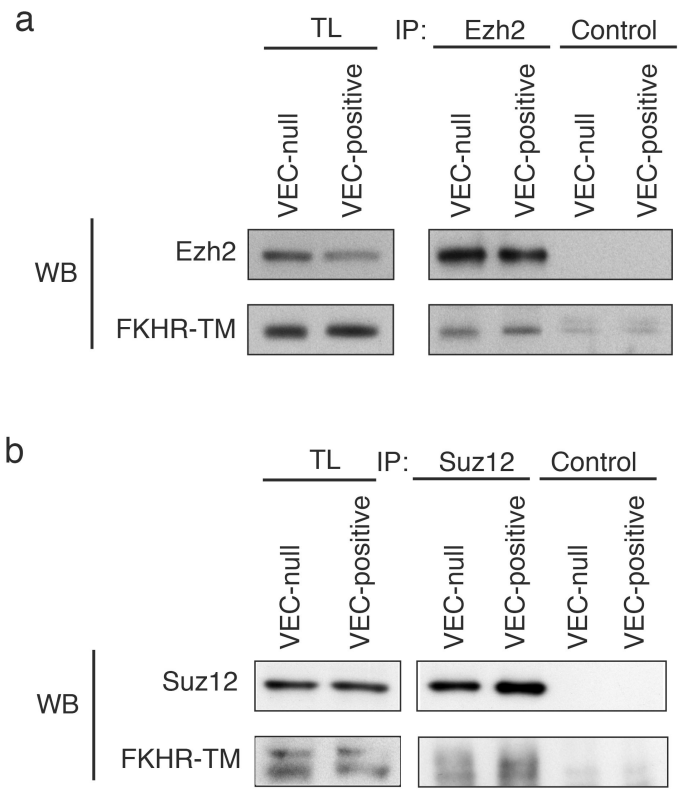

Figure 29 FKHR-TM interacts with PcG proteins

CoIP and WB analysis of either endogenous Ezh2 (**a**) or Suz12 (**b**) and FKHR-TM from extracts of confluent VEC-null and VEC-positive ECs expressing either FKHR-TM (myc tagged) or GFP as negative control. To limit the pro-apoptotic effect of FKHR-TM cells were cultured in the presence of the pan-caspase inhibitor Z-VAD-FMK (see more details in Materials and Methods). Cells were lysed 72h after infection. TL, total lysate. Negative control Abs used in these experiments were anti-HA tag mouse mAb in (**a**) and non-immune rabbit IgG in (**b**).

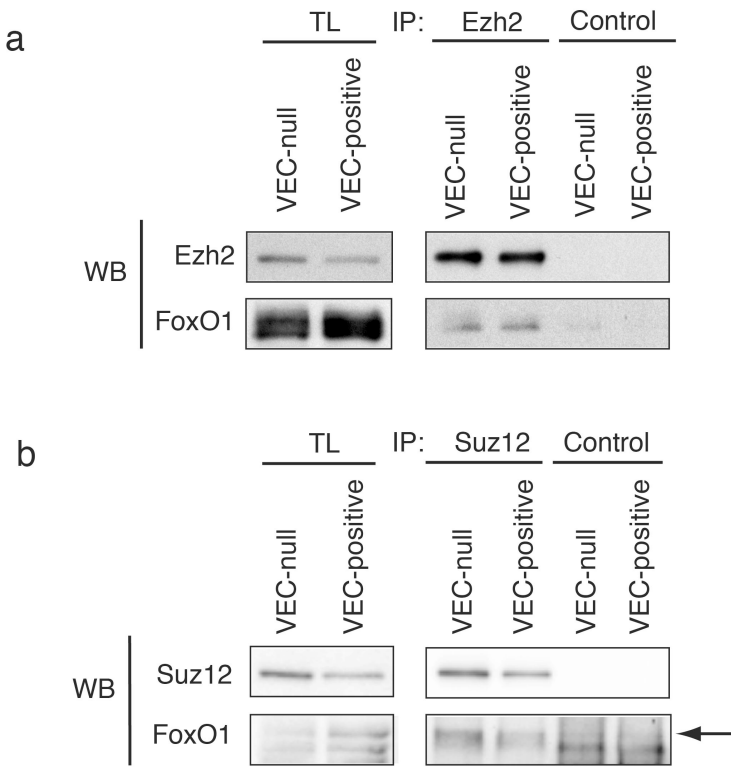

Figure 30 Endogenous FoxO1 interacts with PcG proteins

CoIP and WB analysis of endogenous Ezh2 (**a**) or Suz12 (**b**) and FoxO1 from extracts of confluent VEC-null and VEC-positive ECs. Arrow indicates specific FoxO1 band. TL, total lysate. Negative control Abs used in these experiments were anti-HA tag mouse mAb in (**a**) and non-immune rabbit IgG in (**b**).

Of note, such interaction seemed to occur also in the presence of VE-cadherin expression and clustering in confluent VEC-positive cells (Figure 30). However, given the negligible levels of FoxO1-DNA binding at the promoters of *claudin-5* [26], *VE-PTP* and *vWf* in such condition (Figure 18), this complex is unlikely to be recruited at target sites. FKHR-TM overexpression in VEC-positive confluent cells led to a marked increase of H3K27me3 binding to the TSS of *claudin-5*, *VE-PTP* and *vWf* genes, as shown by H3K27me3 qChIP (Figure 31a). This is in line with the gene downregulation observed upon FKHR-TM overexpression (Figure 14 and see Taddei et al., 2008). Moreover, no increase in Ezh2 protein levels was induced by FKHR-TM (Figure 31b), proving that the augmented H3K27me3 enrichment seen in qChIP was not caused by Ezh2 protein upregulation.

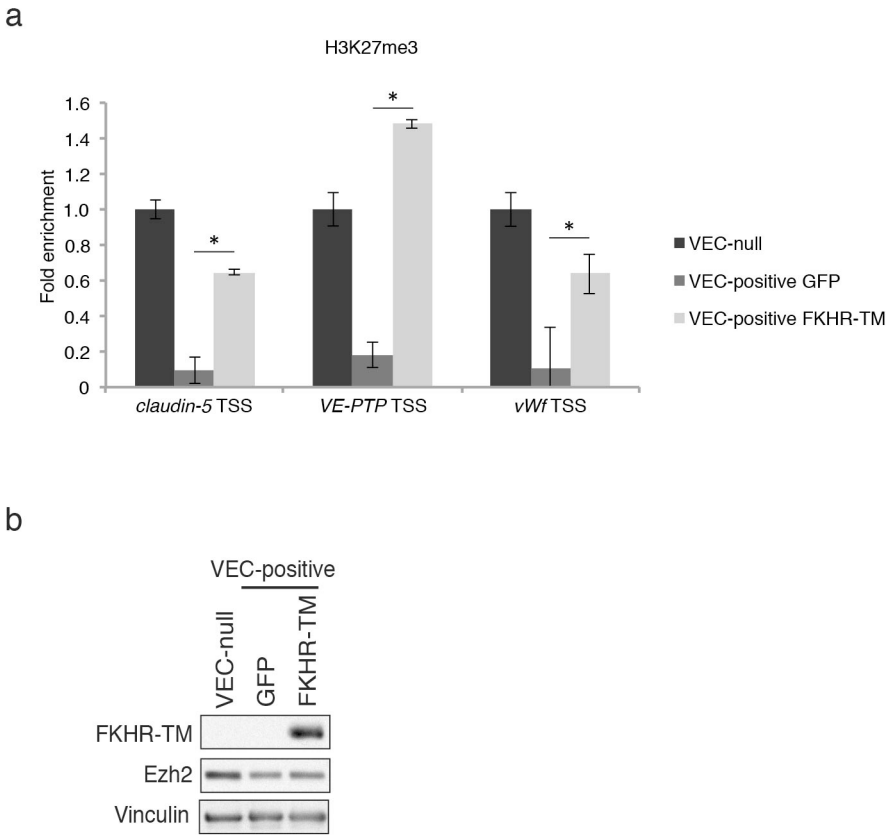

Figure 31 FKHR-TM overexpression increases H3K27me3 levels on the TSS of *claudin-5*, *VE-PTP* and *vWf* genes

(**a**) qRT-PCR for the TSS of *claudin-5*, *VE-PTP* and *vWf* performed on endogenous H3K27me3-bound chromatin immunoprecipitated from confluent VEC-null and VEC-positive ECs expressing either FKHR-TM or GFP as negative control. Columns are means ± s.d. of the fold enrichment normalized on the signal of VEC-null cells (n=3). *t*-test: $*P < 0.01$. (**b**) WB analysis of FKHR-TM and Ezh2 in extracts from confluent VEC-null and VEC-positive ECs expressing either FKHR-TM or GFP. Vinculin was used as loading control.

Conversely, endogenous FoxO1 knockdown strongly reduced Ezh2 recruitment at target sites in VEC-null cells (Figure 32a), in the absence of any Ezh2 downregulation (Figure 32b and c).

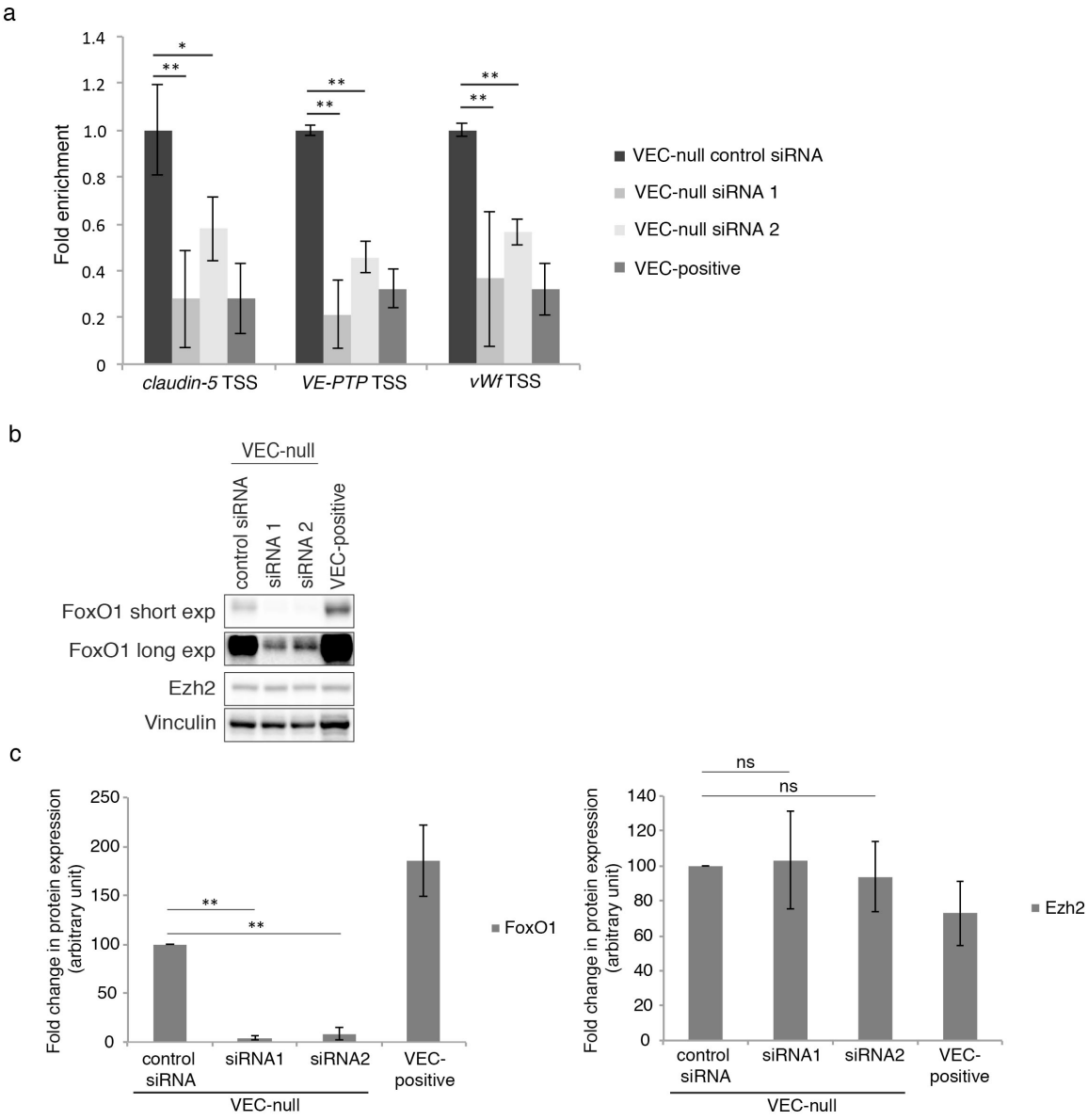

Figure 32 FoxO1 knockdown impairs Ezh2 binding to the TSS of *claudin-5*, *VE-PTP* and *vWf* genes

(**a**) qRT-PCR for the TSS of *claudin-5*, *VE-PTP* and *vWf* performed on endogenous Ezh2-bound chromatin immunoprecipitated from confluent VEC-null ECs either transfected with a control siRNA or with 2 different siRNAs targeting FoxO1 and VEC-positive ECs. Columns are means ± s.d. of the fold enrichment normalized on the signal of VEC-null control siRNA cells (n=3).

(**b**)WB analysis of FoxO1 and Ezh2 on confluent VEC-null ECs transfected either with a control siRNA or with 2 different siRNAs targeting FoxO1 and VEC-positive ECs. Vinculin was used as a loading control.

(**c**) WB quantification. For each protein, bands are normalized on vinculin and represented as percentage of the signal in VEC-null control siRNA cells (n=3). *t*-test: **P* < 0.05; ** *P*<0.01; ns, not significant.

Co-expression of Suz12 and FKHR-TM in VEC-positive confluent cells induced a significantly stronger repression of *claudin-5* (75,3%) than expression of FKHR-TM alone (about 53,1%), further maintaining the hypothesis that FoxO1-mediated downregulation occurs through Polycomb activity (Figure 33).

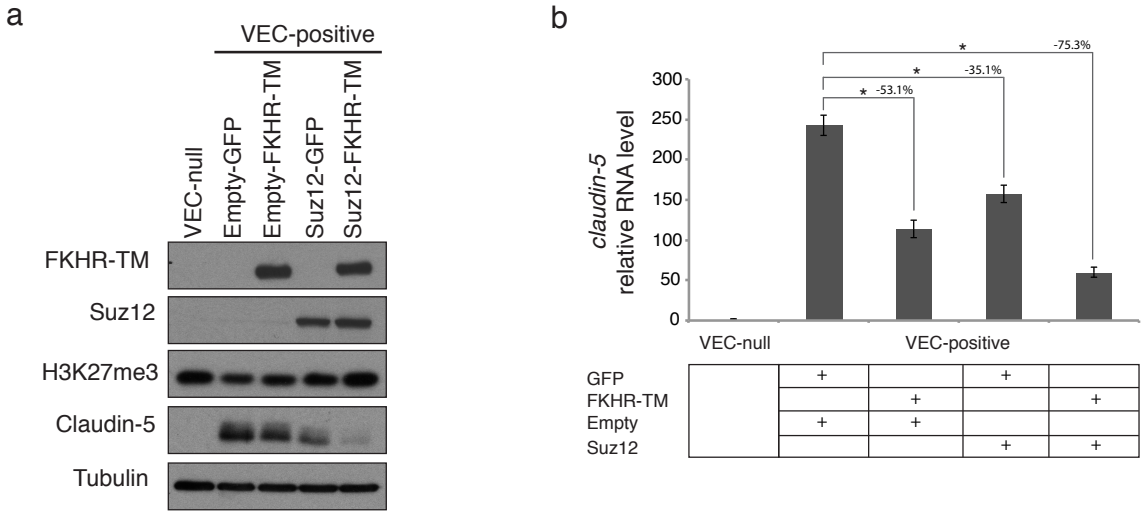

Figure 33 FKHR-TM and Suz12 cooperate in repressing *claudin-5* gene

(**a**) WB analysis of FKHR-TM, Suz12, H3K27me3 and Claudin-5 in extracts of confluent VEC-null, VEC-positive-Empty and VEC-positive-Suz12 ECs expressing either FKHR-TM or GFP as negative control. Tubulin was used as loading control.

(**b**) qRT-PCR analysis of *claudin-5* in VEC-null, VEC-positive-Empty and VEC-positive-Suz12 ECs expressing either FKHR-TM or GFP as negative control. The levels of mRNA are normalized to GAPDH. Columns are means ± s.d. of triplicates from a representative experiment (n=3). *t*-test: * $P<0.01$.

We investigated whether β-catenin was part of FoxO1/PcG protein complex. Co-immunoprecipitation experiments showed an interaction of β-catenin with both Ezh2 (Figure 34a) and Suz12 (Figure 34b). As observed for FoxO1 (see above), also this association was present both in confluent VEC-null and VEC-positive cells but the lack of β-catenin binding to *claudin-5*, *VE-PTP* and *vWf* promoters in confluent VEC-positive

cells (Figure 19 and see Taddei et al., 2008) ruled out a possible recruitment of the complex to the DNA in this latter condition. Surprisingly we detected a strong Ezh2/β-catenin association in VEC-positive confluent cells that was unlikely to be connected to the analysed recruitment mechanism (Figure 34a). The meaning of this interaction will be further explored in the next section.

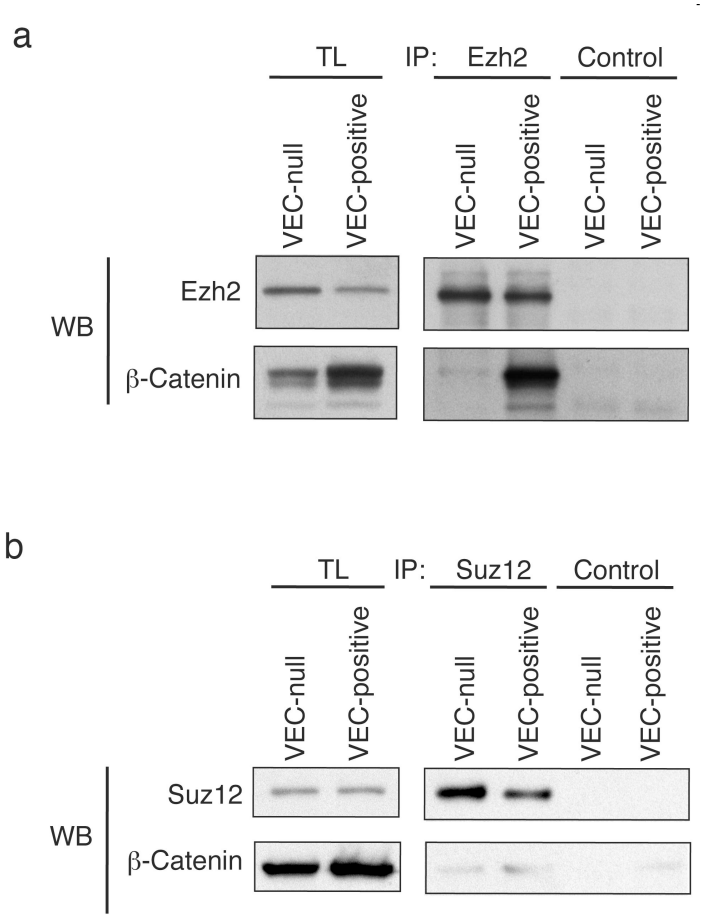

Figure 34 β-catenin interacts with PcG proteins

CoIP and WB analysis of either endogenous Ezh2 (**a**) or Suz12 (**b**) and β-catenin from extracts of confluent VEC-null and VEC-positive ECs. TL, total lysate. Negative control Abs used in these experiments were anti-HA tag mouse mAb in (**a**) and non-immune rabbit IgG in (**b**).

β-Catenin/FoxO1 association is known to stabilise FoxO1 binding to *claudin-5* promoter and β-catenin/DNA interaction occurs via Tcf [26]. To test whether the observed β-

catenin/PcG protein association had a similar stabilizing effect on Polycomb binding to target sites we overexpressed in confluent VEC-null cells a dominant negative form of TCF4 (TCF4-DN) [109], containing the DNA-binding domain but lacking the β-catenin-interacting region. TCF4-DN is able to abolish β-catenin/DNA interaction and weakens FoxO1 binding at *claudin-5* promoter [26]. The expression of such construct weakened Ezh2 binding to *claudin-5* and *VE-PTP* promoters (Figure 35), while *vWf* promoter shows only a trend of downregulation. These findings suggest a stabilizing role for β-catenin on PcG protein association to target sites.

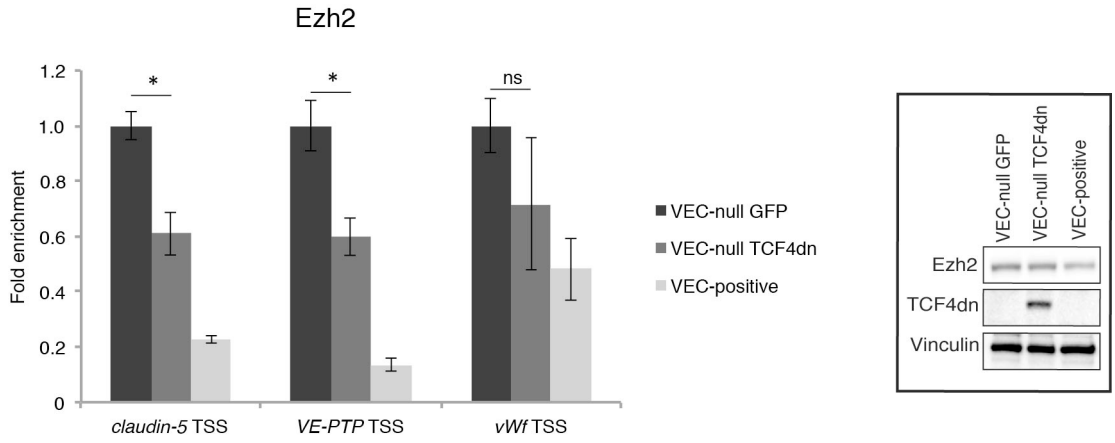

Figure 35 β-catenin stabilises Ezh2 to the the TSS of *claudin-5*, *VE-PTP* genes

qRT-PCR for the TSS of *claudin-5*, *VE-PTP* and *vWf* performed on endogenous Ezh2-bound chromatin immunoprecipitated from confluent VEC-null ECs expressing either TCF4-DN or GFP (as a negative control) and VEC-positive ECs. Columns are means ± s.d. of the fold enrichment normalized on the signal of VEC-null GFP cells (n=3). *t*-test: $*P < 0.05$. Inset: WB analysis of TCF4-DN (V5 tag) and Ezh2 in extracts from confluent VEC-null ECs expressing either TCF4-DN or GFP and VEC-positive ECs. Vinculin was used as loading control.

VE-cadherin associates with Ezh2 and sequesters it at the plasma membrane

The strong Ezh2/β-catenin association detected in confluent VEC-positive cells (Figure 34a) prompted us to hypothesize an alternative role for their interaction in this cell type. Surprisingly, Ezh2 co-immunoprecipitated with endogenous full length VE-cadherin (Figure 36a) suggesting that Ezh2/β-catenin interaction in VEC-positive cells might occur preferentially at cadherin complexes. Conversely, no interaction was detected between Ezh2 and N-cadherin (Figure 36b), which is strongly upregulated in the absence of VE-cadherin in confluent VEC-null cells [19]. Ezh2/VE-cadherin interaction was confirmed both *in vitro* using another anti-Ezh2 antibody (Millipore) (Figure 37) and *in vivo* from adult mice-derived whole lung extracts (Figure 38).

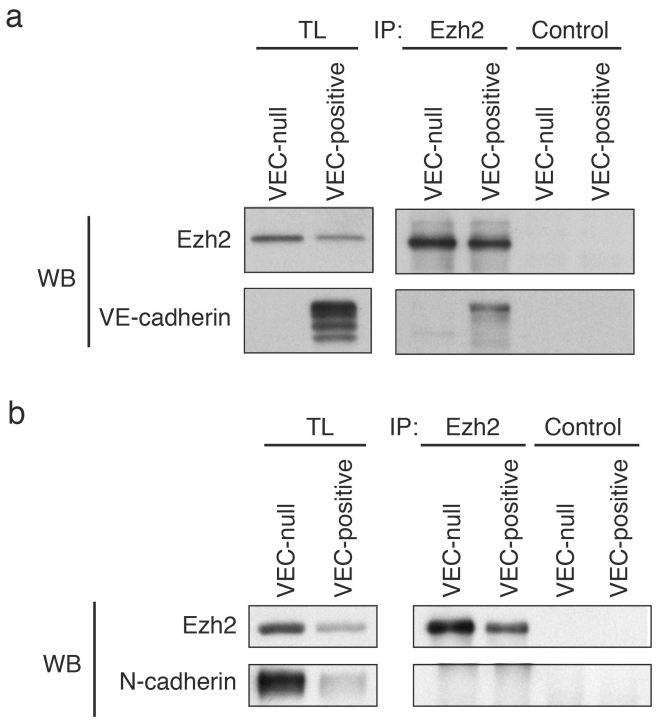

Figure 36 Ezh2 associates with VE-cadherin but not with N-cadherin *in vitro*

CoIP and WB analysis of endogenous Ezh2 with either VE-cadherin (**a**) or N-cadherin (**b**) from extracts of confluent VEC-null and VEC-positive ECs. TL, total lysate. In both (**a**) and (**b**) anti-HA tag mouse mAb was used as negative control Ab.

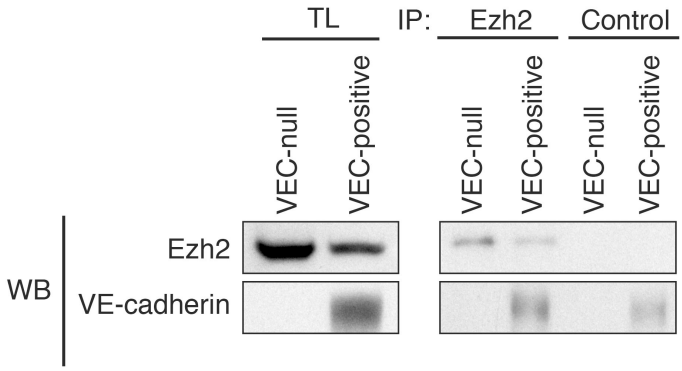

Figure 37 Ezh2 association with VE-cadherin probed with a different antibody (Millipore)

CoIP and WB analysis of endogenous Ezh2 with VE-cadherin from extracts of confluent VEC-null and VEC-positive ECs. TL, total lysate. Non-immune rabbit IgG were used as negative control.

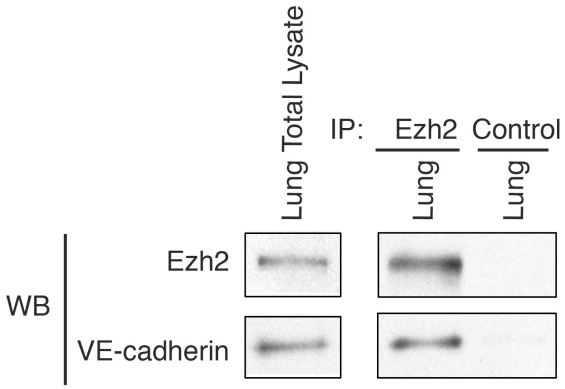

Figure 38 Ezh2 associates with VE-cadherin *in vivo*

CoIP and WB analysis of Ezh2 and VE-cadherin from murine whole lung extracts. Anti-HA tag mouse mAb was used as negative control Ab.

We also checked if VE-cadherin could interact also with other PcG proteins. Surprisingly, we could not see any VE-cadherin co-immunoprecipitated by anti-Suz12 Ab (Figure 39),

thus suggesting that VE-cadherin binds selectively Ezh2 protein and not other PcG proteins.

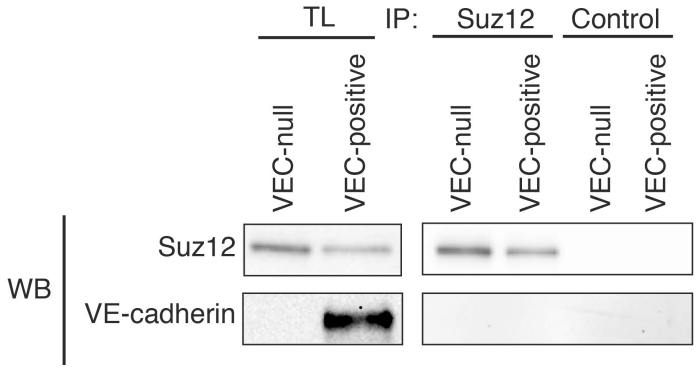

Figure 39 Suz12 does not interact with VE-cadherin

CoIP and WB analysis of endogenous Suz12 with VE-cadherin from extracts of confluent VEC-null and VEC-positive ECs. TL, total lysate. Non-immune rabbit IgG were used as negative control Ab.

Cytoplasmic localization of Ezh2 has been previously described [122]. Moreover, membrane sequestration of another PcG protein, Eed, via interaction with Nef or activated integrins is a known mechanism exploited by human immunodeficiency virus (HIV) to reduce nuclear PcG protein activity and promote Trans-Activator of Transcription (Tat)-/Negative Regulatory Factor (Nef)-mediated transcription of the viral genome [123]. Biotinylation of cell surface proteins further proved that Ezh2 associates with biotinylated VE-cadherin exposed on the membrane (Figure 40), supporting the hypothesis that the observed cadherin-Ezh2 interaction sequesters the Polycomb protein at the cell membrane.

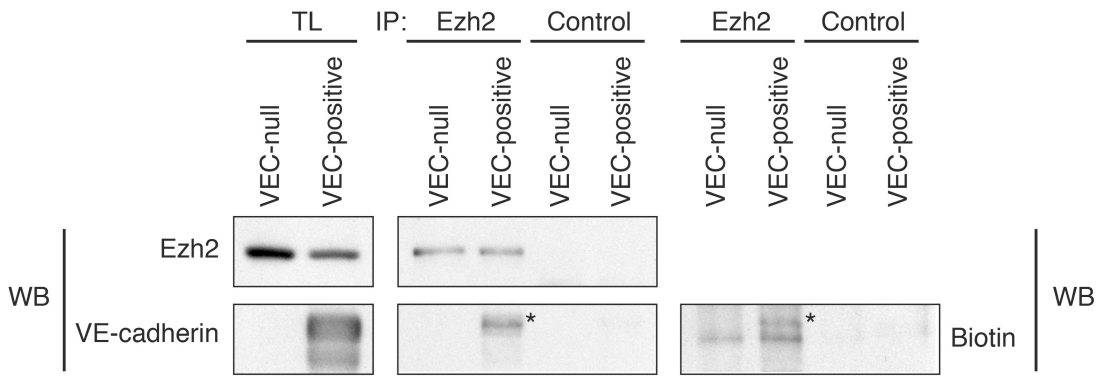

Figure 40 Ezh2 interacts with VE-cadherin at the plasma membrane

CoIP and WB analysis of endogenous Ezh2 and VE-cadherin from extracts of confluent VEC-null and VEC-positive ECs after biotinylation of membrane proteins. TL, total lysate. * marks the biotinylated band of VE-cadherin specifically immunoprecipitated by Ezh2 in VEC-positive ECs. Anti-HA tag mouse mAb was used as negative control Ab.

Within the framework of trying to characterise Ezh2/VE-cadherin interaction, we investigated a putative role for β-catenin. Ezh2-VE-cadherin association was strongly reduced in a β-catenin-knockout endothelial cell line derived from adult mouse lung (β-catenin KO) (Monica Corada, unpublished data) compared to the wild-type counterpart (β-catenin WT) (Figure 41).

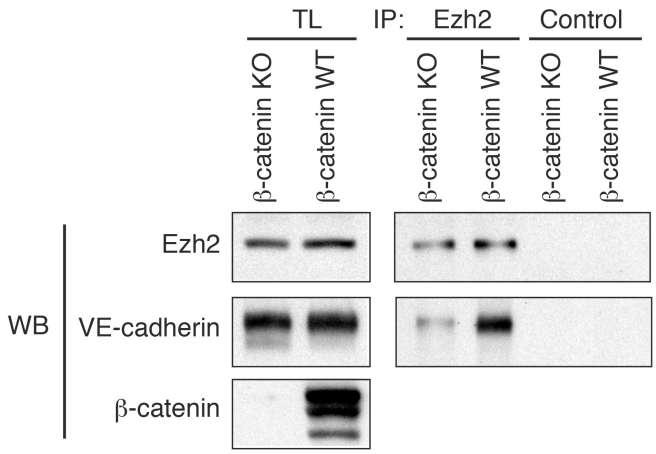

Figure 41 β-catenin mediates Ezh2 binding to VE-cadherin

CoIP and WB analysis of endogenous Ezh2 and VE-cadherin from extracts of confluent β-catenin KO and β-catenin WT ECs. TL, total lysate. Anti-HA tag mouse mAb was used as negative control Ab.

Furthermore, VEC-null cells were reconstituted with a truncated mutant of VE-cadherin lacking the β-catenin-binding domain (Δβcat) [22]. This VE-cadherin mutant is unable to sequester β-catenin at the membrane and displayed a marked reduction of Ezh2 binding (Figure 42). Interestingly, β-catenin was not the only VE-cadherin partner regulating Ezh2 association. The expression of another VE-cadherin mutant, lacking the p120-catenin binding site but still able to bind β-catenin (Δp120) [22] showed an even greater reduction of Ezh2 association (about 90% reduction in Δp120 and 60% reduction in Δβcat compared to wild-type VE-cadherin) (Figure 42a and b).

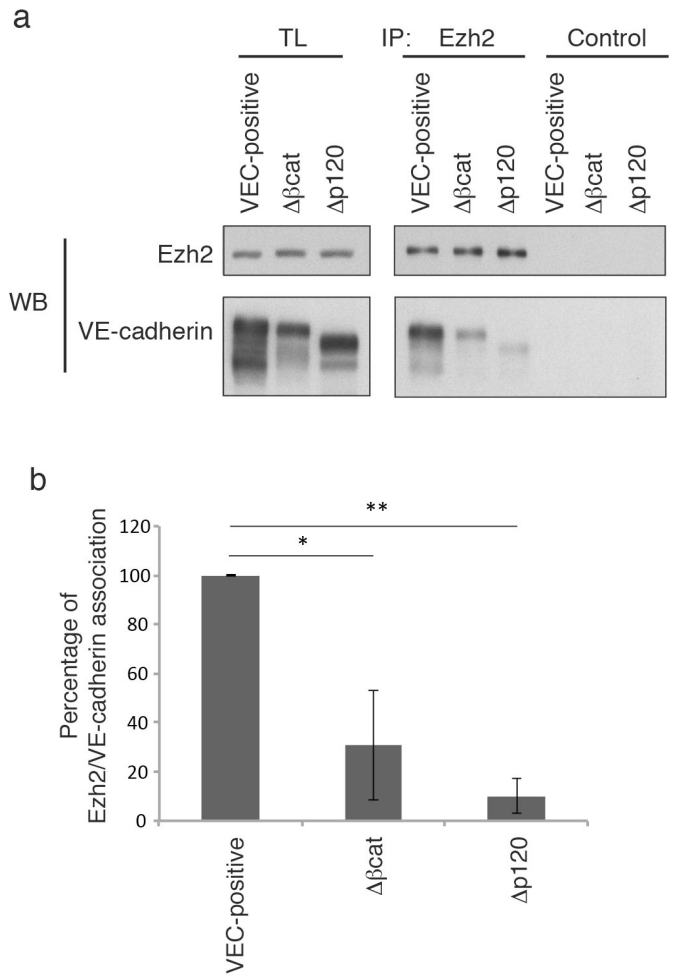

Figure 42 Ezh2/VE-cadherin association is reduced in both Δβcat and Δp120 ECs

(**a**) CoIP and WB analysis of Ezh2 and VE-cadherin from extracts of confluent VEC-positive, Δβcat and Δp120 ECs. TL, total lysate. Δβcat and Δp120 VE-cadherin mutants show a lower molecular weight compared to WT VE-cadherin due to the deletion in their cytoplasmic tail (see also Lampugnani et al., 2002). Anti-HA tag mouse mAb was used as negative control Ab.

(**b**) Quantification of relative Ezh2/VE-cadherin association normalized to VEC-positive ECs (n=3). *t*-test: $*P < 0.05$; $**P < 0.01$.

In line with this observation, Ezh2 co-immunoprecipitated with endogenous p120-catenin as well (Figure 43). Altogether, these results show that Ezh2 is recruited at cell-cell contacts by clustered VE-cadherin and such association depends on cadherin binding to β-catenin and p120-catenin.

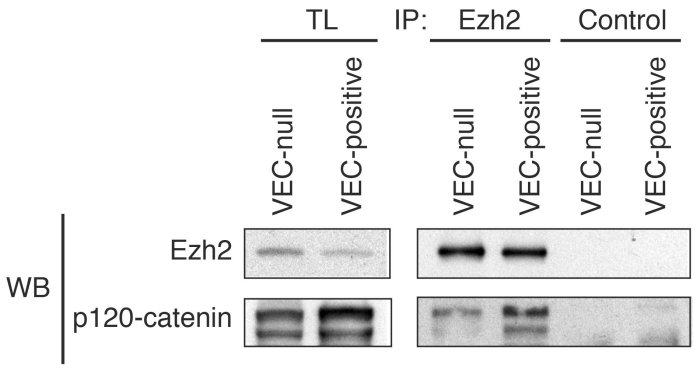

Figure 43 Ezh2 interacts with p120 catenin

CoIP and WB analysis of endogenous Ezh2 with p120-catenin from extracts of confluent VEC-null and VEC-positive ECs. TL, total lysate. Anti-HA tag mouse mAb was used as negative control Ab.

Accordingly, *claudin-5*, *VE-PTP* and *vWf* gene expression was strongly reduced in Δp120 cells (Figure 44). These findings suggest that the inhibition of p120 binding to VE-cadherin most likely reduces the amount of Ezh2 that is sequestered out of the nucleus by VE-cadherin, thus facilitating the repression *claudin-5*, *VE-PTP* and *vWf*.

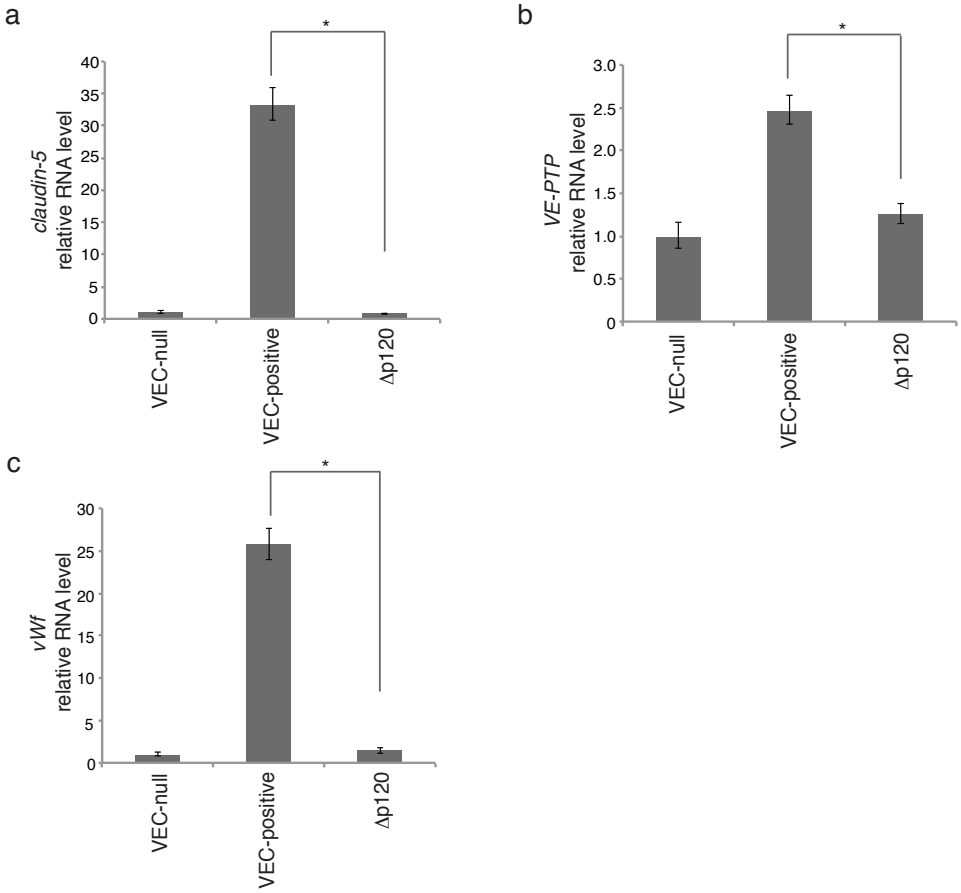

Figure 44 Δp120 ECs fail to upregulate *claudin-5*, *VE-PTP* and *vWf*

qRT-PCR analysis of *claudin-5* (**a**), *VE-PTP* (**b**) and *vWf* (**c**) in confluent VEC-null, VEC-positive and Δp120 ECs. The levels of mRNA are normalized to 18S. Columns are means ± s.d. of triplicates from representative experiments (n=3). *t*-test: * $P<0.01$.

VE-cadherin regulates Ezh2 expression level

The data collected so far proved that VE-cadherin is able to regulate PcG protein activity at *claudin-5*, *VE-PTP* and *vWf* promoters by finely tuning PcG protein recruitment, through the regulation of FoxO1/β-catenin nuclear availability and Ezh2/VE-cadherin association. However, we noticed an additional mechanism through which VE-cadherin expression and clustering might regulate PcG activity. Ezh2 protein levels were higher in confluent VEC-null cells than in confluent VEC-positive cells (Figure 30). This difference was at least in part due to a higher level of transcription of *Ezh2* gene in VEC-null cells (Figure 45).

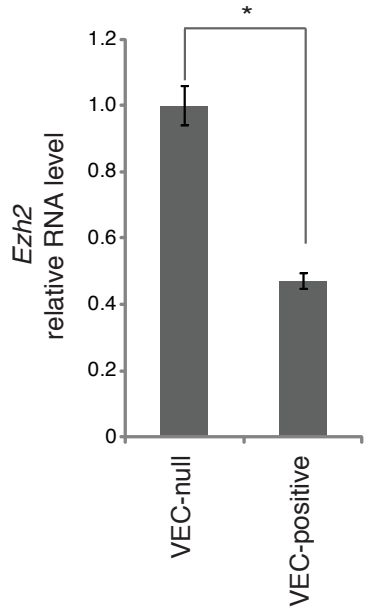

Figure 45 *Ezh2* transcript levels are reduced in VEC-positive ECs

qRT-PCR analysis of *Ezh2* in confluent VEC-null and VEC-positive. The levels of mRNA are normalized to 18S. Columns are means ± s.d. of triplicates from representative experiments (n=3). *t*-test: * $P<0.01$.

Ezh2 has been shown to be a target of hypoxia inducible factor (Hif)1α [124]. Interestingly, we observed that Hif1α was increased both at the mRNA and protein level in VEC-null cells (Figure 46).

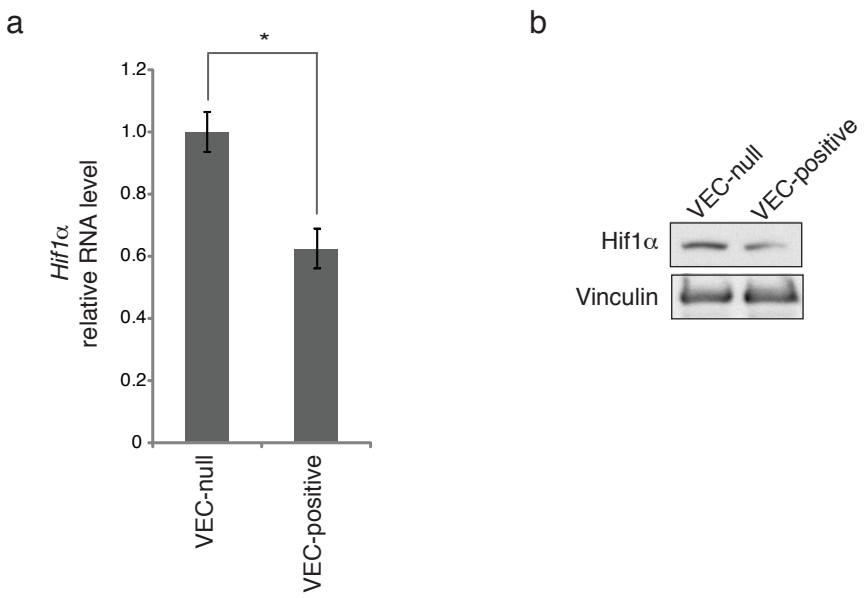

Figure 46 *Hif1α* transcript and protein levels are reduced in VEC-positive ECs

(**a**) qRT-PCR analysis of *Hif1α* in confluent VEC-null and VEC-positive. The levels of mRNA are normalized to 18S. Columns are means ± s.d. of triplicates from representative experiments (n=3). *t*-test: * $P<0.01$. (**b**) WB analysis of Hif1α in extracts from confluent VEC-null and VEC-positive ECs. Vinculin was used as loading control.

Moreover, *Ezh2* is upregulated by E2f transcription factors in endothelial cells [125]. E2f factors are negatively regulated by the binding to hypophosphorylated retinoblastoma protein (pRb) [126]. Confluent VEC-positive cells showed a much higher level of hypophosphorylated pRb than VEC-null cells (Figure 47), in line with a role for E2f factors in determining a reduced *Ezh2* expression in such cell type.

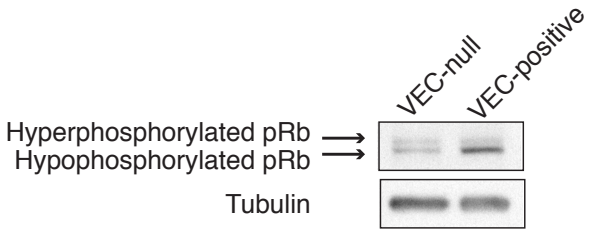

Figure 47 pRb is hypophosphorylated in VEC-positive ECs

WB analysis of hyperphosphorylated (higher band) and hypophoshorylated pRb (lower band) in extracts from confluent VEC-null and VEC-positive ECs. Tubulin was used as loading control.

Polycomb protein overexpression is accompanied by Claudin-5 repression in human ovarian cancer

Previous reports showed that EZH2 is overexpressed by tumour cells and tumour ECs in 66% and 67% of human epithelial ovarian cancer samples analysed, respectively [120, 138]. Increased EZH2 expression in cancer cells and ECs strongly correlates with poor prognosis. We therefore sought to investigate if the reported higher EZH2 levels in human ovarian cancer specimens have an effect on Claudin-5 expression.

By performing double IHC analysis we found that normal ovarian tissue expresses very low, if any, EZH2, both in stromal cells and ECs, as expected for a non-proliferative healthy tissue, while Claudin-5 is massively expressed by virtually every vessel (Figure 48a). Conversely, serous surface papillary ovarian carcinomas show a marked increase in EZH2 protein expression in tumour cells compared to the healthy counterpart, in line with reports by Lu et al. Interestingly, Claudin-5 is strongly reduced in tumour vasculature and this is paralleled by the presence of ECs expressing high EZH2 (Figure 48b). These data show that, at least in the context of serous surface papillary ovarian carcinomas, EZH2 and Claudin-5 levels show an inverse expression pattern in ECs suggesting that Claudin-5 is a PcG protein-target gene *in vivo*.

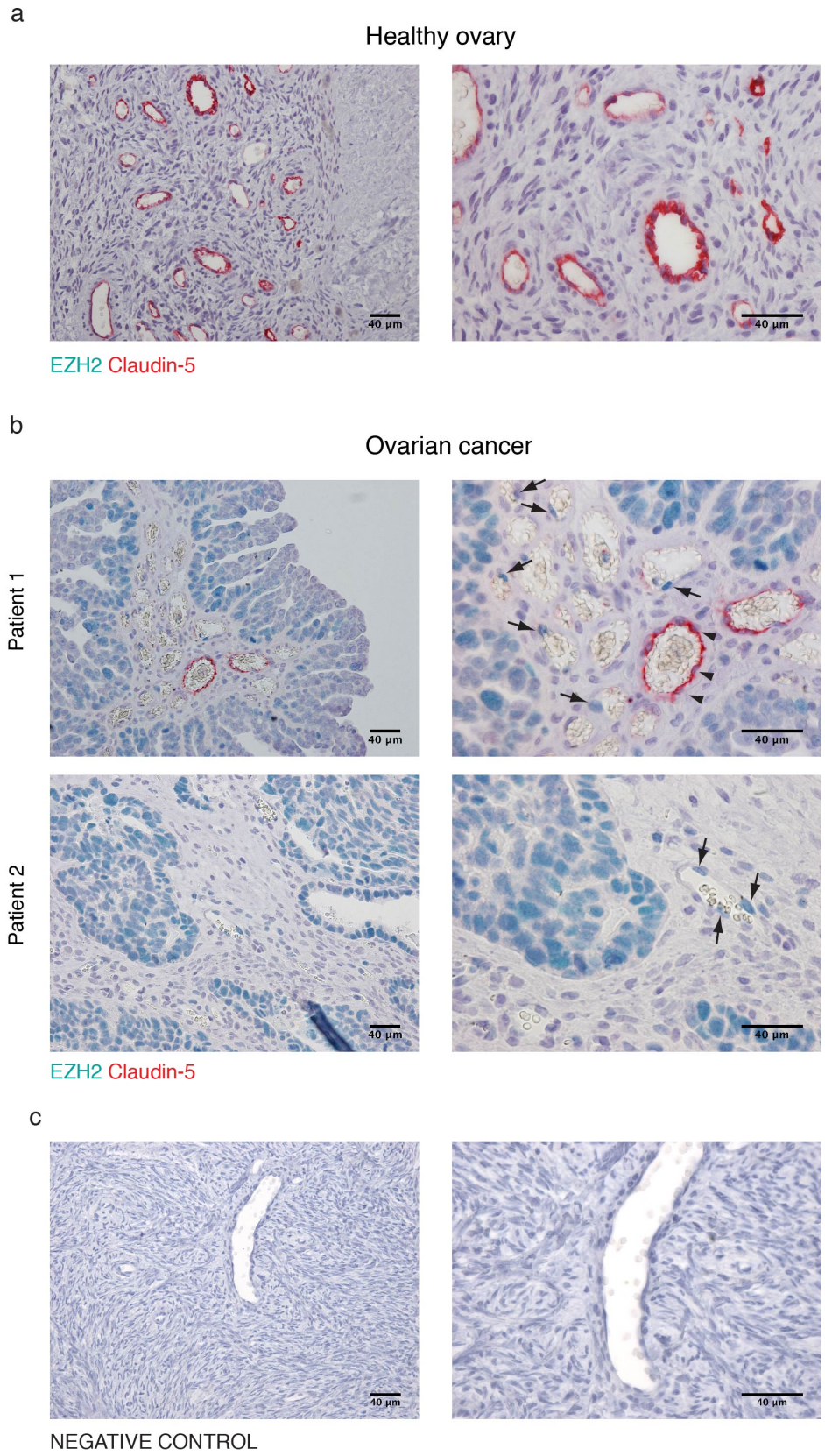

Figure 48 IHC analysis of EZH2 and Claudin-5 in normal and malignant ovarian tissue

Representative images of double IHC analysis showing EZH2 (green) and Claudin-5 (red) in normal ovarian tissue (**a**) and serous surface papillary ovarian carcinoma (**b**). Black arrows in (**b**) indicate blood vessels that contain at least one EZH2-positive ECs and that are simultaneously Claudin-5-negative. Black arrowheads

indicate vessels that express CLAUDIN-5 but no detectable EZH2. (**c**) Double IHC negative control (primary Abs omitted) staining performed on ovarian tissue.

DISCUSSION

We demonstrate here the essential role of VE-cadherin expression and clustering at AJs for the proper expression of endothelial-specific genes linked to vascular stability such as *claudin-5, VE-PTP* and *vWf*. These results confirm and extend previous observations about VE-cadherin-mediated regulation of *claudin-5* expression in ECs [26]. We found that *claudin-5, VE-PTP* and *vWf* are a core set of endothelial-specific genes that are positively regulated by EC-confluency (Figure 10, 11 and 12) and negatively regulated by the activity of FoxO1 and β-catenin (Figure 14, 15 and 16). This is in agreement with the presence of FoxO1 and Tcf/β-catenin-binding sites in the promoter regions of all three analysed genes. Of note, we found also that *claudin-5, VE-PTP* and *vWf* are epigenetically regulated by the activity of PcG and TrxG proteins (Figure 20 and 22), depending on the state of cell confluence and AJ organization. Our data point to a role for FoxO1 and β-catenin in the recruitment of PcG proteins to the promoter of *claudin-5, VE-PTP* and *vWf*, which is necessary to induce gene repression (Figure 31, 32 and 35). Moreover, VE-cadherin facilitates vascular stability gene expression by sequestering Ezh2 at the plasma membrane and this association is dependent on β-catenin- and p120-VE-cadherin binding (Figure 41 and 42). Finally, we show evidence of an inverse expression pattern of endothelial EZH2 and Claudin-5 *in vivo* in human ovarian cancer specimens further supporting the hypothesis of an epigenetic transcriptional regulation of Claudin-5 (Figure 48).

This, to our knowledge, proves for the first time that AJ organisation can influence in multiple ways gene expression at the epigenetic level and provides new insights into the molecular mechanisms governing vascular stabilisation. Here we propose that the presence of VE-cadherin in ECs is necessary to initiate a vascular stability transcriptional programme comprising *claudin-5, VE-PTP* and *vWf* and likely other yet uncharachterized genes. VE-cadherin expression and clustering modulates several genes involved in

different aspects of cellular homeostasis. Among these genes we decided to focus on *claudin-5, VE-PTP* and *vWf* because of their well-known EC-restricted expression pattern and for their previously reported role in promoting vascular stability.

Our findings about EC-confluence-mediated upregulation of *claudin-5, VE-PTP* and *vWf* are in line with data present in the literature. For instance, Nottebaum and coworkers noticed an increase of VE-PTP junctional localization and a partial overlap of VE-PTP with VE-cadherin staining in long-confluent mouse bEnd.3 endothelioma cell line [76]. In addition, Howell *et al.* reported that confluent HUVECs contain a larger pool of vWf protein compared to sub-confluent cells [127].

Conversely, *claudin-5, VE-PTP* and *vWf* are negatively regulated by the activity of FoxO1 and β-catenin (Figure 14, 15 and 16). Our findings are in line with the previously reported role of FoxO1 as a transcription factor with vascular destabilising functions. Indeed, FoxO1 activity leads to an impairment in tube formation and VEGF-dependent migration in HUVECs [51]. In particular, FoxO1 inhibits the expression of endothelial eNOS and promotes that of Ang-2, both effects leading to a destabilised vessel phenotype [74, 128]. Our data further support the role of FoxO1 as an important regulator of angiogenesis and vascular remodelling, showing that FoxO1 activity is linked to vessel destabilisation, as it exerts an inhibitory effect on the expression of genes playing key roles in junctional and extracellular matrix stability such as *claudin-5, VE-PTP* and *vWf*.

Of note, we found also that *claudin-5, VE-PTP* and *vWf* are epigenetically regulated by the activity of PcG and TrxG proteins, depending on the state of cell confluence and AJ organisation. We observed that the presence of VE-cadherin itself is able to modulate PcG protein levels and activity. In the absence of VE-cadherin, ECs display higher levels of PcG proteins and a higher enrichment in H3K27me3 on the TSS of the analysed gene, which correlate with their repressed state (Figure 20). As shown in Figure 45, VEC-null ECs display higher *Ezh2* transcript levels if compared to VEC-positive ECs. This is in line

with the observed higher activity of both E2f transcription factors and Hif1α, two well-known activators of *Ezh2* gene expression [124, 129] (Figure 46, 47 and 49).

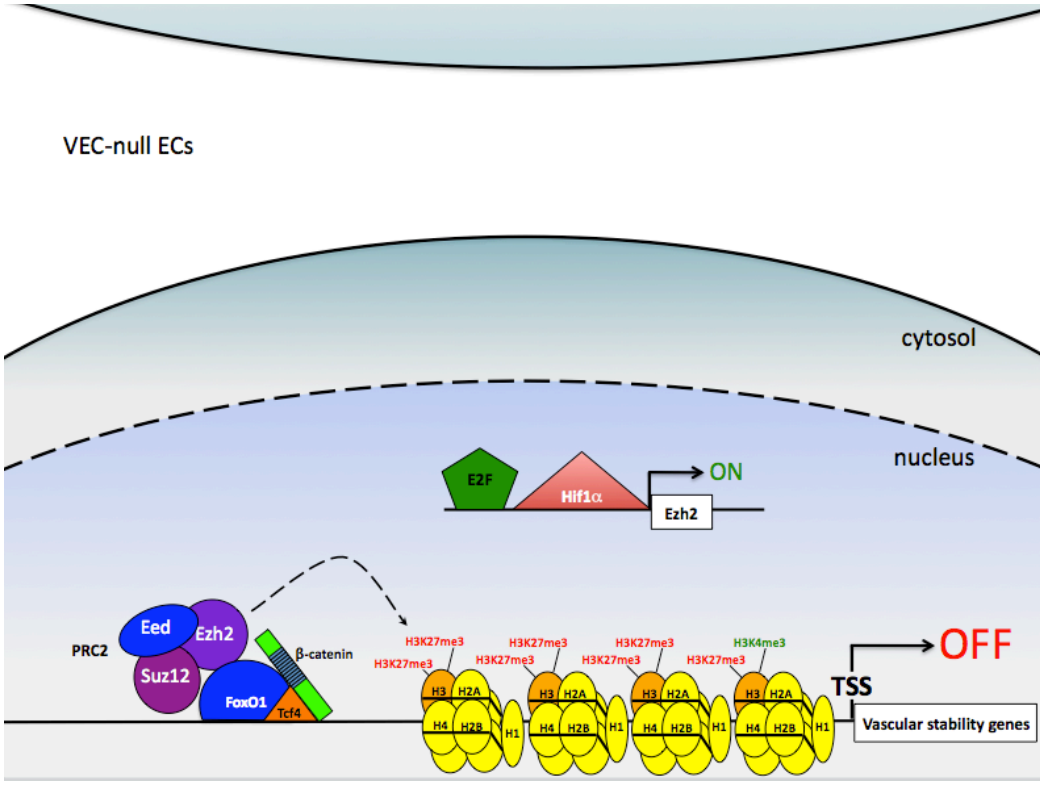

Figure 49 Schematic representation of PcG-protein-dependent regulation of vascular stability genes in VEC-null ECs

In the absence of VE-cadherin the FoxO1/β-catenin/Tcf4 complex binds to the promoter of *claudin-5, VE-PTP* and *vWf* and represses their expression with the help of PcG proteins which catalyse the deposition of the repressive histone mark H3K27me3.

Conversely, VEC-positive ECs display a reduced PcG protein occupancy on the TSS of *claudin-5, VE-PTP* and *vWf*, compared to VEC-null cells. This is due to the aforementioned transcriptional mechanisms (less E2f and Hif1α activity), to the reduced FoxO1 and β-catenin nuclear levels and to the ability of VE-cadherin to sequester part of Ezh2 out of the nucleus. Furthermore VE-cadherin expression is likely to promote post-translational modifications that modulate PcG protein activity [130] (Figure 50).

Interestingly, AKT is reported to phosphorylate Ezh2 on serine 21 resulting in an inhibition of H3K27me3 deposition [131]. Given that the expression and clustering of VE-cadherin in ECs promotes AKT activation [26], we hypothesize that this mechanism could also be involved in dampening PcG protein activity in VEC-positive ECs. Future work will be required to demonstrate this hypothesis but unfortunately specific reagents recognizing phosphorylated PcG proteins are still missing. Strikingly, our biochemical data suggest that the presence of VE-cadherin is able to decrease PcG protein activity in ECs by sequestering at least part of cellular Ezh2 protein away from the nucleus in a p120- and β-catenin-dependent manner (Figure 41, 42 and 50). VE-cadherin/Ezh2 interaction takes place mainly at the plasma membrane, as suggested by membrane protein biotinylation experiments (Figure 40). VE-cadherin/Ezh2 interaction is quite strong as it could be observed also in CoIPs from murine total lung lysates in the absence of crosslinking reactions (Figure 38). Ezh2 binding to VEC was further confirmed by using a second commercial anti-Ezh2 Ab (Rabbit polyclonal 07-689 Millipore) (Figure 37). It is also worth to point out that, in ECs, Ezh2 sequestration at the plasma membrane is selectively exerted by VE-cadherin, as we could not see any Ezh2 binding to N-cadherin neither in VEC-positive nor in VEC-null ECs (which express more N-cadherin compared to VEC-positive ECs [19]). VE-cadherin specifically recruits Ezh2 among PcG proteins, as Suz12 IP did not shows any co-immunoprecipitated VEC (Figure 39). Still, we do not have evidence supporting a direct binding of Ezh2 to VE-cadherin, nor to p120 or β-catenin, so we cannot rule out that Ezh2 sequestration to VE-cadherin at the plasma membrane might be mediated by another protein binding to VE-cadherin cytoplasmic tail. To understand this aspect pull down assays combining full length proteins or deletion mutants are required.

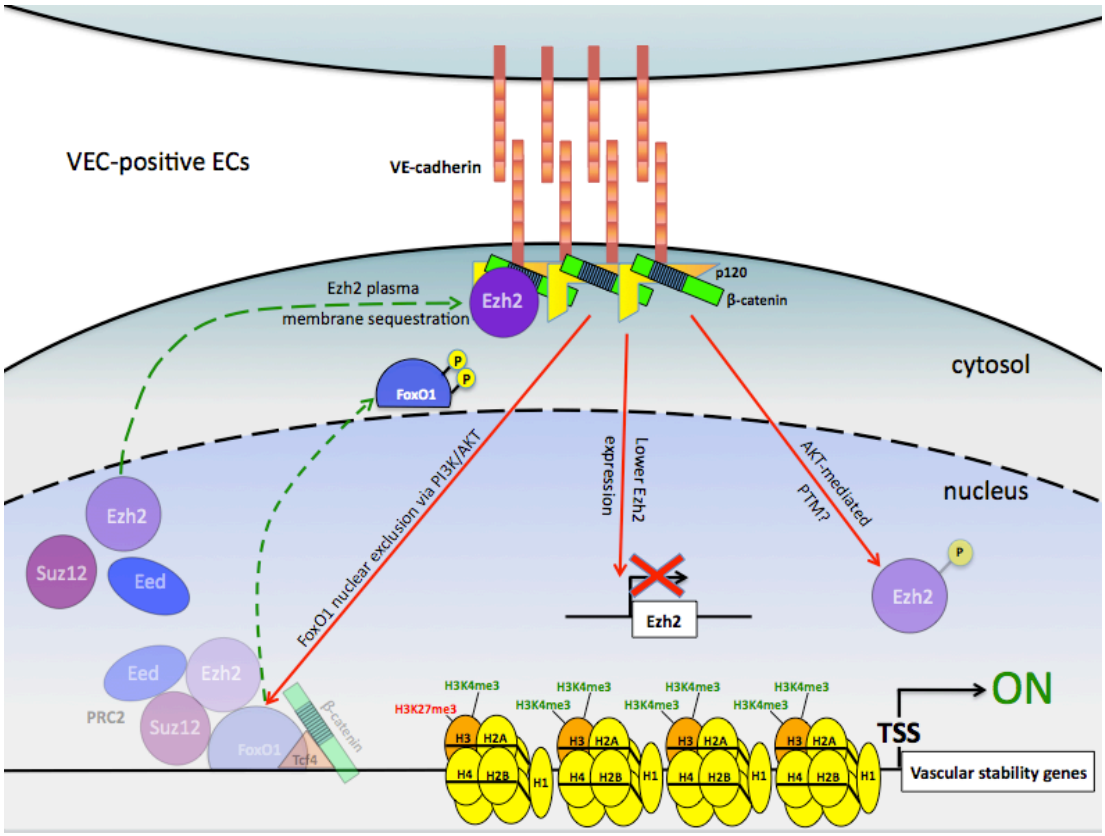

Figure 50 Schematic representation of vascular stability gene activation in VEC-positive ECs

The presence of VE-cadherin promotes the expression of *claudin-5, VE-PTP* and *vWf* vascular stability genes in multiple ways: 1) the nuclear exclusion of the transcription factor FoxO1 through PI3K/AKT pathway activation, 2) the β-catenin- and p-120-dependent sequestration of part of cellular Ezh2 at the plasma membrane, 3) the reduction in *Ezh2* transcript levels and 4) the AKT-mediated post-translational modifications (PTM). These events cooperate to dampen PcG protein activity and to favour vascular stability gene expression.

In the literature PcG proteins were previously reported to have atypical localizations, interactions and functions beside their well-known role as histone modifiers. For instance, Witte *et al.* showed that the PcG protein EED can be bound by the N-terminus of the HIV protein Nef and sequestered at the plasma membrane. This allows a de-repression of the HIV genome in order to permit Tat-dependent viral transcription [123]. Su and coworkers, instead, showed that a cytosolic pool of Ezh2 exists at least *ex vivo* in thymocytes and

purified lymph node T cells and in several cell lines such as Jurkat, mouse embryonic fibroblasts (MEFs) and HEK-293. The authors also show that cytosolic Ezh2 is bound to Suz12, Eed and the GTP/GDP exchange factor Vav1 and still retains histone methyl transferase activity although its cytosolic substrates remain unknown. Strikingly, T-cell-restricted *Ezh2* deletion does not affect H3K27me3 levels while it impairs T-cell Receptor (TCR)-dependent actin polymerization acting upstream of Cdc42 and Rac1 [122]. Altogether these data suggest that, even if the major role of PcG proteins remains modifying histone tails to regulate gene expression, several members of PcG proteins could reside and work also in cellular compartments different from the nucleus exerting functions unrelated to histone modification.

As stated above, different mechanisms most likely work together to reduce PcG protein activity in VEC-positive ECs (Figure 50) resulting in high H3K4me3 levels on the TSS of *claudin-5, VE-PTP* and *vWf* that overcome H3K27me3 and facilitate gene expression. We can speculate that these higher H3K4me3 levels in VEC-positive ECs might be due to a higher activity of TrxG protein complexes. Set1A-, Set1B- and Mll-containing TrxG complexes are reported in the literature to be the only multiprotein complexes able to catalyse the deposition of the activating histone mark H3K4me3 [83, 101]. Future work will be required to address how TrxG proteins are recruited to these loci and how they act at the molecular level in order to turn on the expression of *claudin-5, VE-PTP* and *vWf*.

The presence of PcG protein-derived and TrxG protein-derived histone marks (H3K27me3 and H3K4me3, respectively) on the TSS of *claudin-5, VE-PTP* and *vWf* is not trivial given the well documented roles of these two histone marks in regulating the expression of a wide variety of target genes. PcG proteins have been extensively studied for their involvement in the regulation of developmental genes in ES cells, where they often induce the establishment of the so-called "bivalent domains", regions of the genome harbouring both H3K27me3 and H3K4me3 histone marks [82, 83]. Bivalent domains are eventually resolved during differentiation leading to either H3K27me3-marked (repressed)

or H3K4me3-marked (active) regions. In this way, the regulated developmental genes are believed to be maintained repressed but poised for activation [82]. *Claudin-5, VE-PTP* and *vWf* simultaneously show both H3K27me3 and H3K4me3 on their TSSs and the balance between these two histone marks depends on cell confluence and junction organization. We suggest therefore that bivalent domains exist in ECs and are involved in keeping *claudin-5, VE-PTP* and *vWf* genes in a repressed/poised for activation state in VEC-null or sparse VEC-positive cells. Once ECs reach confluence and VE-cadherin is expressed and clustered at AJs, bivalent domains are resolved towards the full activation state of *claudin-5, VE-PTP* and *vWf*, leading to a quiescent, mature and stabilised endothelial cell layer.

Despite the huge improvements that were made in the last decade in the field of PcG protein biology, we still do not fully understand the molecular mechanisms that drive PcG protein binding to target genes. PcG protein targeting is much better defined in *Drosophila melanogaster* where PcG proteins "land" on *cis*-regulatory binding platforms called PREs ensuring the consequent repression on target genes [86, 87, 132]. Conversely, in mammals, very little is known about how PcG proteins are targeted to specific genes. Previous publications suggested that mammalian PcG proteins might be recruited to chromatin by associating with DNA-binding partners [84, 86, 87, 100]. For instance, the transcription factor Snail1 has been shown to interact with members of the PRC2 complex, such as Suz12 and Ezh2, targeting them to the DNA to specifically inhibit the expression of *E-cadherin* [100]. Recently, two other transcription factors were reported to be involved in the regulation of PcG targeting. Mulero *et al.* showed that Nuclear factor of kappa light polypeptide gene enhancer in B cells inhibitor, alpha (IκBα) interacts with Ezh2, Suz12 and Bmi1 and that, following TNFα treatment, Suz12 detaches from IκBα-target genes suggesting that IκBα could regulate PcG protein association to these regions [133]. Another example of PcG protein-recruiting factor is the RE1-silencing transcription factor (REST). Dietrich and co-workers showed that, in NT2-D1 human teratocarcinoma cells and mouse embryonic stem (mES) cells, REST interacts with both PRC1 and PRC2 and is required for PcG protein

binding to a subset of REST target genes involved in neuronal differentiation [134]. These and many other reports in the literature suggest that PcG protein targeting could be strongly cell type- and genomic context-dependent.

Likewise, in our study we found that the cooperation between PcG proteins and 2 new putative recruiting factors, FoxO1 and β-catenin, is required for the proper repression of specific genes in ECs. The overexpression of FKHR-TM in VEC-positive cells increased H3K27me3 levels on the TSS of *claudin-5, VE-PTP* and *vWf* correlating with their repressed state (Figure 31, 32, 51 and see Taddei et al., 2008). Our experiments demonstrate also that PcG proteins form a complex with FoxO1 both in endogenous and overexpression conditions. Counterintuitively, we found that PcG proteins interact with FoxO1 also in VEC-positive ECs. We still do not know the function of this interaction, however in this cell type the complex is not targeted to chromatin, as VE-cadherin expression promotes FoxO1 phosphorylation and nuclear exclusion and no binding of either FoxO1 or β-catenin was detected to any of the promoter regions of the analysed genes in confluent VEC-positive cells (Figure 18 and 19) [26, 47, 48].

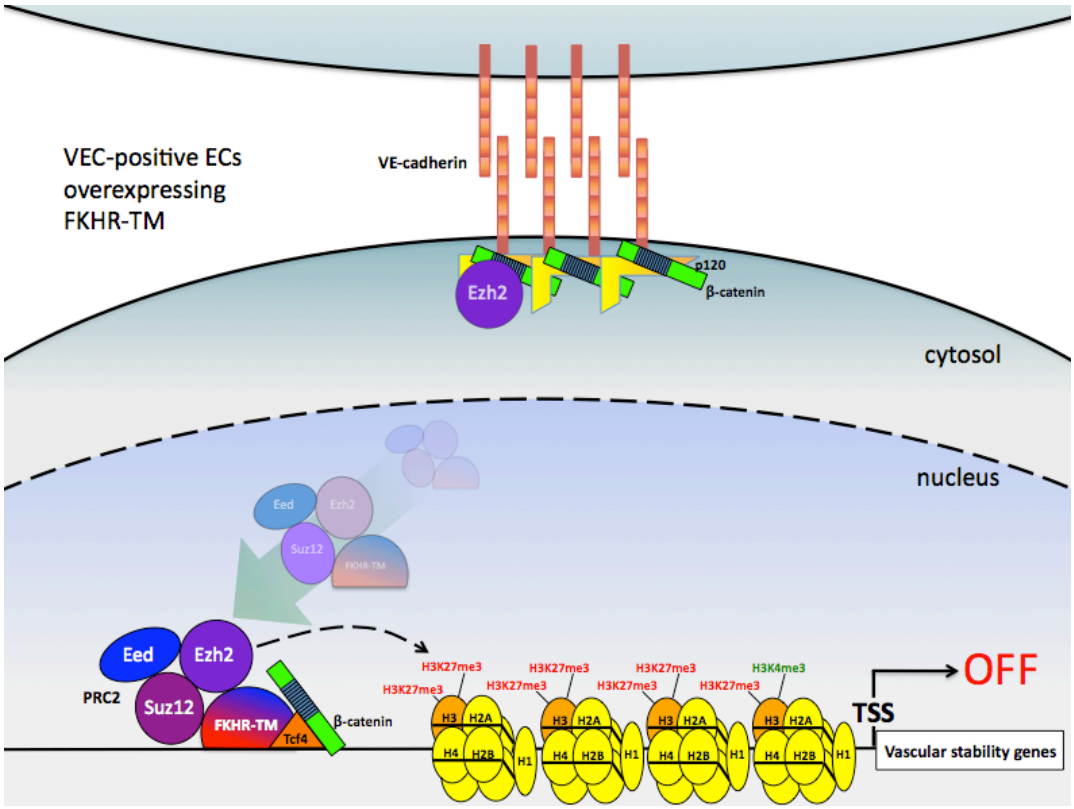

Figure 51 Proposed model for PcG-protein recruitment by FoxO1 (FKHR-TM) in VEC-positive ECs

Upon FKHR-TM overexpression, PcG proteins are recruited to the promoters of *claudin-5, VE-PTP* and *vWf* and, through the deposition of the repressive histone mark H3K27me3, these vascular stability genes undergo repression.

These data explain also why PcG protein overexpression in VEC-positive cells leads to a significant reduction of *claudin-5, VE-PTP* and *vWf* expression which, however, does not reach the levels of repression observed in VEC-null cells. Indeed, in confluent VEC-positive cells, the amount of de-phosphorylated (active) FoxO1 available in the nucleus and able to actively target PcG proteins to chromatin is strongly reduced [26], rendering the recruiting mechanism inefficient.

Concerning β-catenin, our results point to a dual role for this protein in the regulation of *claudin-5, VE-PTP* and *vWf* expression. While membrane-localized β-catenin allows Ezh2/VE-cadherin association (Figure 50), facilitating vascular stability gene expression, on the other hand β-catenin nuclear localization seems to stabilise PcG protein association

to target gene promoters, likely strengthening FoxO1/DNA binding (Figure 49). In line with this hypothesis, the inhibition of β-catenin association to DNA-bound Tcf4 reduces PcG protein targeting to *claudin-5* and *VE-PTP* promoters, while Ezh2 binding to *vWf* promoter is only mildly reduced upon TCF4dn overexpression (Figure 35). Future work will be required to better dissect the molecular mechanisms involved in such dual role.

Our results however suggest that inhibiting PcG activity is not sufficient for a full reactivation of the analysed vessel stabilisation genes. In fact, PcG protein knockdown in VEC-null ECs led only to a modest de-repression of *claudin-5, VE-PTP* and *vWf* reaching an expression level far lower than that observed in confluent VEC-positive ECs. This parallels evidence in literature showing that many genes are unable to undergo a full reactivation after PcG protein knockdown. For example SW-60 cells stably expressing siRNA against either Suz12 or Ezh2 show only a mild de-repression of *E-cadherin* gene [100]. Our results therefore suggest two possible scenarios. PRC1 has been reported to bind certain target genes even in the absence of PRC2 recruitment [135, 136]. This complex itself could therefore be responsible for maintaining *claudin-5, VE-PTP* and *vWf* in a repressed state. Alternatively, VEC-null ECs might lack one or more activators of transcription needed to accomplish the full expression of *claudin-5, VE-PTP* and *vWf*. Previous publications pointed at sex-determining region (SRY)-box (SOX) and E twenty six (ETS) factors as putative activators of *claudin-5* and *vWf* transcription, respectively [112, 137, 138] and preliminary results suggest a lower expression of such TFs in the absence of VE-cadherin expression and clustering. Future work will be required to elucidate the possible involvement of these TFs or of the PRC1 complex in the regulation of the analysed genes.

Vascular stabilisation is altered in many pathological conditions such as stroke and cancer, where blood vessels are strongly disorganised and present a high, uncontrolled permeability. Tumour vessels, for instance, display uneven pericyte coverage and ECs with disorganized cell-cell junctions, often detached from the basal membrane. This has profound consequences at the clinical level. Leaky vessels cause regions of severe

hypoxia, increased interstitial pressure and offer cancer cells a preferential route for metastatic dissemination [54]. Thus, finding therapeutical approaches able to efficiently "normalise" abnormal vessels and restore the physiological control of permeability would be a huge improvement for cancer treatment allowing an increased delivery of chemotherapeutic drugs to tumour cells and creating a barrier against cancer cell intravasation and metastasis dissemination [54, 139].

Recent publications showed vessel normalisation as an efficient approach for cancer treatment. For instance, *Phd2* haploinsufficient mice show normalised tumour blood vessels, increased tumour perfusion, reduced cancer cell intravasation and metastasis and a better response to chemotherapy [139-141]. PcG protein Ezh2 is emerging as a key player regulating neoplastic growth and tumour vessel organization [125, 142-144]. Epithelial ovarian cancer patients expressing high levels of Ezh2 in tumour cells and ECs have worse prognosis [125, 142]. In ovarian cancer-derived ECs Ezh2 has been proved to repress vasohibin1 (VASH1), an inhibitor of angiogenesis, by directly binding to its promoter, leading to abnormal and uncontrolled vessel growth in the tumour mass [125]. The inhibition of Ezh2 by *in vivo* siRNA delivery or using available chemical inhibitors such as 3-Deazaneplanocin A (DZnep) has effects both on tumour vessels and cancer cells [143, 144]. These approaches lead to reduced tumour microvessel density and cancer cell proliferation while increasing vessel pericyte coverage and tumour cell apoptosis, resulting in tumour shrinkage [125, 143, 144]. In addition to this, we found that human ovarian cancer specimens often show an increased EZH2 protein level both in tumour cells and in ECs, thus confirming what previously published by Sood and coworkers [125, 142]. The higher EZH2 expression in ECs is paralleled by a dramatic decrease in Claudin-5. Conversely, fimbriae (not shown) and ovary specimens from healthy donors show no detectable EZH2 expression (neither in stromal cells nor in ECs) and a high expression of Claudin-5 in blood vessels (Figure 48). These findings suggest that an inverse correlation exists between the expression of EZH2 and Claudin-5 *in vivo* and could explain the very high interstitial

fluid pressure (IFP) observed in ovarian cancer tissues by Goel and coworkers [64]. Indeed, lack of Claudin-5 in ovarian cancer could lead to an increase in vascular permeability to cells and solutes, causing a rise in IFP. More *in vivo* experiments are being performed to confirm such regulation also for *VE-PTP* and *vWf*. Data from several research groups [125, 142-144] complement our results and support the idea that Ezh2 activity is linked to vascular proliferation and destabilisation. This makes Ezh2 an interesting therapeutic target that can be exploited to normalize destabilised tumour vessels in ovarian cancer, the fourth most common cause of cancer-related death in women and the most lethal tumour type in gynecological neoplasms [145, 146]. In this perspective, acting on the VE-cadherin/FoxO1/PcG pathway, for example through DZnep-induced Ezh2 inhibition, could result in the upregulation of *claudin-5*, *VE-PTP* and *vWf* in tumour ECs. This would re-establish a correct vascular stability and permeability control and would efficiently obstruct metastatic cell intravasation.

In conclusion, we found that VE-cadherin expression and clustering at endothelial cell-cell junctions and the consequent modulation of the FoxO1/β-catenin pathway have broad effects on EC maturation, beyond the previously reported *claudin-5* upregulation [26]. Indeed, VE-cadherin, by indirectly inhibiting PcG protein activity via multiple mechanisms, drives the expression of a cluster of genes of key importance for vascular stabilisation including *VE-PTP* and *vWf* and likely others not yet identified. This, to our knowledge, proves for the first time that AJ organisation can influence gene expression at the epigenetic level and provides new insights into the understanding of vascular stabilisation control, which might help developing new therapeutic approaches for a set of pathologies characterized by vessel instability such as cancer.

REFERENCES

1. Boron, W. F. & Boulpaep, E. L. in *Medical physiology: a cellular and molecular approach* 1319 (Elsevier Saunders, Philadelphia, Pa., 2005).
2. Carmeliet, P. Angiogenesis in life, disease and medicine. *Nature* **438**, 932-6 (2005).
3. Potente, M., Gerhardt, H. & Carmeliet, P. Basic and Therapeutic Aspects of Angiogenesis. *Cell* **146**, 873-887 (2011).
4. De Val, S. & Black, B. L. Transcriptional control of endothelial cell development. *Developmental cell* **16**, 180-95 (2009).
5. Drake, C. J. & Fleming, P. a. Vasculogenesis in the day 6.5 to 9.5 mouse embryo. *Blood* **95**, 1671-9 (2000).
6. Carmeliet, P. & Jain, R. K. Molecular mechanisms and clinical applications of angiogenesis. *Nature* **473**, 298-307 (2011).
7. Herbert, S. P. & Stainier, D. Y. R. Molecular control of endothelial. *Nature Publishing Group* **12**, 551-564 (2011).
8. Adams, R. H. & Alitalo, K. Molecular regulation of angiogenesis and lymphangiogenesis. **8**, 464-478 (2007).
9. Phng, L. K. & Gerhardt, H. Angiogenesis: a team effort coordinated by notch. *Dev. Cell.* **16**, 196-208 (2009).
10. Hayashi, M. *et al.* VE-PTP regulates VEGFR2 activity in stalk cells to establish endothelial cell polarity and lumen formation. *Nature Communications* **4**, 1615-1672 (2013).
11. Zeeb, M., Strilic, B. & Lammert, E. Resolving cell-cell junctions: lumen formation in blood vessels. *Curr. Opin. Cell Biol.* **22**, 626-632 (2010).
12. Lenard, A. *et al.* In vivo analysis reveals a highly stereotypic morphogenetic pathway of vascular anastomosis. *Dev. Cell.* **25**, 492-506 (2013).
13. Dejana, E. & Giampietro, C. Vascular endothelial-cadherin and vascular stability. *Curr. Opin. Hematol.* **19**, 218-223 (2012).
14. Dejana, E. Endothelial cell-cell junctions: happy together. *Nature reviews.Molecular cell biology* **5**, 261-70 (2004).
15. Patel, S. D., Chen, C. P., Bahna, F., Honig, B. & Shapiro, L. Cadherin-mediated cellâ€“cell adhesion: sticking together as a family. *Curr. Opin. Struct. Biol.* **13**, 690-698 (2003).
16. Harris, T. J. C. & Tepass, U. Adherens junctions: from molecules to morphogenesis. *Nature reviews.Molecular cell biology* **11**, 502-14 (2010).
17. Lampugnani, M. G. *et al.* CCM1 regulates vascular-lumen organization by inducing endothelial polarity. *J. Cell. Sci.* **123**, 1073-80 (2010).
18. Cavallaro, U. & Dejana, E. Adhesion molecule signalling: not always a sticky business. *Nature reviews.Molecular cell biology* **12**, 189-97 (2011).
19. Giampietro, C. *et al.* Overlapping and divergent signalling pathways of N- and VE-cadherin in endothelial cells. *Oncology* (2012).
20. Luo, Y. & Radice, G. L. N-cadherin acts upstream of VE-cadherin in controlling vascular morphogenesis. *J. Cell Biol.* **169**, 29-34 (2005).
21. Carmeliet, P. *et al.* Targeted deficiency or cytosolic truncation of the VE-cadherin gene in mice impairs VEGF-mediated endothelial survival and angiogenesis. *Cell* **98**, 147-57 (1999).
22. Grazia Lampugnani, M. *et al.* Contact inhibition of VEGF-induced proliferation requires vascular endothelial cadherin, beta-catenin, and the phosphatase DEP-1/CD148. *J. Cell Biol.* **161**, 793-804 (2003).
23. Lampugnani, M. G., Orsenigo, F., Gagliani, M. C., Tacchetti, C. & Dejana, E. Vascular endothelial cadherin controls VEGFR-2 internalization and signaling from intracellular compartments. *J. Cell Biol.* **174**, 593-604 (2006).
24. Furuse, M. Molecular basis of the core structure of tight junctions. *Cold Spring Harb Perspect. Biol.* **2**, a002907 (2010).
25. Steed, E., Balda, M. S. & Matter, K. Dynamics and functions of tight junctions. *Trends Cell Biol.* **20**, 142-9 (2010).

26. Taddei, A. *et al*. Endothelial adherens junctions control tight junctions by VE-cadherin-mediated upregulation of claudin-5. *Nat. Cell Biol*. **10**, 923-34 (2008).
27. Liebner, S. *et al*. Wnt/beta-catenin signaling controls development of the blood-brain barrier. *J. Cell Biol*. **183**, 409-17 (2008).
28. Liebner, S. *et al*. Claudin-1 and claudin-5 expression and tight junction morphology are altered in blood vessels of human glioblastoma multiforme. *Acta Neuropathol*. **100**, 323-331 (2000).
29. Staehelin, L. A. Further observations on the fine structure of freeze-cleaved tight junctions. *J. Cell. Sci*. **13**, 763-786 (1973).
30. Krause, G. *et al*. Structure and function of claudins. *Biochim. Biophys. Acta* **1778**, 631-645 (2008).
31. Ikenouchi, J. *et al*. Tricellulin constitutes a novel barrier at tricellular contacts of epithelial cells. *J. Cell Biol*. **171**, 939-945 (2005).
32. Ikenouchi, J., Sasaki, H., Tsukita, S., Furuse, M. & Tsukita, S. Loss of occludin affects tricellular localization of tricellulin. *Mol. Biol. Cell* **19**, 4687-4693 (2008).
33. Itoh, M. *et al*. Direct binding of three tight junction-associated MAGUKs, ZO-1, ZO-2, and ZO-3, with the COOH termini of claudins. *J. Cell Biol*. **147**, 1351-1363 (1999).
34. Ikenouchi, J., Umeda, K., Tsukita, S., Furuse, M. & Tsukita, S. Requirement of ZO-1 for the formation of belt-like adherens junctions during epithelial cell polarization. **176**, 779-786 (2007).
35. Umeda, K. *et al*. ZO-1 and ZO-2 independently determine where claudins are polymerized in tight-junction strand formation. *Cell* **126**, 741-754 (2006).
36. Mandell, K. J. & Parkos, C. A. The JAM family of proteins. *Adv. Drug Deliv. Rev*. **57**, 857-867 (2005).
37. Bazzoni, G. The JAM family of junctional adhesion molecules. *Curr. Opin. Cell Biol*. **15**, 525-530 (2003).
38. Bazzoni, G. Endothelial tight junctions : permeable barriers of the vessel wall. , 36-42 (2006).
39. Dejana, E., Orsenigo, F. & Lampugnani, M. G. The role of adherens junctions and VE-cadherin in the control of vascular permeability. *J. Cell. Sci*. **121**, 2115-22 (2008).
40. Clevers, H. & Nusse, R. Wnt/Î²-Catenin Signaling and Disease. *Cell* **149**, 1192-1205 (2012).
41. Stadeli, R., Hoffmans, R. & Basler, K. Transcription under the control of nuclear Arm/beta-catenin. *Curr. Biol*. **16**, R378-85 (2006).
42. Maher, M. T., Flozak, A. S., Stocker, A. M., Chenn, A. & Gottardi, C. J. Activity of the beta-catenin phosphodestruction complex at cell-cell contacts is enhanced by cadherin-based adhesion. *J. Cell Biol*. **186**, 219-28 (2009).
43. McCrea, P. D., Gu, D. & Balda, M. S. Junctional music that the nucleus hears: cell-cell contact signaling and the modulation of gene activity. *Cold Spring Harb Perspect. Biol*. **1**, a002923 (2009).
44. St Croix, B. *et al*. E-Cadherin-dependent growth suppression is mediated by the cyclin-dependent kinase inhibitor p27(KIP1). *J. Cell Biol*. **142**, 557-71 (1998).
45. Shimizu, M., Fukunaga, Y., Ikenouchi, J. & Nagafuchi, A. Defining the roles of beta-catenin and plakoglobin in LEF/T-cell factor-dependent transcription using beta-catenin/plakoglobin-null F9 cells. *Mol. Cell. Biol*. **28**, 825-835 (2008).
46. Balda, M. S., Garrett, M. D. & Matter, K. The ZO-1-associated Y-box factor ZONAB regulates epithelial cell proliferation and cell density. *J. Cell Biol*. **160**, 423-432 (2003).
47. Dejana, E., Taddei, A. & Randi, A. M. Foxs and Ets in the transcriptional regulation of endothelial cell differentiation and angiogenesis. *Biochim. Biophys. Acta* **1775**, 298-312 (2007).
48. Tang, E. D., Nun, G., Barr, F. G. & Guan, K. Negative Regulation of the Forkhead Transcription Factor FKHR by Akt *. **274**, 16741-16746 (1999).
49. Hosaka, T. *et al*. Disruption of forkhead transcription factor (FOXO) family members in mice reveals their functional diversification. *Proc. Natl. Acad. Sci. U. S. A*. **101**, 2975-80 (2004).
50. Furuyama, T. *et al*. Abnormal angiogenesis in Foxo1 (Fkhr)-deficient mice. *The Journal of biological chemistry* **279**, 34741-9 (2004).
51. Potente, M. *et al*. Involvement of Foxo transcription factors in angiogenesis and postnatal neovascularization. **115** (2005).
52. Daly, C. *et al*. Angiopoietin-1 modulates endothelial cell function and gene expression via the transcription factor FKHR (FOXO1). , 1060-1071 (2004).
53. Jain, R. K. Molecular regulation of vessel maturation. *Nat. Med*. **9**, 685-693 (2003).
54. Carmeliet, P. & Jain, R. K. Principles and mechanisms of vessel normalization for cancer and other angiogenic diseases. *Nature reviews.Drug discovery* **10**, 417-27 (2011).

55. von Tell, D., Armulik, A. & Betsholtz, C. Pericytes and vascular stability. *Exp. Cell Res.* **312**, 623-629 (2006).
56. Armulik, A., Genove, G. & Betsholtz, C. Pericytes: developmental, physiological, and pathological perspectives, problems, and promises. *Dev. Cell.* **21**, 193-215 (2011).
57. Sottile, J. Regulation of angiogenesis by extracellular matrix. *Biochim. Biophys. Acta* **1654**, 13-22 (2004).
58. O'Reilly, M. S. *et al.* Endostatin: an endogenous inhibitor of angiogenesis and tumor growth. *Cell* **88**, 277-285 (1997).
59. George, E. L., Georges-Labouesse, E. N., Patel-King, R. S., Rayburn, H. & Hynes, R. O. Defects in mesoderm, neural tube and vascular development in mouse embryos lacking fibronectin. *Development* **119**, 1079-1091 (1993).
60. George, E. L., Baldwin, H. S. & Hynes, R. O. Fibronectins are essential for heart and blood vessel morphogenesis but are dispensable for initial specification of precursor cells. *Blood* **90**, 3073-3081 (1997).
61. Pereira, L. *et al.* Targetting of the gene encoding fibrillin-1 recapitulates the vascular aspect of Marfan syndrome. *Nat. Genet.* **17**, 218-222 (1997).
62. Liu, X., Wu, H., Byrne, M., Krane, S. & Jaenisch, R. Type III collagen is crucial for collagen I fibrillogenesis and for normal cardiovascular development. *Proc. Natl. Acad. Sci. U. S. A.* **94**, 1852-1856 (1997).
63. Jain, R. K. & Carmeliet, P. SnapShot: Tumor angiogenesis. *Cell* **149**, 1408-1408.e1 (2012).
64. Goel, S. *et al.* Normalization of the vasculature for treatment of cancer and other diseases. *Physiol. Rev.* **91**, 1071-1121 (2011).
65. Jain, R. K., Duda, D. G., Clark, J. W. & Loeffler, J. S. Lessons from phase III clinical trials on anti-VEGF therapy for cancer. *Nat. Clin. Pract. Oncol.* **3**, 24-40 (2006).
66. Ohsugi, M., Larue, L., Schwarz, H. & Kemler, R. Cell-Junctional and Cytoskeletal Organization in Mouse Blastocysts Lacking E-Cadherin. **271**, 261-271 (1997).
67. Nitta, T. *et al.* Size-selective loosening of the blood-brain barrier in claudin-5-deficient mice. *J. Cell Biol.* **161**, 653-60 (2003).
68. Morita, K., Sasaki, H., Furuse, M. & Tsukita, S. Endothelial claudin: claudin-5/TMVCF constitutes tight junction strands in endothelial cells. *J. Cell Biol.* **147**, 185-194 (1999).
69. Ba, S. *et al.* Vascular endothelial cell â€“ specific phosphotyrosine phosphatase (VE-PTP) activity is required for blood vessel development. *Angiogenesis* **107**, 4754-4762 (2006).
70. Dominguez, M. G. *et al.* Vascular endothelial tyrosine phosphatase (VE-PTP) -null mice undergo vasculogenesis but die embryonically because of defects in angiogenesis BIOLOGY. (2006).
71. Carra, S. *et al.* Ve-ptp Modulates Vascular Integrity by Promoting Adherens Junction Maturation. **7**, 1-12 (2012).
72. Fachinger, G., Deutsch, U. & Risau, W. Functional interaction of vascular endothelial-protein-tyrosine phosphatase with the angiopoietin receptor Tie-2. *Oncogene* **18**, 5948-53 (1999).
73. Winderlich, M. *et al.* VE-PTP controls blood vessel development by balancing Tie-2 activity. **185**, 657-671 (2009).
74. Saharinen, P. *et al.* Angiopoietins assemble distinct Tie2 signalling complexes in endothelial cell-cell and cell-matrix contacts. *Nat. Cell Biol.* **10**, 527-37 (2008).
75. Nawroth, R. VE-PTP and VE-cadherin ectodomains interact to facilitate regulation of phosphorylation and cell contacts. *EMBO J.* **21**, 4885-4895 (2002).
76. Nottebaum, A. F. *et al.* VE-PTP maintains the endothelial barrier via plakoglobin and becomes dissociated from VE-cadherin by leukocytes and by VEGF. **205**, 2929-2945 (2008).
77. Vischer, U. M. von Willebrand factor, endothelial dysfunction, and cardiovascular disease. *Journal of thrombosis and haemostasis : JTH* **4**, 1186-93 (2006).
78. Ruggeri, Z. M. The role of von Willebrand factor in thrombus formation. *Thromb. Res.* **120 Suppl**, S5-9 (2007).
79. Sadler, J. E., Mancuso, D. J., Randi, A. M., Tuley, E. A. & Westfield, L. A. Molecular biology of von Willebrand factor. *Ann. N. Y. Acad. Sci.* **614**, 114-124 (1991).
80. Starke, R. D. *et al.* Cellular and molecular basis of von Willebrand disease: studies on blood outgrowth endothelial cells. *Blood* **121**, 2773-2784 (2013).
81. Starke, R. D. *et al.* Endothelial von Willebrand factor regulates angiogenesis Endothelial von Willebrand factor regulates angiogenesis. *Starke*, 1071-1080 (2012).

82. Bernstein, B. E. *et al*. A bivalent chromatin structure marks key developmental genes in embryonic stem cells. *Cell* **125**, 315-326 (2006).
83. Voigt, P., Tee, W. W. & Reinberg, D. A double take on bivalent promoters. *Genes Dev*. **27**, 1318-1338 (2013).
84. Margueron, R. & Reinberg, D. The Polycomb complex PRC2 and its mark in life. *Nature* **469**, 343-9 (2011).
85. Mills, A. a. Throwing the cancer switch: reciprocal roles of polycomb and trithorax proteins. *Nature reviews.Cancer* **10**, 669-82 (2010).
86. Simon, J. a. & Kingston, R. E. Mechanisms of polycomb gene silencing: knowns and unknowns. *Nature reviews.Molecular cell biology* **10**, 697-708 (2009).
87. Simon, J. A. & Kingston, R. E. Review Occupying Chromatin : Polycomb Mechanisms for Getting to Genomic Targets , Stopping Transcriptional Traffic , and Staying Put. *Mol. Cell* **49**, 808-824 (2013).
88. Cao, R., Zhang, Y., Hill, C. & Carolina, N. SUZ12 Is Required for Both the Histone Methyltransferase Activity and the Silencing Function of the EED-EZH2 Complex University of North Carolina at Chapel Hill. **15**, 57-67 (2004).
89. Pasini, D., Bracken, A. P., Hansen, J. B., Capillo, M. & Helin, K. The polycomb group protein Suz12 is required for embryonic stem cell differentiation. *Mol. Cell. Biol*. **27**, 3769-79 (2007).
90. Margueron, R. *et al*. Role of the polycomb protein EED in the propagation of repressive histone marks. *Nature* **461**, 762-7 (2009).
91. Hansen, K. H. *et al*. A model for transmission of the H3K27me3 epigenetic mark. *Nat. Cell Biol*. **10**, 1291-300 (2008).
92. Margueron, R. *et al*. Ezh1 and Ezh2 maintain repressive chromatin through different mechanisms. *Mol. Cell* **32**, 503-518 (2008).
93. Nekrasov, M. *et al*. Pcl-PRC2 is needed to generate high levels of H3-K27 trimethylation at Polycomb target genes. *EMBO J*. **26**, 4078-4088 (2007).
94. Sarma, K., Margueron, R., Ivanov, A., Pirrotta, V. & Reinberg, D. Ezh2 requires PHF1 to efficiently catalyze H3 lysine 27 trimethylation in vivo. *Mol. Cell. Biol*. **28**, 2718-2731 (2008).
95. Pasini, D. *et al*. JARID2 regulates binding of the Polycomb repressive complex 2 to target genes in ES cells. *Nature* **464**, 306-10 (2010).
96. Schmitges, F. W. *et al*. Histone Methylation by PRC2 Is Inhibited by Active Chromatin Marks. *Mol. Cell* **42**, 330-41 (2011).
97. Li, B., Carey, M. & Workman, J. L. The role of chromatin during transcription. *Cell* **128**, 707-719 (2007).
98. Gao, Z. *et al*. Article PCGF Homologs , CBX Proteins , and RYBP Define Functionally Distinct PRC1 Family Complexes. *Mol. Cell* **45**, 344-356 (2012).
99. Tavares, L. *et al*. RYBP-PRC1 Complexes Mediate H2A Ubiquitylation at Polycomb Target Sites Independently of PRC2 and H3K27me3. *Cell* **3** (2012).
100. Herranz, N. *et al*. Polycomb complex 2 is required for E-cadherin repression by the Snail1 transcription factor. *Mol. Cell. Biol*. **28**, 4772-4781 (2008).
101. Schuettengruber, B., Martinez, A., Iovino, N. & Cavalli, G. Trithorax group proteins: switching genes on and keeping them active. *Nature Reviews Molecular Cell Biology* **12**, 799-814 (2011).
102. Schuettengruber, B., Chourrout, D., Vervoort, M., Leblanc, B. & Cavalli, G. Genome regulation by polycomb and trithorax proteins. *Cell* **128**, 735-45 (2007).
103. Balconi, G., Spagnuolo, R. & Dejana, E. Development of Endothelial Cell Lines From Embryonic Stem Cells. *Arteriosclerosis & Thrombosis* (2000).
104. Navarro, P. *et al*. Catenin-dependent and -independent functions of vascular endothelial cadherin. *J. Biol. Chem*. **270**, 30965-30972 (1995).
105. Lampugnani, M. G. *et al*. VE-Cadherin Regulates Endothelial Actin Activating Rac and Increasing Membrane Association of Tiam. *Mol. Biol. Cell* **13**, 1175-1189 (2002).
106. Xiao, K. *et al*. Mechanisms of VE-cadherin processing and degradation in microvascular endothelial cells. *J. Biol. Chem*. **278**, 19199-19208 (2003).
107. Lampugnani, M. G. *et al*. Cell confluence regulates tyrosine phosphorylation of adherens junction components in endothelial cells. *J. Cell. Sci*. **110 (Pt 17)**, 2065-2077 (1997).
108. Dull, T. *et al*. A third-generation lentivirus vector with a conditional packaging system. *J. Virol*. **72**, 8463-8471 (1998).

109. Quasnichka, H. *et al*. Regulation of smooth muscle cell proliferation by beta-catenin/T-cell factor signaling involves modulation of cyclin D1 and p21 expression. *Circ. Res.* **99**, 1329-1337 (2006).
110. Spagnuolo, R. *et al*. Gas1 is induced by VE-cadherin and vascular endothelial growth factor and inhibits endothelial cell apoptosis. *Blood* **103**, 3005-3012 (2004).
111. Cartharius, K. *et al*. MatInspector and beyond: promoter analysis based on transcription factor binding sites. *Bioinformatics* **21**, 2933-2942 (2005).
112. Fontijn, R. D. *et al*. SOX-18 controls endothelial-specific claudin-5 gene expression and barrier function. *American journal of physiology.Heart and circulatory physiology* **294**, H891-900 (2008).
113. Schwachtgen, J. L. *et al*. Ets transcription factors bind and transactivate the core promoter of the von Willebrand factor gene. *Oncogene* **15**, 3091-3102 (1997).
114. Burek, M. & Forster, C. Y. Cloning and characterization of the murine claudin-5 promoter. *Mol. Cell. Endocrinol.* **298**, 19-24 (2009).
115. Collins, C. J. *et al*. Molecular cloning of the human gene for von Willebrand factor and identification of the transcription initiation site. *Proc. Natl. Acad. Sci. U. S. A.* **84**, 4393-4397 (1987).
116. Guan, J., Guillot, P. V. & Aird, W. C. Characterization of the mouse von Willebrand factor promoter. *Blood* **94**, 3405-3412 (1999).
117. Nakae, J. *et al*. The forkhead transcription factor Foxo1 regulates adipocyte differentiation. *Dev. Cell.* **4**, 119-129 (2003).
118. Corada, M. Monoclonal antibodies directed to different regions of vascular endothelial cadherin extracellular domain affect adhesion and clustering of the protein and modulate endothelial permeability. *Blood* **97**, 1679-1684 (2001).
119. Brookes, E. & Pombo, A. Modifications of RNA polymerase II are pivotal in regulating gene expression states. *EMBO Rep.* **10**, 1213-9 (2009).
120. Pasini, D., Bracken, A. P., Jensen, M. R., Lazzerini Denchi, E. & Helin, K. Suz12 is essential for mouse development and for EZH2 histone methyltransferase activity. *EMBO J.* **23**, 4061-4071 (2004).
121. Bracken, A. P., Dietrich, N., Pasini, D., Hansen, K. H. & Helin, K. Genome-wide mapping of Polycomb target genes unravels their roles in cell fate transitions. *Genes Dev.* **20**, 1123-1136 (2006).
122. Su, I. -. *et al*. Polycomb Group Protein Ezh2 Controls Actin Polymerization and Cell Signaling. **121**, 425-436 (2005).
123. Witte, V. *et al*. HIV-1 Nef Mimics an Integrin Receptor Signal that Recruits the Polycomb Group Protein Eed to the Plasma Membrane Nikolaus-Fiebiger-Center for Molecular Medicine Institute for Experimental Pathology. *Group* **13**, 179-190 (2004).
124. Chang, C. J. *et al*. EZH2 promotes expansion of breast tumor initiating cells through activation of RAF1-beta-catenin signaling. *Cancer. Cell.* **19**, 86-100 (2011).
125. Lu, C. *et al*. Regulation of tumor angiogenesis by EZH2. *Cancer cell* **18**, 185-97 (2010).
126. Nicolay, B. N. & Dyson, N. J. The multiple connections between pRB and cell metabolism. *Curr. Opin. Cell Biol.* (2013).
127. Howell, G. J. *et al*. Endothelial cell confluence regulates Weibel-Palade body formation. *Mol. Membr. Biol.* **21**, 413-421 (2004).
128. Thomas, M. & Augustin, H. G. The role of the Angiopoietins in vascular morphogenesis. *Angiogenesis* **12**, 125-37 (2009).
129. Bracken, A. P. *et al*. EZH2 is downstream of the pRB-E2F pathway , essential for proliferation and ampli Â® ed in cancer. *EMBO J.* **22**, 5323-5335 (2003).
130. Niessen, H. E., Demmers, J. A. & Voncken, J. W. Talking to chromatin: post-translational modulation of polycomb group function. *Epigenetics Chromatin* **2**, 10-8935-2-10 (2009).
131. Cha, T. L. *et al*. Akt-mediated phosphorylation of EZH2 suppresses methylation of lysine 27 in histone H3. *Science* **310**, 306-310 (2005).
132. Schuettengruber, B. & Cavalli, G. Recruitment of Polycomb group complexes and their role in the dynamic regulation of cell fate choice. *Development* **3542**, 3531-3542 (2009).
133. Mulero, M. C. *et al*. Chromatin-Bound IkappaBalpha Regulates a Subset of Polycomb Target Genes in Differentiation and Cancer. *Cancer. Cell.* **24**, 151-166 (2013).

134. Dietrich, N. *et al*. REST-mediated recruitment of polycomb repressor complexes in mammalian cells. *PLoS Genet*. **8**, e1002494 (2012).
135. Leeb, M. *et al*. Polycomb complexes act redundantly to repress genomic repeats and genes. *Genes Dev*. **24**, 265-76 (2010).
136. Schoeftner, S. *et al*. Recruitment of PRC1 function at the initiation of X inactivation independent of PRC2 and silencing. **25**, 3110-3122 (2006).
137. Yuan, L. *et al*. ERG controls endothelial cell permeability via transcriptional regulation of claudin-5 (CLDN5). *The Journal of biological chemistry* **5**, 1-15 (2012).
138. Liu, J. *et al*. Vascular bed-specific regulation of the von Willebrand factor promoter in the heart and skeletal muscle. *Blood* **117**, 342-51 (2011).
139. Bautch, V. L. Endothelial cells form a phalanx to block tumor metastasis. *Cell* **136**, 810-2 (2009).
140. Mazzone, M. *et al*. Heterozygous deficiency of PHD2 restores tumor oxygenation and inhibits metastasis via endothelial normalization. *Cell* **136**, 839-51 (2009).
141. Oliveira, R. L. D. *et al*. Article Gene-Targeting of Phd2 Improves Tumor Response to Chemotherapy and Prevents Side-Toxicity. , 263-277 (2012).
142. Lu, C. *et al*. Gene alterations identified by expression profiling in tumor-associated endothelial cells from invasive ovarian carcinoma. *Cancer Res*. **67**, 1757-68 (2007).
143. Tan, J. *et al*. Pharmacologic disruption of Polycomb-repressive complex 2-mediated gene repression selectively induces apoptosis in cancer cells. (2007).
144. Smits, M. *et al*. Down-regulation of miR-101 in endothelial cells promotes blood vessel formation through reduced repression of EZH2. *PloS one* **6**, e16282-e16282 (2011).
145. Ahmed, A. A., Becker, C. M. & Bast, R. C.,Jr. The origin of ovarian cancer. *BJOG* **119**, 134-136 (2012).
146. Zecchini, S. *et al*. The Differential Role of L1 in Ovarian Carcinoma and Normal Ovarian Surface Epithelium. , 1110-1118 (2008).

ACKNOWLEDGEMENTS

Four years have passed and, thanks to the experiences I had and the people I met, I hope I grew both from the scientific and the personal sides. At this point I hope I became a little closer to what I want to be, even if I know that it's still a long way to go.

First I want to thank my boss, Elisabetta Dejana, for giving me the opportunity to work in her group, for pushing me always in the right direction and for letting me pursue my scientific interests.

I acknowledge my supervisors, Holger Gerhardt and Giuseppe Testa for their very helpful and constructive feedback during these years.

The work done on human tissue samples was done thanks to the frutiful collaboration with Ugo Cavallaro who kindly shared with us many samples and gave us insightful advice.

I am grateful to Federica Pisati who gave me a tremendous help in performing the stainings on human tissues and for being always so nice to me.

I deeply thank Andrea Taddei for teaching me how to think and to work in the lab and for his precious help every time I needed it during these years.

A special thank goes to Costanza Giampietro who is a person whom I could always count on. That's what real friends are for.

I thank all the past and present members of the Vascular Biology Group for their help and the great moments we spent together, especially I want to acknowledge Ganesh, Matteo, Marianna, Monica C, Monica G, Luca B, Annamaria, Azzurra, Benedetta, Roberto, Noemi, Gigi and Eleanna.

I am particularly grateful to Lisa who, apart from being a unique person to me, is also my personal "proof-reader". Your help has been so precious to me and I am so lucky to have you close to me.

To conclude, I thank my family and my friends, Federico, Francesca and Ilaria without whom it would have been much much harder.